

USE OF ELECTRICAL RESISTIVITY AND MULTICHANNEL  
ANALYSIS OF SURFACE WAVE GEOPHYSICAL  
TOMOGRAPHY IN GEOTECHNICAL SITE  
CHARACTERIZATION OF DAM

by

JOSHUA LEE HUBBARD

Presented to the Faculty of the Graduate School of  
The University of Texas at Arlington in Partial Fulfillment  
of the Requirements  
for the Degree of

MASTER OF SCIENCE IN CIVIL ENGINEERING

THE UNIVERSITY OF TEXAS AT ARLINGTON

DECEMBER 2009

Copyright © by Joshua Lee Hubbard 2009

All Rights Reserved

## ACKNOWLEDGEMENTS

I would like to thank the members of the committee; Dr. Laureano Hoyos and Dr. Stefan Romanaschi, for their time and participation in the completion of this project. I would like to give special thanks to the committee chair, Dr. Sahadat Hossain, for his advisement throughout my graduate studies and for my introduction into geophysical testing.

The completion of this thesis would not have been possible without the corroborative efforts of several individuals and organizations. The following individuals and organizations have contributed time and resources to the completion of this study: the City of Gladewater, Texas, Apex Geoscience, Inc, Advanced Geosciences, Inc., Geometrics, Inc and the Kansas Geologic Survey.

I would like to thank David Wright and Mitch Bernhard, for the encouragement and opportunity to accomplish my personal and professional goals. I would like to give a special thanks to John Tayntor, for his ongoing professional and personal support as well as the willingness to participate in whatever capacity necessary to make this venture a success.

I would like to thank my family for all their support. Specifically, I would like to thank my mother and brothers; Patricia, David and Jeremy, for their continual support and guidance.

This work is dedicated to my loving wife, Melissa. Without your love and sacrifice, I would not be achieving this milestone. Thank you.

December 7, 2009

## ABSTRACT

# USE OF ELECTRICAL RESISTIVITY AND MULTICHANNEL ANALYSIS OF SURFACE WAVE GEOPHYSICAL TOMOGRAPHY IN GEOTECHNICAL SITE CHARACTERIZATION OF DAM

Joshua Lee Hubbard, M.S.

The University of Texas at Arlington, 2009

Supervising Professor: MD. Sahadat Hossain

Performance of geotechnical site characterization is a primary function of geotechnical engineers. Generalizations required to extrapolate conventional geotechnical boring data can limit the effectiveness of site assessments. Advancements in geophysical technology have simplified means of data acquisition and interpretation of electrical and seismic testing, allowing a broader audience of practitioners to utilize methods for various engineering and environmental applications. In this study, electrical resistivity and multichannel analysis of surface waves (MASW) seismic geophysical methods are used to expound upon previous geotechnical sampling and in situ testing conducted at an earthen dam site in East Texas. Findings from this study show: results of geophysical testing are comparable with those from conventional geotechnical field and laboratory testing, dissimilarities between geophysical profiles and geotechnical data can exist due to soil heterogeneity, resolution capabilities and data smoothing

associated with geophysical interpretation, and areas of low resistivity and low density corresponded with observations of seepage and seepage related issues.

## TABLE OF CONTENTS

ACKNOWLEDGEMENTS .....	iii
ABSTRACT .....	iv
LIST OF ILLUSTRATIONS.....	xi
LIST OF TABLES .....	xiii
Chapter	Page
1. INTRODUCTION.....	1
1.1    Background and Significance.....	1
1.2    Objectives.....	2
1.3    Organization .....	3
2. REVIEW OF LITERATURE.....	4
2.1    Geotechnical Site Characterization.....	4
2.1.1    Document Review .....	6
2.1.2    Visual Assessment .....	6
2.1.3    Subsurface Sampling .....	7
2.1.3.1    Drilling .....	7
2.1.3.2    Sampling .....	8
2.1.4    In-Situ Testing .....	10
2.1.5    Laboratory Testing.....	12
2.1.6    Geophysical Testing .....	14
2.2    Electrical Resistivity.....	14
2.2.1    Theoretical Background .....	15

2.2.2	Natural Conditions Affecting Measurements of Resistivity.....	18
2.2.3	Arrays .....	19
2.2.3.1	Wenner Array.....	19
2.2.3.2	Schlumberger Array.....	21
2.2.3.3	Dipole-Dipole Array.....	22
2.2.4	Electrical Resistivity Testing Methods.....	23
2.2.4.1	One Dimensional Electrical Resistivity Surveying .....	24
2.2.4.2	Two Dimensional Electrical Resistivity Surveying .....	24
2.2.4.3	Three Dimensional Electrical Resistivity Surveying.....	25
2.2.4.4	Time Variant Resistivity Measurements .....	25
2.2.5	Equipment .....	25
2.2.5.1	Transmitter/Receiver.....	25
2.2.5.2	Cables.....	26
2.2.5.3	Current and Potential Electrodes.....	26
2.2.5.4	Power Source .....	27
2.2.6	Data Acquisition.....	27
2.2.7	Data Interpretation.....	29
2.3	Multichannel Analysis of Surface Waves (MASW) .....	32
2.3.1	Seismic Wave Theory .....	32
2.3.1.1	Physical Background .....	32
2.3.1.2	Wave Types .....	33
2.3.1.3	Methods of Surface Wave Analysis.....	36
2.3.2	Performance of MASW Testing.....	38
2.3.2.1	Equipment.....	38
2.3.2.1.1	Seismic Source .....	38

2.3.2.1.2	Trigger Mechanism.....	39
2.3.2.1.3	Geophones.....	40
2.3.2.1.4	Geophone Cable .....	41
2.3.2.1.5	Seismograph .....	41
2.3.2.2	Field Survey Setup.....	42
2.3.3	Data Acquisition.....	44
2.3.4	Data Interpretation.....	45
2.4	Case Histories .....	48
2.4.1	Examples of Site Characterization and Assessment .....	48
2.4.1.1	Detailed Site Assessment in Anguilla, BWI .....	48
2.4.1.2	Missouri Department of Transportation Field Test of MASW.....	50
2.4.1.3	Site Characterization for Retaining Wall near Atlanta, Georgia.....	51
2.4.1.4	Time-lapse Analysis of Texas Levee.....	53
2.4.2	Attempts to Correlate Geophysical and Geotechnical Data.....	54
2.4.2.1	Analysis from Thermal Power Plant Sites in India.....	54
2.4.2.2	Field Testing of Geophysical Techniques in Garchy, France .....	55
2.4.2.3	Analysis of Shear Wave Velocity Penetration Testing.....	57
3.	FIELD DATA COLLECTION .....	59
3.1	Site Assessment and Geotechnical Sampling .....	59
3.1.1	In-Situ Geotechnical Testing .....	60
3.1.2	Laboratory Testing.....	62
3.1.3	Comments .....	63
3.2	Electrical Resistivity Survey .....	63



3.2.1	Survey Preparations .....	63
3.2.2	Equipment .....	64
3.2.3	Data Acquisition.....	66
3.2.4	Data Processing and Inversion .....	69
3.2.5	Comments .....	70
3.3	Multi-Channel Analysis of Surface Wave (MASW) Survey .....	71
3.3.1	Survey Preparations .....	71
3.3.2	Survey Setup .....	71
3.3.3	Data Acquisition.....	74
3.3.4	Data Processing and Inversion .....	75
3.3.5	Comments .....	78
4.	FINDINGS AND OBSERVATIONS .....	79
4.1	Geotechnical Site Assessment .....	79
4.1.1	Findings .....	79
4.1.2	Observations .....	81
4.2	Electrical Resistivity Survey .....	83
4.2.1	Findings .....	83
4.2.2	Observations .....	85
4.3	Multichannel Analysis of Surface Waves (MASW) Survey .....	88
4.3.1	Findings .....	88
4.3.2	Observations .....	90
5.	CONCLUSIONS .....	94
5.1	Findings and Conclusions .....	94
5.2	Recommendations for Future Work .....	95
APPENDIX		

A. PROCEDURE FOR DEVELOPMENT OF TWO DIMENSIONAL MASW PROFILE .....	97
B. BORING LOGS FROM LAKE GLADEWATER DAM .....	99
C. DEVELOPMENT OF SUBSURFACE MAPPING SCHEME FROM DIPOLE-DIPOLE ARRAY USING AGI ADMINISTRATOR PROGRAM .....	103
D. ENLARGED ERT AND MASW TOMOGRAPHY IMAGERY .....	107
E. MASW DISPERSION CURVE AND SHEAR WAVE PROFILE EXAMPLES .....	110
REFERENCES .....	119
BIOGRAPHICAL INFORMATION .....	124

## LIST OF ILLUSTRATIONS

Figure	Page
2.1 General Application of Ohm's Law for Derivation of Geometric Factor for Apparent Resistivity Measurement.....	17
2.2 Wenner Array (a) Layout and (b) Sensitivity Pattern .....	20
2.3 Schlumberger Array (a) Layout and (b) Sensitivity Pattern.....	22
2.4 Dipole-Dipole Array (a) Layout and (b) Sensitivity Pattern .....	23
2.5 Example of a Roll-Along for (a) Two-Dimensional Tomography Survey and (b) Three-Dimensional Survey .....	29
2.6 Example of Developed Psuedosection Model Using a Wenner Array and 28 Electrodes .....	30
2.7 Flow Chart of Resistivity Inversion Processing .....	31
2.8 Translational Behavior of (a) P-waves and (b) S-waves .....	34
2.9 (a) Love and Rayleigh Wave Propagation and (b) Retrograde, Elliptical Particle Motion of Rayleigh Wave Propagation .....	35
2.10 Example of Sledgehammer Triggering Device .....	40
2.11 Example of Spike-coupled Geophone.....	41
2.12 Instrumentation of MASW Tomography Survey.....	42
2.13 Progression of MASW Tomography Survey .....	43
2.14 Suggested Parameters for Setup of MASW Survey .....	44
2.15 Processing Steps to Estimate Shear Wave Velocity.....	46
3.1 Map of Lake Gladewater Dam from Gladewater Quadrangle.....	60
3.2 Approximate Boring Locations along Crest of Dam .....	62

3.3 Psuedosection Model of Dipole-Dipole Array Used During Data Acquisition .....	66
3.4 Origination Point and Direction of Electrical Resistivity Tomography Survey. ....	67
3.5 Performance of Electrical Resistivity Tomography Survey at Lake Gladewater.....	69
3.6 Electrical Resistivity Profile of Lake Gladewater Dam .....	70
3.7 Instrumentation and Setup for MASW Field Testing.....	73
3.8 Example of Acquired Shot Record during Lake Gladewater MASW Survey.....	75
3.9 Dispersion Curve from Sounding No. 45 of Lake Gladewater Dam .....	77
3.10 Inversion of Sounding No. 45 from Lake Gladewater Dam.....	77
3.11 Shear Wave Profile using MASW Seismic Tomography. ....	78
4.1 Boring Moisture Content Profiles .....	80
4.2 Neglected Areas of Electrical Resistivity Profile .....	84
4.3 Location of Borings and Downstream Slope Observations.....	85
4.4 Variations in Moisture Content and Resistivity with Depth.....	86
4.5 MASW Shear Wave Profile of Lake Gladewater Dam Scaled in Linear Feet.....	89
4.6 Variation in SPT N-Values and Shear Wave Velocity with Depth.....	90
4.7 Comparison of General Soil Conditions and Shear Wave Velocity with Depth at Boring No. 1 .....	91
4.8 Electrical Resistivity and MASW Tomography with Boring Overlay .....	92

## LIST OF TABLES

Table	Page
2.1 Correlations between SPT N-Values and Cohesionless Soil Properties .....	11
2.2 Correlations between SPT N-Values and Cohesive Soil Properties .....	11
2.3 Common Geotechnical Laboratory Testing Methods .....	13
2.4 Typical Values of Electrical Resistivity for Various Subsurface Materials .....	18
2.5 Derived Correlations between Shear Wave Velocity and Penetration Resistance .....	57
3.1 Summary of Assigned Testing Program .....	62
4.1 Percent Fine Content and Plasticity Index Test Summary .....	80
4.2 Correlations between Material Stiffness and Shear Wave Velocity.....	90

## CHAPTER 1

### INTRODUCTION

#### 1.1 Background and Significance

Geotechnical site characterization is performed by completing document reviews, soil sampling, in-situ testing, and/or laboratory analysis of samples from an area of interest (Day 2006). The effort provided to a site characterization is based on the cost-benefit to a given project (Bowles 1984). Advancements in the field of in-situ testing have improved the quality of collected soils data; however, known conditions are still limited to a confined area and data must be extrapolated amongst an entire soil mass for design purposes. Undetected natural and/or man-made anomalies can nullify constant earth assumptions often used during the analysis and evaluation of geotechnical data. Encountering anomalous conditions during site development and construction can result in interruptions to projected schedule, additional labor and material costs, and potentially pose safety risks.

It is for these reasons that the burden for improved site characterization has since fallen on the geotechnical/environmental engineering consultant. Geotechnical engineers need sound means to bridge point data acquired during conventional geotechnical field operations, in a timely and cost efficient manner.

Geophysicist and practitioners of geophysics have improved and developed innovative near-surface geophysical testing methods, increasing the ease and ability to visualize subsurface conditions and anomalies. Advancements in data acquisition and interpretation have improved efficiency and have made the use of geophysical surveying fiscally and logistically feasible for several different project applications (Steeple 2001). Unfortunately, there is still resistance by members of the engineering community to accept results derived from geophysical testing. Some

practitioners see methods and results as ambiguous, and are uncomfortable with the non-unique nature of interpretations and level of precision that are characteristic of geophysical testing methods. Views from geophysical practitioners suggest that the hesitance is caused by improper presentation of findings on the part of the geophysicist or geophysical provider. Issues also spawn from unrealistic expectations of the testing on the part of the engineer or owner requesting the testing. By understanding proper application and associated limitations of testing methods, near-surface geophysics can provide tools for improving the quality of geotechnical site characterization (Butler 2005).

## 1.2 Objectives

The main purpose of this study is to evaluate improvements made on a previous geotechnical site characterization through the use of two geophysical tomography methods: electrical resistivity and multichannel analysis of surface wave (MASW) seismic tomography. The following are means of accomplishing this objective:

- Collect and analyze conventional geotechnical field data from the test location;
- Perform an electrical resistivity tomography survey at the test location, encompassing the data points evaluated during the original geotechnical site characterization;
- Use inversion techniques to analyze collected electrical resistivity and generate representative two dimensional (2D) profiles of the test site;
- Perform a MASW tomography survey at the test location, encompassing the data points evaluated during the original geotechnical site characterization;
- Use inversion and interpolative techniques to analyze collected MASW data and generate a representative 2D profile of the test site; and
- Compare the results of the original geotechnical site characterization and the two tomography surveys, highlighting improvements in site characterization and discussing limiting factors in the geophysical interpretations.

### 1.3 Organization

An introduction of the subject matter and statement of purpose were provided in Chapter 1. The following commentary discusses the presentation of the aforementioned study in the remainder of the document. Chapter 2 provides a review of literature concerning conventional geotechnical site characterization, electrical resistivity and MASW methodology and testing. Also provided are summaries of case histories demonstrating the usefulness of electrical resistivity and MASW surveying methods in site characterization applications as well as case histories attempting to correlate geotechnical testing to geophysical interpretation. Chapter 3 discusses field data acquisition and analysis performed in conjunction with original geotechnical site characterization, and supplemental electrical resistivity and MASW tomography surveys. Chapter 4 gives findings and observations from geotechnical and geophysical field studies. Conclusions drawn from the site characterization and geophysical testing are presented in Chapter 5. Additional comments discussing areas of improvement and potential items for future research are also provided. Appendices are included to supplement information and/or data presented at various locations within the text.



## CHAPTER 2

### REVIEW OF LITERATURE

#### 2.1 Geotechnical Site Characterization

Unlike other civil engineering professions, materials at the focus of geotechnical engineering are not manufactured and do not possess a consistent set of properties. Soil and rock formations are unique based on location and geologic histories. In light of this fact, it is important to properly characterize the site prior to initiating design and construction. Site characterization can be broadly described as the defining of existing soil properties at a given site (Coduto 1999). This task is often the focal point of the geotechnical engineering analysis, more so than the associated development and/or foundation design. Likewise, the means of performing site characterization generally utilizes the greatest portion of the project budget for geotechnical services. Understanding the properties of the subsurface allows the geotechnical engineer to predict soil behavior under a myriad of scenarios. Recommendations are made regarding applicable foundation types, means for mitigating or preparing existing soil conditions for construction, and forecasting potential issues during construction.

Although the objectives of a site characterization program must be project specific, the fundamental objectives are often consistent. These objectives include (Bowles 1984, Coduto 1999, Sowers and Sowers 1970):

- Determination of site stratigraphy and lithology, including location and layer thickness of existing soil and/or rock formations;
- Determination and evaluate physical properties of existing soil and/or rock;
- Determination of site hydrologic conditions;
- Performance of pertinent in-situ testing;

- Acquisition of soil and/or rock samples;
- Performance of applicable laboratory testing; and
- Definition of site specific issues pertinent to the project.

The performance of site characterization is dictated by the project schedule and funding available to conduct the required analyses. Such limitations restrict the amount of testing and analysis performed, thus limiting the understanding of the existing site condition. The estimated budget for geotechnical studies 25 years ago ranged from 0.1 percent to 0.3 percent of the total project budget (Bowles 1984). More recent data indicates that similar percentages are consistent with current budget allowances (Look 2007). The value of the geotechnical evaluation is related to the amount of money that would be spent in the absence of the site characterization; suggesting that in order to compensate for a lesser degree of data, the final project will often be overdesigned resulting in additional project costs related to design and implementation. The extraneous cost of overdesign is greater than the cost to perform additional testing or analysis (Sowers and Sowers 1970).

Geotechnical engineers recognize that acquired data represents only a fraction of the present geologic conditions, and engineering judgment is necessary in order to discern what conditions can be expected as the project progresses. The absence of absolutes lends site characterization to significant amounts of engineering judgment and the inherent acceptance of risk (Sowers and Sowers 1970). The job of the geotechnical engineer is to devise a site characterization plan which maximizes site understanding, satisfies project budget and time constraints, and while maintain an acceptable risk level.

Site characterization is conducted by completing a series of tasks aimed at defining the conditions of the site. Conventional means of achieving this objective may include any combination of the following:

- Review of available site geologic and topographic data;

- Review of historical geotechnical data;
- Planning and performance of drilling program, including soil sampling acquisition and in-situ testing;
- Excavation and evaluation of site test pits or trenches;
- Initiation of in-situ testing program, including down-hole geotechnical testing; and
- Monitoring of groundwater levels, either by means of installation and development of test wells or piezometers or monitoring groundwater conditions encountered during the course of drilling.

These items are representative actions which comprise the majority of geotechnical studies. Geophysical testing is incorporated as well; however, testing is often limited due to project scope or the client's or practitioner's unfamiliarity with the methodology (United States Corps of Engineers 2001).

#### *2.1.1 Document Review*

A document review is helpful in providing a generalization of the site, prior to visiting the site or initiating field activities. Documents which may be available include geologic, seismic and/or topographic maps, aerial photography, past development records (i.e. construction plans, past geotechnical reports), and field reports by state or federal agencies (Day 2006). Such documentation may assist with planning of field activities and also help during the interpretation of collected field and laboratory data. In some cases, a review of local building codes may provide guidance in planning or directing field activities (Day 2006).

#### *2.1.2 Visual Assessment*

In certain situations, it is advantageous for the engineer to visit and visualize the site either prior to or during field activities. There are natural conditions, such as topography changes, unknown bodies of water, or man-made features that impact the analyses or interpretation of collected data. Unfortunately, due to schedule and budgetary constraints, a

visual site assessment is not always performed by the geotechnical engineer (United States Corps of Engineers 2001).

Visual assessment of collected samples is also needed during the assessment of retrieved soil specimens. Although field and laboratory testing define the necessary physical properties for soil classification, visually assessing collected material may provide additional insight into the history or current state of the site. Such conditions may include the presence of organic and/or inorganic debris from past development, chemical contamination, thin laminations of various soils or rock, mineral concentrations (United States Corps of Engineers 2001).

### *2.1.3 Subsurface Sampling*

Site assessments require subsurface observation and/or sampling. Since geotechnical site characterization primarily focuses on the underlying properties and characteristics soil and rock, it is imperative that these conditions be properly delineated. For most projects, this is accomplished by drilling test borings for sampling and in-situ testing. Other means of sampling or observation may include the construction of test pits or trenches, or by using direct push methods of sampling and in-situ testing (United States Corps of Engineers 2001).

#### *2.1.3.1 Drilling*

The completion of borings is the most common means of collecting geotechnical data. Borings are holes drilled into the ground for the purpose of collecting information related to subsurface conditions, primarily by obtaining samples for analysis and performing in-situ testing. Several means of completing borings are available due to the need for drilling and obtaining samples in varying subgrade conditions. Methods include the use of continuous dry auger drilling, hollow stem auger drilling, rotary drilling, wash drilling and percussion drilling (Day 2006). For the purposes of this paper, dry auger and hollow stem auger methods are applicable for further discussions and are expanded upon herein.

Dry auger drilling is accomplished by rotating an auger into the earth while simultaneously applying a downward thrust to the stem of augers, using the weight of the drilling

rig (Day 2006). Dry auger drilling is a preferred means of drilling in soil conditions not prone to caving, and for soils above the groundwater table. Strata changes are readily determined by the cutting or spoils returned to the surface. Boreholes can easily be prepared for in-situ testing. This method is completed quickly and reduces the degree of sample disturbance as opposed to rotary or wash methods. Drilling using solid continuous flight augers is also adaptable to rock conditions by quickly switching end bits, for better penetration (Bowles 1984).

Hollow stem augers have hollow cores that allow for drilling and sampling in conditions which are prone to caving, as the auger itself serves as casing supporting the anterior walls of the borehole excavation. As the auger is advanced, the interior core is used to run sampling and testing equipment through the borehole to the desired depth without disturbance from intruding soils or groundwater. Drilling and sampling using hollow stem augers is similar to dry auger drilling in that the stem of augers is advanced into the earth using the weight of the drilling rig. Hollow stem augers may also be used as casing during coring operations (Day 2006).

The number of borings required for site characterization is subjective. Although local or federal codes may provide guidance (Day 2006), the quantity of sampling is often defined by the design team based on the scope of the project. Considerations for determining depth and quantity of borings includes; the size of the site, potential grading, soils conditions anticipated, degree of subsurface variability, type and purpose of the proposed development, and accessibility of the drilling equipment (Coduto 1999). The boring program must provide the geotechnical engineer assurance that the underlying soil conditions have been adequately defined (Bowles 1984).

#### 2.1.3.2 Sampling

Samples of soil and rock are collected in either a disturbed or undisturbed condition. Disturbed sampling is performed when maintaining the physical structures or integrity of the sample is not required for further evaluation of physical properties. Undisturbed sampling is used to evaluate in-situ soil structure and stress history (Bowles 1984).

Disturbed sampling is performed using several different methods. Bulk disturbed samples are collected directly off of flight augers during drilling, or manual excavated from the ground. Samples collected using a split-spoon sampling device or California sampler are also considered disturbed. Disturbance is caused by the shape and configuration of the sampling device and also by the impact drive used to advance the sampler. Disturbed samples are suitable for the determination of some physical properties, but are not appropriate for testing that requires test specimens to retain the original physical structure or properties related to past stresses. Disturbed sampling is performed for the collection of cohesionless and cohesive soil types.

Undisturbed sampling is most commonly used for acquiring samples of cohesive soils, and is typically performed using thin or thick walled Shelby tube samplers. The sampler is continuously inserted into the soil, to a depth equivalent to the sampler length, and then retracted from the borehole (Bowles 1984). No driving of the sampler is involved. The sample is then extruded from the tube using hydraulic equipment, and preserved for further evaluation. In other situations, coring methods can be used to collect necessary samples of both soil and rock. During coring, a cutting shoe is affixed to the end of a sampling barrel. The barrel is rotated into the ground and the sample is retained in the sampling barrel. Upon completing a core run, the split barrel sampling assembly is opened and samples are removed from the barrel half. (United States Corps of Engineers 2001). It is generally accepted that an undisturbed sample will have some degree of disturbance is introduced, either related to sampling, handling, and transporting the given sample. The degree of disturbance is generally related to the experience of personnel collecting the samples, and the implementation and execution of proper sampling methods (Bowles 1984). Undisturbed specimens of cohesionless materials can be acquired; however, this generally requires a significant effort during sampling to maintain the physical structure of the granular sample. Developed correlations exist between in-situ testing and the physical properties

of cohesionless materials, therefore the collection of and testing of undisturbed granular soils is typically not warranted for most projects (Day 2006).

#### *2.1.4 In-Situ Testing*

During the course of drilling, in-situ testing of the subsurface is performed as the boring is being advanced. The style of testing is determined by the geotechnical engineer based on the scope of the given project. Several methods of testing have been researched and developed for use in geotechnical applications; however, two of the most commonly used methods are the Standard Penetration Test (SPT) and the Cone Penetration Test (CPT) (United States Corps of Engineers 2001).

One of the most established field testing procedures is the Standard Penetration Test (Bowles 1984). The method for performing standard penetration testing is documented by the American Society of Testing and Materials (ASTM), in ASTM D 1586: Standard Test Method for Penetration Test and Split Barrel Sampling of Soils. A split barrel sampling unit, termed a “split spoon,” is hammered into the undisturbed soil a distance of 18 inches. The driving force is provided by a free-falling, 140 pound (63.5 kilogram) anvil or weight. The energy transfer is standardized by routinely dropping the anvil from a height of 30 inches (760 millimeters). Each hammer strike is documented and noted through three consecutive six inch (152 millimeter) intervals. The first interval is considered a seating interval, allowing the sampler to penetrate any disturbed soils caused by drilling. The summation of hammer strikes in the final two intervals is considered the “blow count” or “N-value.” N-Values are evaluated for the purpose of determining soil properties and conditions. If within any single interval 50 blows is achieved prior to advancing the sampler six inches, the test is stopped and the sampler is thought to have achieved “refusal” due to failure to advance the sampler (American Society of Testing and Materials 1999). SPT is scrutinized due to variability and inconsistency related to the crudeness of the methodology, mechanical efficiency, and proper implementation by the operator. However, SPT remains a prevalent field method due to the extensive database of recorded testing (Bowles 1984).

SPT N-values have been related to several physical soil properties and directly tied to the analysis of foundations bearing capacity and settlement. Table 2.1 and Table 2.2 below provide example correlations between N-values and properties of cohesionless and cohesive soils.

Table 2.1 Correlations between SPT N-Values and Cohesionless Soil Properties

N-value	0-10	11-30	31-50	50+
State	Loose	Medium Dense	Dense	Very Dense
Unit Weight, $\gamma$ (pcf)	75-100	90-115	100-125	115-145
Unit Weight, $\gamma$ (kN/m <sup>3</sup> )	12-16	14-18	16-20	18-23
Friction Angle, $\Phi$ (degrees)	25-32	28-36	30-40	>35

Table 2.2 Correlations between SPT N-Values and Cohesive Soil Properties

N-value	0-4	4-6	6-15	16-25	25+
Consistency	Very Soft	Soft	Medium Stiff	Stiff	Stiff
Unit Weight, $\gamma$ (pcf)	90-115	100-115	100-115	100-125	>125
Unit Weight, $\gamma$ (kN/m <sup>3</sup> )	14-18	16-18	16-18	16-20	>20
Shear Strength, $q_u$ (psf)	<500	400-1,000	600-1,250	800-4,000	>2,000
Shear Strength, $q_u$ (kPa)	<25	20-50	30-60	40-200	>100

The method for performing Cone Penetration Testing (CPT) is described in ASTM standard D 5778, Standard Testing Method for Electronic Friction Cone and Piezocone Penetration Testing of Soils (American Society of Testing and Materials 2007). Unlike SPT, CPT does not require a pre-drilled borehole. A continuously pushed, transducer-equipped, cone into subgrade soils at a constant rate using specially equipped testing rigs. During the constant feed of the cone, transducers in the cone continuously collect resistance measurements at the tip of



the cone and along the perimeter surface of the cone (National Cooperative Highway Research Program 2007).

Cones with different instrumentation can be used in different testing applications. Depending on the application of the testing, the utilized cone can be equipped with various transducers or receivers. Piezocones, commonly used for CPT analysis, are equipped with a transducer capable of measuring fluctuations in soil pore water pressure. Seismocones or conductance cones are used to create one dimensional profiles depicting changes in shear wave velocity and soil conductance, respectively (National Cooperative Highway Research Program 2007).

Research has been focused on correlating various soil properties with results from CPT soundings. In addition to correlations with mechanical properties, correlations are available relating cone resistance values to generalized soil descriptions (National Cooperative Highway Research Program 2007).

CPT can be performed rapidly in the field and provides instantaneous and continuous feedback on tested soil profiles. However, the test method does not readily allow for sample retrieval, and without the use of heavy equipment or anchoring systems, CPT analysis is generally limited to softer subgrade profiles (National Cooperative Highway Research Program 2007).

#### *2.1.5 Laboratory Testing*

Laboratory testing is used to define various material properties, including index, mechanical, and chemical properties. Laboratory testing may also be used to assess soil shear strength properties of native or reconditioned soils. The assignment of tests is generally dictated by the complexity of the project and/or the complexity of the site.

In order to maintain consistency within the industry, it is considered prudent to use and follow standardized testing methods when performing laboratory activities. Standardized methods are researched and reviewed by specialized panels prior to publication and distribution

to the public. Entities such as the American Society of Testing and Materials (ASTM), American Association of State Highway and Transportation Officials (AASHTO), and Texas Department of Transportation (TxDOT) publish reference documents dictating acceptable means of performing, recording, and evaluating various laboratory testing methods. Table 2.3 provides a listing of common geotechnical laboratory testing methods, as referenced by ASTM (Day 2006).

Table 2.3 Common Geotechnical Laboratory Testing Methods (Day 2006)

Classification of Test	Description	ASTM Test Designation
Index Test	Moisture Content Specific Gravity Relative Density Atterberg Limit	D 2216 D 854 D 4253 D 4318
Particle Size Analysis	Sieve Analysis Hydrometer Test	D 422 D 422
Settlement Analysis	Consolidation Test	D 2435
Expansive Activity	Expansion Index Swell Test	D 4829 D 4546
Shear Strength	Direct Shear Test Unconfined Compressive Strength UU Triaxial Test CU Triaxial Test	D 3080 D 2166 D 2850 D 4767
Compaction	Standard Proctor Modified Proctor	D 698 D 1557
Permeability	Constant Head Test Falling Head Test	D 2434 D 5084

### 2.1.6 *Geophysical Testing*

For engineering applications, geophysical testing is used to assist in characterizing near-surface conditions. Near surface is generally considered to be depths less than one hundred feet or thirty meters (Butler 2005). Examples of applications include: study of lithology, evaluation of faulting and karst conditions, mapping of bedrock, determination groundwater elevations, determination of material layer thicknesses, location of construction materials, determination of seismic site classifications, and monitoring of dams or levee strength (Steeple 2001). The performance of geophysical testing can be performed either prior beginning an assessment, to improve sampling and testing efficiency by isolating and targeting observed conditions, or after the completion of a study, to verify results and conclusions. The selection of method is dictated by the objectives of the survey, required resolution, budget constraints and existing geologic and cultural conditions. Available geophysical methods of analysis include seismic, electrical, magnetic, and gravitational testing methods, of which testing methods can either be performed on from the surface or in downhole arrangements (Benson and Yuhr 1996).

Geophysical methods can be useful; however, the practitioner must be cognizant of the limitations related to a given geophysical method. Typical limitations include effects of natural cultural conditions on data acquisition and data interpretation, depth of penetration and non-unique interpretations (Benson and Yuhr 1996). The use of multiple methods can provide an enhanced understand of the site and/or the desired measureable property at a given site (Steeple 2001). For the purposes of this study, the discussion of geophysical testing methods will focus on the measurement and analysis of electrical resistivity and near surface seismic surface wave analysis.

## 2.2 Electrical Resistivity

Just as soil and rock materials have both physical and chemical properties; subsurface materials also present unique electrical characteristics. Practitioners in geologic, environmental, and engineering fields utilize electrical resistivity soundings and tomography to map fluctuations

in conductive behavior. Recent advancements in equipment and software have automated both data acquisition and processing, making electrical resistivity one of the most versatile methods for both the practicing geophysicist and engineering professionals (Steeple 2001).

### 2.2.1 Theoretical Background

The fundamental principle behind collection and interpretation of electrical resistivity measurements originates in the electrical physical theory of Ohm's Law. Ohm's Law, Equation 2.1, states that the product of the electrical current,  $I$ , through a conductor and the resistance of the conductor,  $R$ , for which the current passes, is equivalent to the potential difference,  $V$ , across the conductor.

$$V = IR \quad (2.1)$$

This relationship is best represented by envisioning current passing through a thin wire. The expounded application of the Ohm's Law has made this relationship a capstone concept in the study of electrical theory (Gibson and George 2003). Units for electrical potential, current, and resistance are volts, amperes, and ohms, respectively.

As suggested, the conductor element can tangibly be described as a wire element. The resistance of the wire is related to both the geometric shape and material attributes of the wire. The geometry of the wire is typically cylindrical, therefore possessing a length and cross-sectional area, and is made of a conductive material. The total resistance of the wire element,  $R$ , is the product of the material resistivity,  $\rho$ , and the ratio of the wire length and cross-sectional area.

$$R = \rho \left( \frac{L}{A} \right) \quad (2.2)$$

Considering the physical relationship between the geometry of the conductor and the material property, Equation 2.2 can be manipulated to determine the material resistivity of the conductor element.

$$\rho = R \left( \frac{L}{A} \right) \quad (2.3)$$

This form states that the units for resistivity are dependent on the volume of space for which the current travels. Typical units for resistivity,  $\rho$ , include ohm-meter and ohm-centimeter (Gibson and George 2003).

In similar context, the measurement of potential difference can be related to the dissipation of electrical current within an infinite, homogenous half-space. In this scenario, the application of an electrical current is travels in radial fashion out from the point of origin. During the current application, the resistance at any location away from the point of origin within the homogeneous mass can be found by determining the radius from the point of origin and the surface area of the respective hemispherical equipotential surface. Relating this model to the original wire example, Equation 2.2 can be rewritten using the radius,  $r$ , as the distance for which the current travels and the surface area of the resulting equipotential surface,  $2\pi r^2$ . Equation 2.4 describes the system resistance at any point away from the point source, within the homogeneous mass.

$$R = \rho \left( \frac{r}{2\pi r^2} \right) = \frac{\rho}{2\pi r} \quad (2.4)$$

Using the resistance term from the aforementioned homogeneous earth model, Equation 2.5 relates the resistance of the earthen model to Ohm's Law.

$$V = IR = I \left( \frac{\rho}{2\pi r} \right) \quad (2.5)$$

Likewise, the potential difference between any two points within the homogeneous mass would be the difference between the two equipotential surfaces, as expressed in Equation 2.6 (Gibson and George 2003).

$$\begin{aligned} V &= I \left[ \left( \frac{\rho}{2\pi r_1} \right) - \left( \frac{\rho}{2\pi r_2} \right) \right] = \left( \frac{I\rho}{2\pi} \right) \left[ \left( \frac{1}{r_1} \right) - \left( \frac{1}{r_2} \right) \right] \\ \therefore \rho &= \left( \frac{2\pi V}{I} \right) \left[ \frac{1}{\left( \frac{1}{r_1} \right) - \left( \frac{1}{r_2} \right)} \right] \end{aligned} \quad (2.6)$$

Equation 2.6 relates the applied current,  $I$ , and measured potential difference,  $V$ , to a constant value which accounts for spatial considerations, or the way in which the reading was acquired.

This model and concept of equipotential surfaces and means of measuring potential differences between various surfaces is fundamental to the interpretation of collected field data (Gibson and George 2003).

In a homogenous media, the measured resistivity will be equivalent to the true value of resistivity at a given location with the media. However, the occurrence of a homogenous condition is rare, if not non-existent in practice. In order to account for the inherent heterogeneity of the earth, a collected reading is considered an apparent resistivity measurement. Apparent resistivity is the resistivity of a theoretical, homogeneous half-space which complements the measured current and potential difference for a particular measurement scheme (United States Corps of Engineers 2001). Essentially, the apparent resistivity value is an average reading of the energized soil mass engaged during the measurement. Numerically, apparent resistivity can be expressed by Equation 2.7.

$$\rho_a = \left(\frac{V}{I}\right) G \quad (2.7)$$

The geometric coefficient,  $G$ , varies with array types. The spacing and layout of current and potential electrodes impacts the induced equipotential fields generated within the earthen mass (refer to Figure 2.2 through Figure 2.4 for Wenner, Schlumberger, and Dipole-Dipole arrays). Referencing Equation 2.6, the geometric factor for a general four probe system can be derived (Gibson and George 2003).

$$\rho_a = \left(\frac{V}{I}\right) \left\{ (2\pi) \left[ \frac{1}{\left(\frac{1}{r_1}\right) - \left(\frac{1}{r_2}\right) - \left(\frac{1}{r_3}\right) + \left(\frac{1}{r_4}\right)} \right] \right\} \quad (2.8)$$

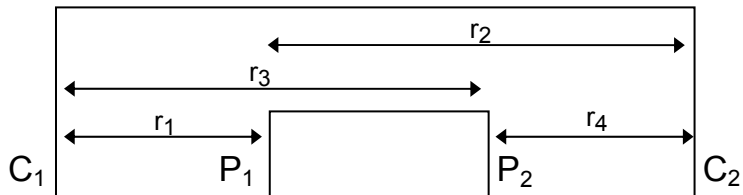


Figure 2.1 General Application of Ohm's Law for Derivation of Geometric Factor for Apparent Resistivity Measurement

Although apparent resistivity measurements are not equivalent to actual measurements of the earthen resistivity, readings are useful during final analysis to forward model and approximate “true” resistivity measurements (Advanced Geosciences, Incorporated 2009).

### 2.2.2 Natural Conditions Affecting Measurements of Resistivity

Electrical current flow is analogous to water flow, in that both travel along paths of least resistance (Greenhouse, Gudjurgis and Slaine 1998). The matrix of both soil and rock are composed of solid material and interstitial void space. Void spaces can be filled with air, water, or even organic contamination. With the exception of metallic ore, mineral bodies and clay particles, the solid fraction of the soil and rock matrices is relatively non-conductive. Therefore, the material porosity and degree of saturation play an intricate role in measureable resistivity. The primary mode of conduction through soil and rock is by current flow through electrolyte-laden pore water (Bryson 2005). As noted, current is not readily transferred through intra-particle contact. However, ionic properties of clay particles do provide a more conductive environment for current flow. Table 2.4 provides a compilation of documented ranges of measureable resistivity for various subsurface materials.

Table 2.4 Typical Values of Electrical Resistivity for Various Subsurface Materials (Advanced Geosciences Incorporated 2008, Gibson and George 2003, Loke 2000, Society of Exploration Geophysicist of Japan 2004, United States Corps of Engineers 2001)

Common Materials	Cited Resistivity Values (ohm-meters)				
	SEGJ	USOCE	Gibson	Loke	AGI
Clay	1-300	1-20	1-100	1-100	10-100
Sand	10-1,100	20-200	50-1,050	10-800	600-10,000
Gravel	20-7,000	----	100-1,400	600-10,000	600-10,000
Limestone	----	100-1 x 10 <sup>6</sup>	50-1 x 10 <sup>6</sup>	50-400	100-1 x 10 <sup>6</sup>
Shale	3-200	1-500	----	20-2,000	----
Sandstone	10-700	----	1-7.4 x 10 <sup>8</sup>	8-4,000	100-1,000
Granite	300-40,000	----	102-1 x 10 <sup>6</sup>	5,000-1 x 10 <sup>6</sup>	----

As noted, a wide range of values exist amongst similar materials; this is a demonstration as of how the condition and composition of a particular subsurface material provide significant variance from location to location. Also note that typical values often overlap one another, making interpretations of soil types difficult since different soil and/or rock types, possessing different degrees of saturation, may present as like materials.

### 2.2.3 Arrays

Theoretically, soil resistivity could be measured by using a single current source and receiver element. In practice, this is not feasible due to the contact resistance between the earth and the electrode pair. To overcome this phenomenon, four electrodes are used for measurement; two electrodes providing current to the earth and two electrodes for measuring potential difference within the earth (Milson 1996). Current electrodes are identified as C1 and C2 (or A and B), and potential electrodes are identified as P1 and P2 or (M and N) (Loke 2000). Figure 2.1 shows a generic representation of a four electrode array, denoting current and potential electrodes with C1, C2, P1 and P2 designations.

Considerable research and development has been done to find different four electrode configurations optimizing resistivity measurements for both vertical and lateral resolution, in different settings and applications. The most commonly used resistivity arrays are the Wenner, Schlumberger, and dipole-dipole arrays (Society of Exploration Geophysicist of Japan 2004). Other arrays include pole-pole, pole-dipole, Wenner-Schlumberger, and gradient arrays (Zonge, Wynn and Urquatt 2005).

#### 2.2.3.1 Wenner Array

The Wenner array is described by the equal spacing between all four electrodes. The two current electrodes, C1 and C2, are placed on the outside of the array, while the potential electrodes, P1 and P2, reside on the interior of the array. Potential difference measurements are taken at the mid span of the potential electrodes, at a depth approximately 0.5 to 1.0 times the



electrode spacing (also known as the “a” spacing). Different depth measurements are made by varying the interval spacing of the array.

In an idealized homogeneous earth model, the sensitivity pattern of the Wenner array provides a pattern with strong horizontal layering immediately below the potential electrode pair. Since the focus of vertical electrical sounding (VES) is to differentiate between horizontal layering beneath a common point, the Wenner Array is a practical array for this application. The strong signal of the Wenner Array also makes the array suitable for use in more noisy environments. (Loke 2000, Society of Exploration Geophysicist of Japan 2004).

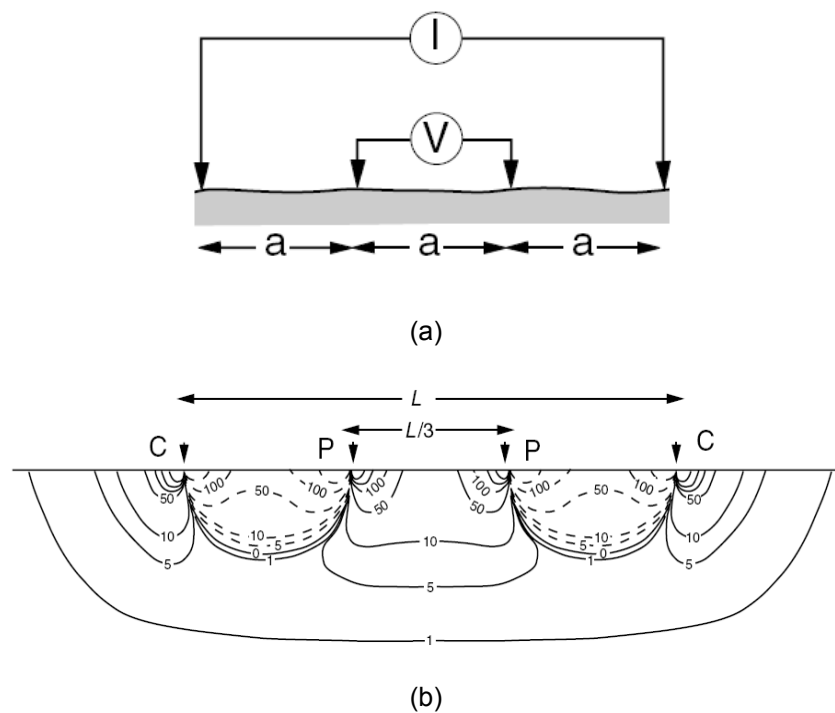


Figure 2.2 Wenner Array (a) Layout and (b) Sensitivity Pattern (Milson 1996)

For the Wenner Array, the apparent resistivity measurement can be represented by Equation 2.9 (Society of Exploration Geophysicist of Japan 2004).

$$\rho_a = (2\pi a) \frac{V}{I} \quad (2.9)$$

### 2.2.3.2 Schlumberger Array

The Schlumberger array is arranged with two current electrodes on the outside of the array, set apart by a distance at least five times the spacing between the two interior potential electrodes. The potential difference measurement is believed to lie at the mid span of the interior potential electrodes, at a depth approximately one half of the length between the exterior current electrodes. Similar to the Wenner array, the Schlumberger array provides a strong signal immediately below the potential electrode pair. The Schlumberger Array is preferred for VES applications due to the strong horizontal resolution and ease of setup in the field. As compared with the Wenner array, where all four electrodes must be repositioned after each test, the Schlumberger array only requires that the exterior two current electrodes be moved to acquire a new measurement. The interior potential electrodes are moved only as the current electrodes are spaced beyond the practical limits of the survey, which occurs when the ratio between the potential electrode spacing and the distance between the exterior current electrode and the mid span of the potential electrodes is greater than 0.4 (United States Corps of Engineers 1995). The apparent resistivity measurement for the Schlumberger Array can be represented Equation 2.10.

$$\rho_a = \left[ \frac{\pi(L^2 - l^2)}{2l} \right] \frac{V}{I} \quad (2.10)$$

In Equation 2.10, the spread length or distance between current electrodes is  $L$ , and the length between the potential electrodes is expressed by the variable  $l$ . As mentioned previously, the Schlumberger Array is valid through a certain range of spacing. With respect to  $L$  and  $l$ , the apparent resistivity measurement is valid as long as the spread length,  $L$ , does not exceed 5 times the potential electrode spacing,  $l$  (Society of Exploration Geophysicist of Japan 2004).

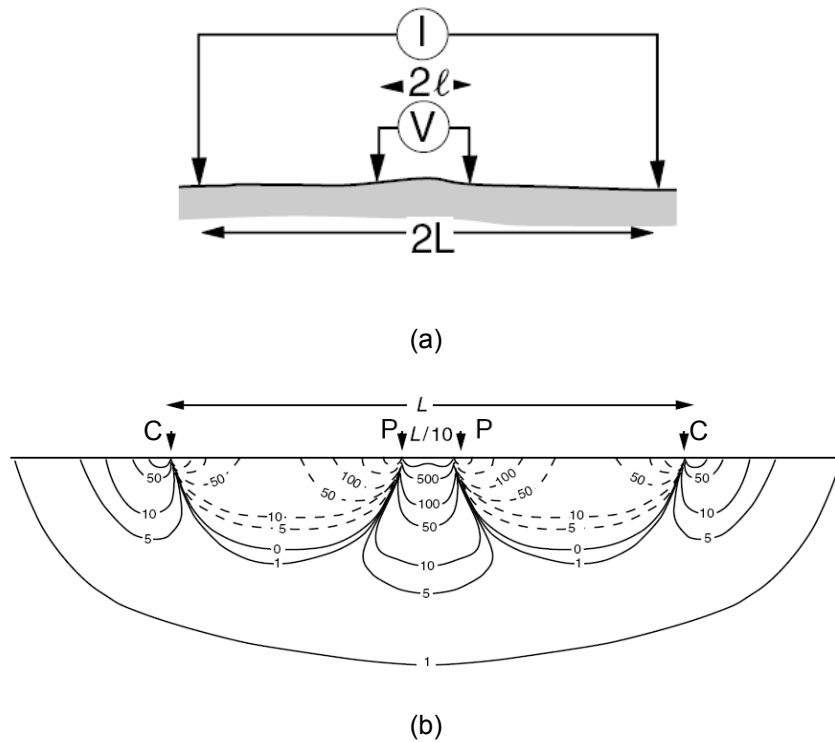


Figure 2.3 Schlumberger Array (a) Layout and (b) Sensitivity Pattern (Milson 1996)

### 2.2.3.3 Dipole-Dipole Array

Unlike the Wenner and Schlumberger arrays, the configuration of the dipole-dipole array does not place the potential electrode pair inside the current electrode pair. Current and potential electrode pairs have common interior spacing, and separated by a distance ten times the interior spacing of the electrode pair. The dipole-dipole array is commonly used for performing tomography surveying due to the array's ability to resolve lateral variations. In comparison to the Wenner and Schlumberger arrays, the dipole-dipole array has a weaker signal and is more susceptible to the effects of ambient or cultural noise. The apparent resistivity reading recorded using the dipole-dipole array represents a condition present at the mid span of the array length, at a depth equivalent to one half the product of the dipole electrode spacing,  $a$ , and one plus the separation factor  $(n+1)$ .

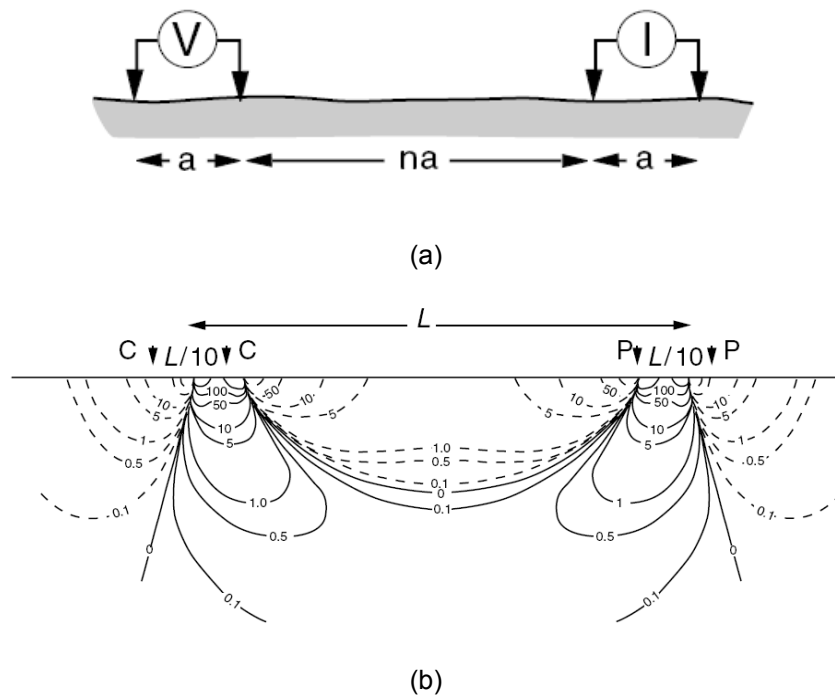


Figure 2.4 Dipole-Dipole Array (a) Layout and (b) Sensitivity Pattern (Milson 1996)

The apparent resistivity measurement for the dipole-dipole array can be represented by Equation 2.11.

$$\rho_a = \pi a [n(n+1)(n+2)] \frac{V}{I} \quad (2.11)$$

#### 2.2.4 Electrical Resistivity Testing Methods

Electrical resistivity testing represents a broad category of geophysical testing, including measurements of spontaneous potential, induced polarization, and apparent resistivity measurements. Spontaneous potential (SP) is a method designed to measure variations in conductive behavior occurring without introducing an auxiliary current source. Flow behavior, such as ionic, thermal or fluid flow, can cause a measureable SP signal. Induced polarization is a method measuring the time-rate decay of polarizing effects resulting from the induced current.

This method is effective in delineating contaminant plumes and mineral ore bodies, which often present with unique decay signatures when compared against other ambient conditions (Gibson and George 2003).

The most utilized method for engineering applications is the measurement of apparent resistivity. Apparent resistivity can be analyzed in either by vertical sounding, two dimensional profile, three dimensional model, or time variant analysis (Gibson and George 2003).

#### 2.2.4.1 One Dimensional Electrical Resistivity Surveying

One-dimensional resistivity surveys, or vertical resistivity soundings (VES), are used to define horizontal layering, vertically below a single location. Point readings are collected by using a four probe array, such as the Wenner or Schlumberger array. The variation in probe spacing affects the equipotential fields produced by the current electrode; therefore, as the probe spacing increases, more earthen mass is engaged in the reading and deeper measurements are made. Therefore, deeper readings of potential difference can be evaluated. However, signal strength diminishes as probe spacing increases. VES surveys are generally conducted at the surface using a four electrode array; however, advancements in cone penetration testing methods now allows for vertical profiles to be generated using conductive cone attachments and data processors (National Cooperative Highway Research Program 2007).

#### 2.2.4.2 Two Dimensional Electrical Resistivity Surveying

Two-dimensional surveying, or electrical resistivity tomography (ERT) surveying, is performed by measuring fluctuations in both the vertical and lateral planes. During this type of survey, readings are assumed to lie within a single, vertical plane. Two dimensional surveys are generally performed at the surface; however, readings may also be collected using downhole or surface to borehole methods of measurement. For surface measurements, the dipole-dipole array is preferred due to the array's sensitivity in both lateral and vertical directions, as well as the versatility of the array setup and progression when used with multi-channel equipment transmitters and receivers (Advanced Geosciences, Incorporated 2009).

#### 2.2.4.3 Three Dimensional Electrical Resistivity Surveying

During a three-dimensional survey, measurements of potential difference are made in all three spatial coordinate planes. This allows for the analysis of a target volume, as opposed to planar section. Three-dimensional surveys may either be performed along the surface, using crosshole methods, or using surface to borehole measurements. Analytical software now allows for the compilation of multiple two-dimensional survey data, into a three-dimensional representation (Advanced Geosciences Incorporated 2008).

#### 2.2.4.4 Time Variant Resistivity Measurements

Fluctuations in conductive behavior over time can be resolved by analyzing multiple resistivity records. This application used in plume delineation to assess the time rate and direction of migrating trace contaminants or fluid travel can be monitored over time to evaluate rates of travel. The time component of this measurement can be applied to either one, two or three dimensional surveys (Gibson and George 2003).

#### 2.2.5 *Equipment*

The basic setup required for field measurements includes a transmitter, receiver, conductive cables, a set of electrodes and a power source (United States Corps of Engineers 1995).

##### 2.2.5.1 Transmitter/Receiver

The function of the transmitter is to apply and regulate a known current through the instrumentation, to the earth. To acquire the desired survey penetration and resolution, it is important that the chosen transmitter is capable of emitting ample current through the system. Previous instrumentation required manual current adjustments until applicable readings were made. However, with advancements in technology, newer transmitters are capable of self-regulating current flow to promote the best possible signal for data acquisition. In addition, various instruments are now capable of conveying larger currents, also improving signal strength and resolution. Advanced Geosciences, Incorporated (AGI) produces three different automated

units, with maximum current outputs ranging from 500 milliamps to 2,000 milliamps. The most recent development by AGI is a system capable of transmitting a current up to 27 amps. (Advanced Geosciences, Incorporated 2009).

As the transmitter applies a known current, a receiver is needed to measure the resulting potential reading. Newer instrument, equipped with digital processing capabilities, are capable of sending the required current, as well as measuring and receiving the respective potential difference measurement. The sensitivity of the receiver should be established prior to initiating a survey to ensure that goals of the survey are met (Advanced Geosciences Incorporated 2008).

Single channel transmitters/receivers are only capable of collecting one reading at a time. Although single channel instruments are still in use for VES surveys, two and three dimensional surveys are optimized by multi-channel systems allowing for the acquisition of multiple readings in a single current output (Advanced Geosciences Incorporated 2008).

#### 2.2.5.2 Cables

Metallic cables are used to convey current from the transmitter and to return measurements of difference to the receiver. The use of highly conductive metallic material, such as copper, helps minimize losses during data acquisition. Depending on the transmitter/receiver system utilized, the cables are either composed of a single wire strand, or a core housing multiple strands accommodating each of the available channels. Cables are needed for connecting the transmitter/receiver with the potential electrodes (Advanced Geosciences Incorporated 2008).

#### 2.2.5.3 Current and Potential Electrodes

Electrodes are used by the transmitter to transfer current to the subgrade, and by the receiver to detect fluctuations in electrical potential. For general use, steel, copper or bronze stakes are common. For applications requiring refined measurements, readings taken in noisy environments or areas with high contact resistance, using electrodes with of ceramic components emitting a metallic aqueous solution, such as copper sulfate, is a viable alternative. Sufficient bedding of electrodes is required in order to couple the resistivity setup with the earth. As noted,

surface conditions with high contact resistance can be overcome by using ceramic electrodes with a metallic aqueous solution, or, if using metallic stakes, by placing a saline solution around the base of the electrode (Advanced Geosciences Incorporated 2008).

When using a direct current for testing purposes, there is a potential that the charges on the exterior of the electrode will take on a common charge over the surface of the electrode, effectively polarizing the electrode, if the current is applied in one direction for an extended period of time. In order to prevent polarization, most modern instruments routinely reverse signals to reverse potential charge buildups (United States Corps of Engineers 1995).

#### 2.2.5.4 Power Source

The transmitter requires a power source in order to pull a current for the data acquisition system. Required power sources vary by instrument, and range from internal rechargeable batteries to external generator power sources. For newer instruments, due to the low power emission required and short duration of discharge, dry cell batteries can be used for this application. Dry cell batteries are preferred because the ability to drain and recharge the battery without damaging the core (Advanced Geosciences Incorporated 2008).

#### 2.2.6 Data Acquisition

Previous single channel instruments required that electrodes be reconfigured after each measurement. For ERT applications, this methodology is time consuming and laborious. Newer instruments are equipped with multiple channels, which allows for multiple electrodes to be engaged and measurement to be taken through each channel. For instance, the SuperSting R8 resistivity meter, produced by Advanced Geosciences, Incorporated, is equipped with eight channels. Therefore, for each current injection, the system engages nine electrodes to collect eight different potential difference measurements (Advanced Geosciences, Incorporated 2006). Unlike the single channel transmitter, multiple channel equipment has to receive instruction on the proper triggering sequence of electrodes. This information can either be programmed directly into the instrument through manual entry, or indirectly by uploading coded command file. The

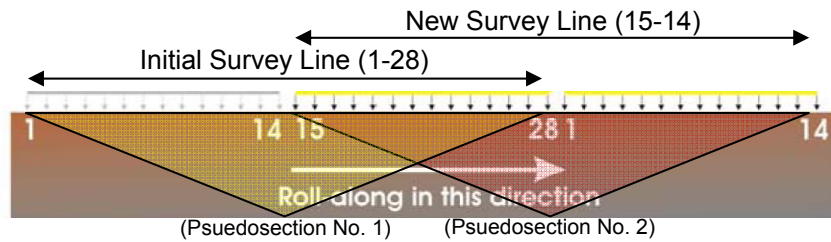


sequencing information considers the array style and information pertaining to the electrode locations or electrode address during each measuring sequence.

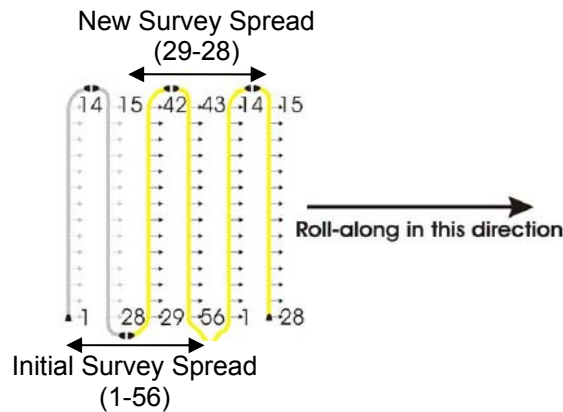
There are no theoretical limits to the depth of penetration. However, as the electrode spacing increases signal strength decreases. At a certain electrode separation distance, the signal strength is too low to provide reliable measurements of potential difference. Practical limits should be instilled considering the signal strength of the particular array type and equipment capabilities. When considering depth of penetration for tomography applications, practitioners can generally assume that the depth of penetration is approximately 15 to 25 percent of the length of the electrode spread (Advanced Geosciences Incorporated 2008). Survey resolution is also related to electrode spacing. Current practices suggest that the electrode spacing not be greater than twice the size of the object or feature to be imaged. The design of the survey (i.e. survey run length, electrode spacing, and array type) directly impacts the depth of penetration and resolution (Advanced Geosciences Incorporated 2008).

It is not always possible or practical to image a survey line or area in one deployment of electrodes. To continue a survey after completion of the initial data collection, electrodes may be configured to collect additional data along a common survey line or area, using roll-along survey techniques. Figure 2.5 shows examples of both two- and three- dimensional roll along patterns. As shown, a segment of electrodes is detached from the original survey line and relocated to the end of the cable system, effectively advancing the survey along the desired imaging path. Since the entire line is not advanced at once, not all readings in the next data acquisition will be new readings. This is demonstrated in Figure 2.5 (a) by the overlapping triangular patterns which represent the respective field of data points, or pseudosection, generated during each survey. Depending on the instrument and survey design, these readings may either be repeated providing redundancy to the survey, or disregarded after acknowledging that measurements of the same area have already been made. It is evident that by advancing multiple cables, the amount of data overlap is reduced and more of the survey can be performed with fewer

movements. However, a decrease in data overlap will subsequently increase the void left below the two overlapping pseudosections (Advanced Geosciences Incorporated 2008).



(a)



(b)

Figure 2.5 Example of a Roll-Along for (a) Two-Dimensional Tomography Survey and (b) Three-Dimensional Survey (Advanced Geosciences, Incorporated 2006)

### 2.2.7 Data Interpretation

Field measurements must be converted into a visual representation for analysis purposes. Referring to Equation 2.7, calculation of apparent resistivity requires a geometric factor. Measurements taken from the field provide readings of induced current and respective potential difference, so by coordinating field data with respective electrode coordinates and known array type, the geometric factor can be determined and apparent resistivity is calculated. In addition, recorded field measurements are assigned a coordinate location, which correlate to the array type used and electrode spacing at the time of the potential difference reading. As

mentioned, the mapping of apparent resistivity values creates a profile termed a pseudosection. (Milson 1996, Loke 2000, Gibson and George 2003). Pseudosections provide a crude representation of the environment surveyed. Attempting an interpretation from a pseudosection can be difficult, but was a common practice before the development of analytical software (Zonge, Wynn and Urquatt 2005). Pseudosections are not unique to the measured subsurface, and can vary depending on the array type used (Advanced Geosciences, Incorporated 2009). Pseudosections provide a crude representation of the resistive environment surveyed, and attempting an interpretation from a pseudosection can be misleading (Zonge, Wynn and Urquatt 2005).

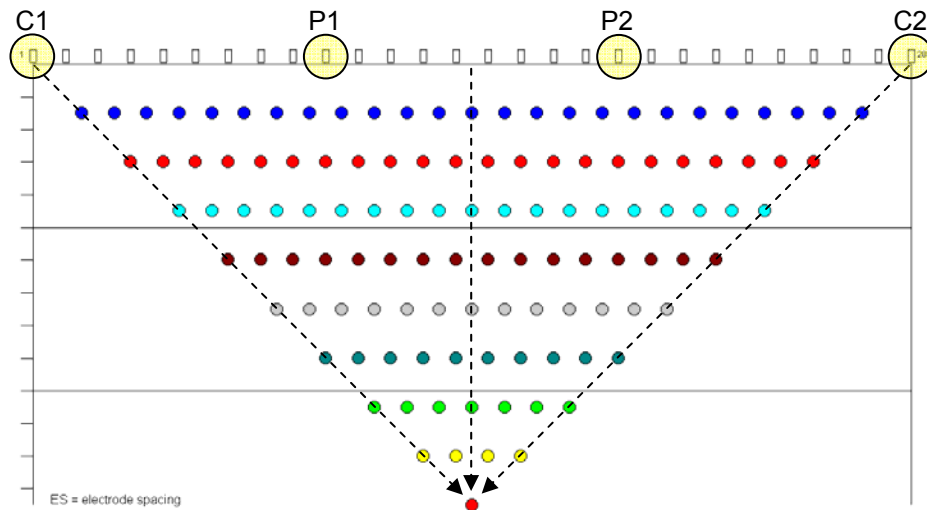


Figure 2.6 Example of Developed Pseudosection Model Using a Wenner Array and 28 Electrodes

Although the “true” point measurements is unattainable using surface survey methods, apparent values can be effectively used to estimate “true” subsurface conditions. Apparent resistivity pseudosections provide the necessary data to complete an iterative inversion process. The purpose of the inversion is to produce a matching or representative earth model which would produce a like pseudosection. Iterations continue until the modeled pseudosection approaches convergence with the measured pseudosection. Currently there are no means of directly

correlating apparent resistivity measurements to an earthen model (Zonge, Wynn and Urquatt 2005). Figure 2.7 provides a generalized flow chart demonstrating the typical processes required to complete the inversion process. The convergence criterion is usually a predetermined tolerance for calculated error between the measured and modeled resistivity. Statistical analysis of data (e.g. root mean square error analysis, L2 normalization) is used gauge the refinement of the final model. Smoothing algorithms are also used to eliminate or lessening the impact of data points not conforming to the trends of the model (Advanced Geosciences, Incorporated 2009, Zonge, Wynn and Urquatt 2005). The inversion process is best performed using numerical analysis software due to the quantity of data involved and iterative processes. Software packages such as RES2DINV, RES3DINV and EarthImager 1D, 2D, and 3D are examples of products available for inversion processing and inversion (Advanced Geosciences Incorporated 2008, 2009, Loke 2000).

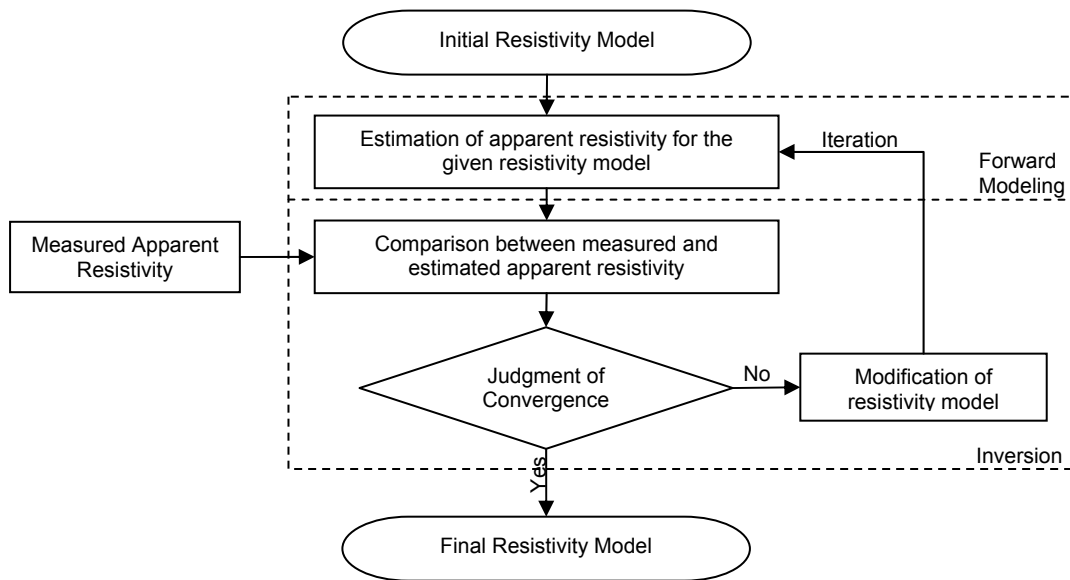


Figure 2.7 Flow Chart of Resistivity Inversion Processing (Society of Exploration Geophysicist of Japan 2004)

In survey situations with significant variations in terrain, estimated resistivity measurements may mask subsurface features if site topography is not considered (Zonge, Wynn and Urquatt 2005). The effects of topographic changes on generated tomography images can be resolved during the inversion process (Advanced Geosciences Incorporated 2008).

### 2.3 Multichannel Analysis of Surface Waves (MASW)

The measurement of shear wave velocity is beneficial for analyzing variations in subsurface stiffness (Park et al. 2003). Small strain parameters of subsurface materials can be studied by evaluating change in stress. Multichannel analysis of surface waves (MASW) is a non-destructive seismic method which analyzes the dispersion properties of horizontal traveling Rayleigh surface waves (Park et al. 2003). The following commentary provides a discussion of wave theory, description of seismic wave types and background information pertaining to MASW theory and analysis.

#### 2.3.1 *Seismic Wave Theory*

##### 2.3.1.1 Physical Background

Seismic theory is dependent on the idea that elastic waves travel at speeds which correlate with the physical properties the respective media (Parasnis 1997). Recognizing this requires an initial physical understanding of material elastic behavior and wave velocity.

Hooke's law states that the strain,  $\epsilon$ , experienced by an object is directly related to the imposed stress,  $\sigma$ , on that given object. When no permanent deformation is experienced, the elastic material property that directly correlates strain to stress is termed the elastic modulus,  $E$ . (Callister Jr. 2001).

$$\sigma = \epsilon E \quad (2.12)$$

Wave propagation is dependent on the ability to elastically deform particles within a given media. The propagation of different wave types is caused by the different forms of stress imposed (e.g. compressive stress, shearing stress). In different situations, the applicability of the small strain assumption has been questioned and other models relating stress and strain have been applied

to seismic analysis. However, the principle of Hooke's law remains one of the prominent models for elasticity in seismic theory (Parasnis 1997).

The wave velocity,  $v$ , is directly related to the frequency of the wave,  $f$ , and the length of the wave,  $\lambda$ , as shown in Equation 2.13.

$$v = f\lambda \quad (2.13)$$

The wavelength is the distance between two consecutive wave peaks or troughs. The frequency of a wave is the reciprocal of the wave period,  $T$ , which is the duration required to complete one wave oscillation.

$$f = \frac{1}{T} \quad (2.14)$$

Although basic in concept, the understanding of the basic wave relationships is beneficial when evaluating and interpreting seismic wave activity (Steeple 1998).

#### 2.3.1.2 Wave Types

Seismic waves are grouped as either body waves or surface waves (Steeple 1998). Body waves are non-dispersive and travel through a given media at a speed proportional to the material density and modulus. Body waves can either travel longitudinal or transverse to the direction of the traveling wave. Longitudinal movements are called P-waves or compression waves, and the transverse movements are called S-waves or shear waves. P-waves transfer energy through media by compressing and dilating particles as the wave passes through the media. In S-wave propagation, particles move perpendicular to the direction of wave movement. In a homogeneous environment, the velocity of a body can be expressed by the general equation provided below.

$$v = \sqrt{\left(\frac{\text{material elastic modulus}}{\text{material density, } \rho}\right)} \quad (2.15)$$

For P-waves, the material elastic modulus is related to both the bulk modulus,  $K$ , and shear modulus,  $\mu$ . However, for S-waves, the material modulus is only related to the shear modulus (Kearey, Brooks and Hill 2002). P-waves transmit faster than S-waves, and S-waves do not

propagate through liquids or gases (Parasnis 1997). The direct measurement of P- and S- waves can be used to calculate soil properties such as Poisson's ratio and bulk and shear moduli (Kearey, Brooks and Hill 2002).

Surface waves are waves that travel along free surfaces or along the boundary of dissimilar materials (Kearey, Brooks and Hill 2002). Surface waves represent the strongest portion of the signal received during a seismic survey. It is estimated that over 70 percent of the received signal during a given shot is attributed to the arrival of surface waves (Ivanov, Park and Xia 2009). For this reason, the reception of surface waves has long since been thought of noise during the performance of body wave surveys (Parasnis 1997).

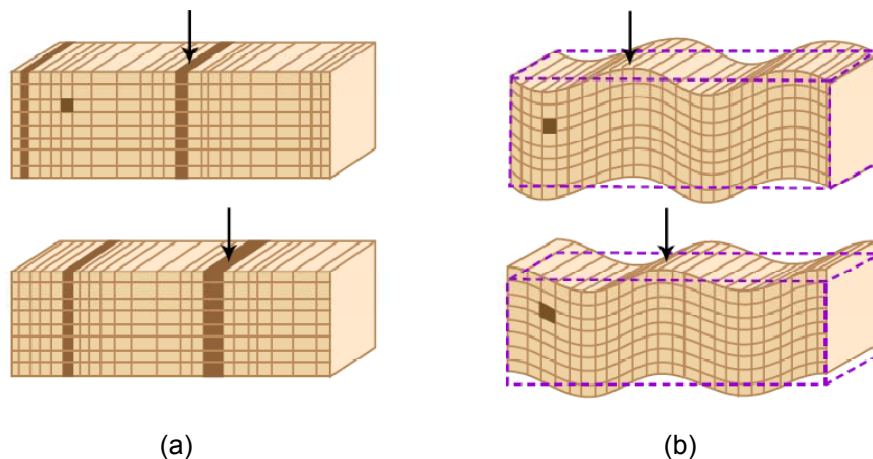


Figure 2.8 Translational Behavior of (a) P-waves and (b) S-waves (Van Der Hilst 2004)

The two main types of surface waves are Love Waves and Rayleigh Waves. Love waves are a form of polarized shear wave, which travels parallel to the free surface and perpendicular to the direction of the wave (Kearey, Brooks and Hill 2002). Love waves are observed in a multilayer media, when the shear wave velocity of the top layer is less than that of the lower layer (Parasnis 1997). Rayleigh waves move perpendicular to the surface, while traveling along the wave path. The shape of the Rayleigh waveform is described as a retrograde, elliptical motion. The retrograde elliptical motion can be compared to the observable path of a cork present in a

gentle wave motion of a pond or lake. The respective Love and Rayleigh waveforms are also termed ground roll, as these are the waves (or rolling feeling) which might be felt in an explosion or seismic event (Steeple, 1998, United States Corps of Engineers 1995).

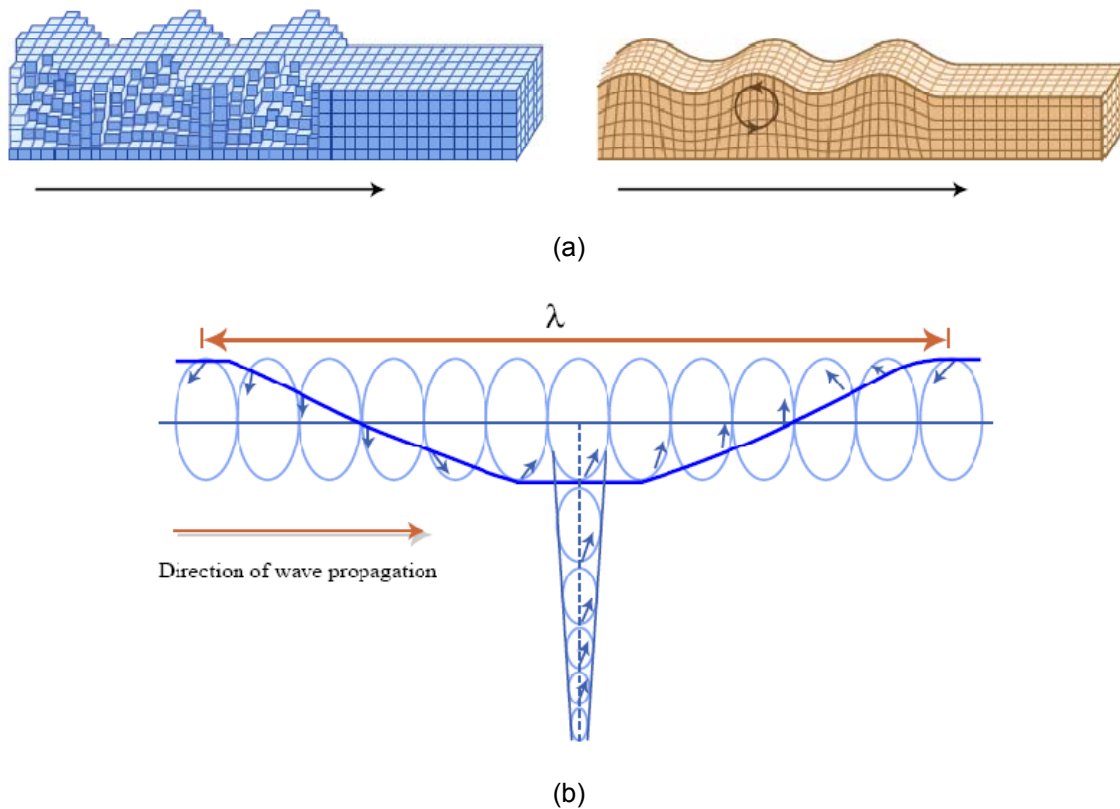


Figure 2.9 (a) Love and Rayleigh Wave Propagation and (b) Retrograde, Elliptical Particle Motion of Rayleigh Wave Propagation (Van Der Hilst 2004)

Surface waves are inherently dispersive, meaning that the amplitude of the surface wave decreases with depth and with distance away from the source. Given the dispersive characteristics, it is understood that surface waves travel exclusively within near-surface soils. This depth is estimated to be within approximately one surface wavelength from of the Earth's surface (Steeple 1998).



The velocity of Rayleigh Waves are comparable to shear waves velocities. In a rock formation with a Poisson's Ratio of approximately 0.25, the velocity of the Rayleigh wave is approximately 92 percent of the velocity of shear wave. In materials with ratios from 0.4 to 0.5, the percentage increases to 94 to 95.5 percent, respectively (Steeple 1998). As a general rule, velocity of Rayleigh waves are assumed to be approximately 90 to 92 percent of the respective shear wave (Ivanov, Park and Xia 2009, Parasnis 1997). The estimation of shear wave velocity can be made within a ten percent margin of error using these assumptions (United States Corps of Engineers 1995).

Surface waves travel in modes, analogous to harmonic modes of a stringed musical instrument. The modes consist of a fundamental mode, and numerous higher modes. In a study performed by Rix, the fundamental mode carried up to 87 percent of the wave energy through a frequency of 50 hertz; therefore it was concluded that the higher modes of the Rayleigh wave could be neglected without a significant impact to the interpretation (Steeple 1998).

#### 2.3.1.3 Methods of Surface Wave Analysis

Until the late 1980s and early 1990s, surface wave artifacts in a shot record were deemed a nuisance in body wave surveys (Parasnis 1997). Researchers discovered that, when properly acquired and analyzed, the evaluation of surface wave behavior provided beneficial information related to near-surface stiffness parameters. In 1994, Dr. Kenneth Stokoe published a document describing the applications of a surface wave analysis technique called the Spectral Analysis of Surface Waves (SASW) (Steeple 1998). In order for the method to derive a representative earth model from surface wave measurements, the method needed the capability of assessing the relationship between surface wave velocity and frequency, and the ability derive an earthen model based on the dispersive properties of the measured surface wave (United States Corps of Engineers 1995). Measurements are carried out at the surface, using a swept-frequency source and at least two receivers, or geophones. The swept-frequency source provides a known frequency for the velocity calculation. Received signals are used determine the

phase difference for each frequency. Travel time is represented in Equation 2.16, where the frequency,  $f$ , is represented in hertz and the phase difference,  $\phi(f)$ , is in radians.

$$t(f) = \left[ \frac{\phi(f)}{(2\pi f)} \right] \quad (2.16)$$

The wave velocity,  $V$ , can then be measured by relating the known distance between the receiver spread and travel time, as seen in Equation 2.17.

$$V = \left[ \frac{d_2 - d_1}{t(f)} \right] \quad (2.17)$$

The velocity is then used to determine the wavelength of the respective Rayleigh wave, using the general wave relationship presented in Equation 2.13. Multiple measurements of phase velocity and wavelength are made by reconfiguring the receiver spread and/or varying the transmitted frequency. The relationship between phase velocity and wave length is then plotted to develop a surface wave dispersion curve. Through an inversion process, the dispersion curve can be transformed into a representative earth model relating shear wave velocity with depth (Steeple 1998).

The SASW method has been successfully used in geotechnical site characterization and pavement analysis applications. However, issues have been identified with the practice. The SASW data acquisition process is labor intensive and time consuming (Park, et al. 2000). The method assumes horizontal layering from the location of the source to the recording point, and that only the fundamental mode of the Rayleigh wave is recorded. In practice these assumptions may not be accurate. In addition, a complex geology present within the spread of the receivers may also complicate measurements as the receiver spread is varied. Further, high frequencies can be difficult to produce and record; therefore resolution of shallow features may be difficult (United States Corps of Engineers 1995).

The Multichannel Analysis of Surface Waves (MASW) was developed in an effort to address the issues related to the SASW method and improve the overall quality of surface wave analysis (Park et al. 2003). Fundamentally, the objectives of the MASW method are similar to

that of the SASW. The differences between the two methods are primarily related to the physical representation and actual means of data acquisition. Rather than a single pair of receivers used during SASW, the MASW uses 12 or more receivers for recording purposes. The multiple receiver spread allows for data acquisition over a larger area, adds redundancy to the measurement, and provides a means of efficient and continuous data acquisition (Park et al. 2000). The multiple receiver spread improves modal separation. Receivers are generally deployed in a linear array pattern, which is maintained through the course of the survey. With an increased efficiency in both the data acquisition and interpretation, analysis tools are now capable of converting one-dimensional shear wave profiles into two-dimensional shear wave profiles (Ivanov, Park and Xia 2009).

### 2.3.2 *Performance of MASW Testing*

Evaluations using MASW can be completed in three general steps. First, the multiple seismic records must be recorded during field testing. Secondly, each seismic record is processed and inverted into individual one dimensional shear wave profiles. If desired, the process could end after generating a one dimensional profile, similar to that accomplished with the SASW method. However, with the efficiency of the MASW method, multiple shot records are acquired rapidly, thus providing multiple one-dimensional profiles along a common survey line. The final step involves combining individual profiles, through interpolation, into a single tomography image representing subsurface shear wave characteristics (Ivanov, Park and Xia 2009). A visual representation of the procedure is provided in Appendix A.

#### 2.3.2.1 Equipment

Equipment required to conduct MASW analyses is comprised of five elements: a seismic source, a triggering device, receivers, transmitting cables and a multichannel seismograph.

##### 2.3.2.1.1 Seismic Source

A seismic source is used to transfer energy to the ground for the purposes of inducing seismic wave activity. In practice, a source can be an impact force applied to the ground by a

hammer or falling weight, a small scale explosion detonated within the subsurface, or a mechanical vibratory device. A sledgehammer with either a metallic or stiff rubber strike plate provides an inexpensive and easily transferrable impact source. However, for surveys requiring a higher degree of energy transfer, a falling weight may also be used to provide an impact source. Explosive sources such as downhole gun fire or explosives used during quarry operations are less frequently used due to expense and safety; however, given the application explosive sources can provide strong surface wave signals for data acquisition. Swept frequency sources provide a signal with a constant frequency. The selection of a seismic source should be based on the signal requirements of the survey, cost and relative safety (Kearey, Brooks and Hill 2002). For most shallow surface evaluations, the use of a sledgehammer and striker plate provides an adequate seismic signal (Ivanov, Park and Xia 2009).

#### 2.3.2.1.2 Trigger Mechanism

The triggering mechanism is needed to signal the seismography and synchronize the time with the arrival of the transmitted surface wave. For impact sources, such as a sledgehammer or drop weight, an open circuit mechanism is attached to the source, which closes at the moment of contact. An example of a simple triggering system attached to a sledgehammer is provided in Figure 2.10. In an ideal situation, the trigger would provide an instantaneous signal marking the initiation of the survey (Milson 1996). However, in practice it is understood that there is a small lag in between the actual strike event and the time for which the signal is transmitted to the seismography that the strike event has occurred. Lag time can be predetermined for a particular trigger instrument and subsequently programmed into seismograph use during data acquisition (Geometrics Incorporated 2003).

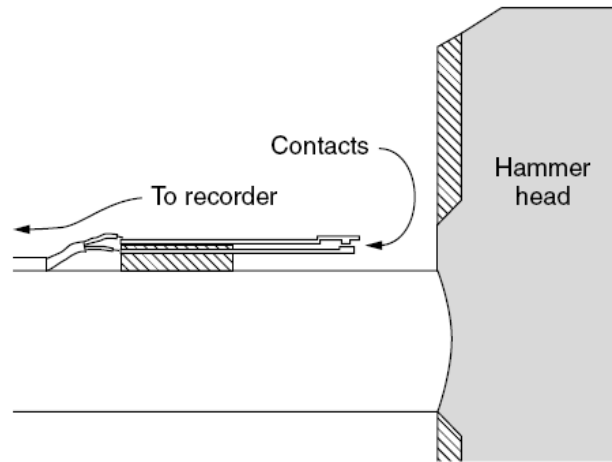


Figure 2.10 Example of Sledgehammer Triggering Device (Milson 1996)

#### 2.3.2.1.3 Geophones

Receivers, or geophones, are electromechanical transducers that convert ground motion into an electrical analog signal (Pelton 2005). The current, or signal, produced is proportional to the velocity of the oscillating coil system through the internal magnetic core (Milson 1996). The movement of the internal core is relative to the ground movement below the geophone, as the seismic wave(s) pass the respective receiver (Kearey, Brooks and Hill 2002). Figure 2.11 provides an example of the configuration of a spike-coupled geophone. Geophones with single, vertical axis of vibration are commonly used to measure incoming signals immediately below the receiver. Other geophones with horizontal or multiple axis capabilities are available, but are not commonly used for MASW applications (United States Corps of Engineers 1995).

The geophone must be well coupled with the earth. Steel spikes are typically used for bedding geophones; however, in some applications the use of steel plates has proven to be comparable to the use of steel spikes. Advancements in receiver deployment have led to towable instruments such as the LandStreamer, which uses a weighted geophones and cable system equipped with robust steel plates for coupling. For MASW applications, lower frequency

receivers (e.g. 2 Hz, 4.5 Hz) provide better performance due to the ability to capture deeper transmitted signals (Ivanov, Park and Xia 2009).

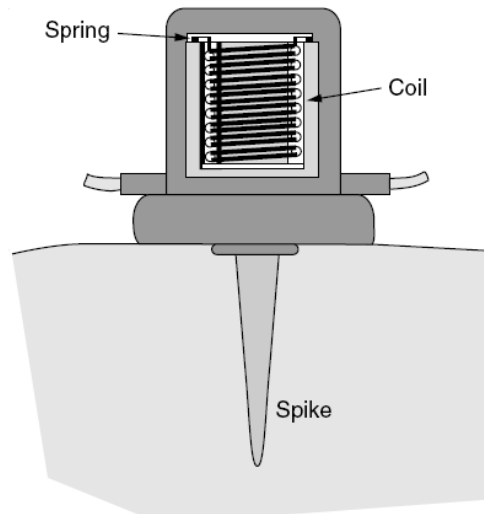


Figure 2.11 Example of Spike-coupled Geophone (Milson 1996)

#### 2.3.2.1.4 Geophone Cable

Analog electrical impulses are transmitted from the individual geophones to the seismograph through a cable system. The cable is metallic and transmits the signal with little resistance; however, due to the potential for “cross-talk” between the geophone cable and the trigger switch, consideration should be given during data acquisition to maintaining a sufficient distance between the two elements (Milson 1996).

#### 2.3.2.1.5 Seismograph

Seismographs are used to record and interpret the transmitted signal from the geophone into a discernable trace or shot record. Seismographs can range in complexity from simple timing instruments to microcomputers capable of digitizing, storing and displaying received shot records. Multichannel seismographs allow for the acquisition of multiple independent readings. Systems

with 24 channels are common in shallow surface investigations; however, deeper applications may utilize a greater number of channels (Milson 1996).

### 2.3.2.2 Field Survey Setup

Field setup for data acquisition is similar to that of the common midpoint reflection survey. Figure 2.13 is an exhibit showing the typical linear layout and the progressive movement of a survey during a profiling application (Ivanov, Park and Xia 2009). Consideration should be given to the geophone interval spacing, as an increased length will improve depth and modal separation but will also increase the amount of spatial averaging of data during processing (Park 2005).

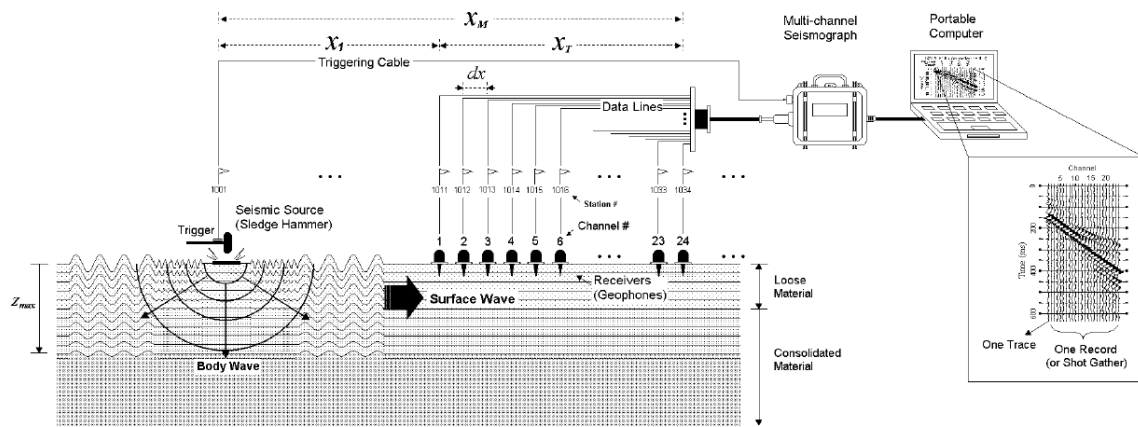
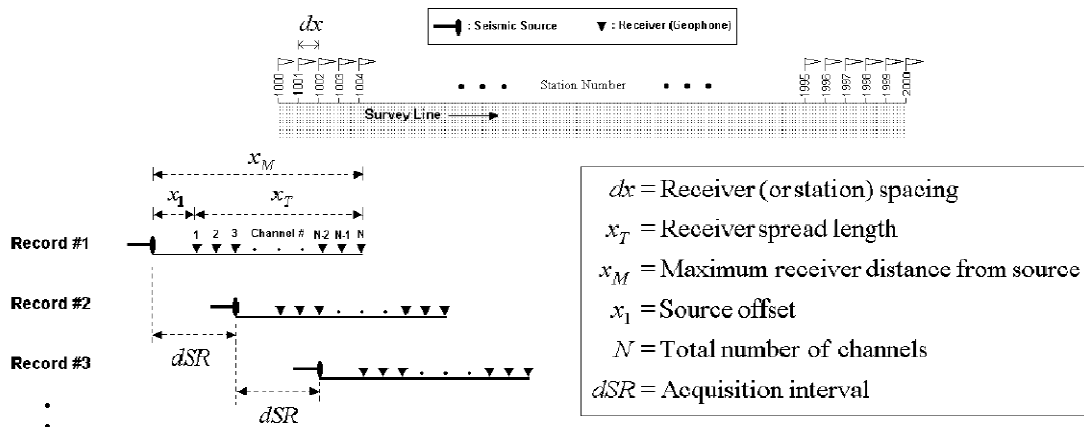


Figure 2.12 Instrumentation of MASW Tomography Survey (Park et al. 2004)



(b)

Figure 2.13 Progression of MASW Tomography Survey (Park et al. 2004)

As shown in Figure 2.12, receivers are laid out using uniform linear spacing, and the seismic source is located at a set distance from the first receiver in the array. The distance should be far enough from the first receiver to ensure that the received surface wave signal is of a horizontal and planar nature. If the source is initiated too close to the receiver, an irregular, non-planar motion may be experienced. This effect is termed the near-field effect. The offset distance suggested to avoid near-field effects should be greater than half the maximum desired wavelength. Far-field effect is experienced when the source is positioned too far from the receiver array. This condition results in a received signal dominated by higher mode surface wave activity and possibly interference from received body waves. Optimization of the source offset can be performed prior to the survey by collecting trial shots at various offset distances (Ivanov, Park and Xia 2009). Figure 2.14 provides guidance related to the parameters which may be used to setup a given survey.



Material Type* ( $V_s$ in m/sec)	$x_1$ (m)	$dx$ (m)	$x_M$ (m)	Optimum Geophone (Hz)	Optimum Source* (Kg)	Recording Time (ms)	Sampling Interval (ms)
<b>Very Soft</b> ( $V_s < 100$ )	1 – 5	0.25 – 0.5	$\leq 20$	4.5	$\geq 5.0$	1000	1.0
<b>Soft</b> ( $100 < V_s < 300$ )	5 – 10	0.5 – 1.0	$\leq 30$	4.5	$\geq 5.0$	1000	1.0
<b>Hard</b> ( $200 < V_s < 500$ )	10 – 20	1.0 – 2.0	$\leq 50$	4.5 – 10.0	$\geq 5.0$	500	0.5
<b>Very Hard</b> ( $500 < V_s$ )	20 – 40	2.0 – 5.0	$\leq 100$	4.5 – 40.0	$\geq 5.0$	500	0.5

\* Average properties within about 30-m depth range

+ Weight of sledge hammer

Figure 2.14 Suggested Parameters for Setup of MASW Survey (Park et al. 2004)

### 2.3.3 Data Acquisition

The survey begins at the instance that the seismic source initiates the wave signal. The triggering system notifies that seismograph when data recording should begin. In order to acquire strong surface signals, it is recommended that sampling intervals range from 0.5 to 1.0 millisecond and recordings times range from 500 milliseconds to 1,000 milliseconds. A variation in required recording times and sampling intervals is generally a function of subsurface conditions (e.g. slower velocities from softer soil conditions). As demonstrated in Figure 2.12, the shot record is created from the trace signals returned to the seismography by the geophones. The individual geophone records are known as traces. After recording the first shot record, the line of geophones is advanced a predetermined interval down the survey line, and preparations are made to collect the next shot (Ivanov, Park and Xia 2009). The length of the geophone array shift dictates the resolution of the tomography profile. Research performed by varying the interval distance between shots in a synthetic environment indicated that the overall resolution of the

tomography profile shows little sign of distortion until the interval distance exceeded a distance equivalent to the geophone spread. Shot Interval distances beyond the spread length increased the required averaging of soil properties and introduced smearing to the imagery. In the synthetic environment, interval spacing less than the shot length did not improve the resolution of the image; however, it is believed that the reduced length adds redundancy to the survey measurement (Park 2005).

Discussions herein have mainly focused on the acquisition of active measurements, which are measurements acquired by means of inducing a seismic signal for the measurement purposes. Although not detailed herein, it should be noted that passive MASW measurements may also be collected using a similar equipment setup. Passive measurements of surface wave activity are made by monitoring ambient vibrations, such as those generate by near-by equipment vibration or traffic. Passive measurements require longer sampling intervals and generally record lower frequency and higher velocity measurements. In some instances, passive measurements can be stacked with active measurements at the same locations to define the low frequency range of the dispersion curve (Ivanov, Park and Xia 2009).

#### *2.3.4 Data Interpretation*

Three steps must be performed in order to convert shot record data to estimations of shear wave velocity: initial processing of shot record for surface wave phase velocity and frequency for development of dispersion curves, identification of fundamental mode, and inversion of the fundamental mode curvature into a representative shear wave profile.

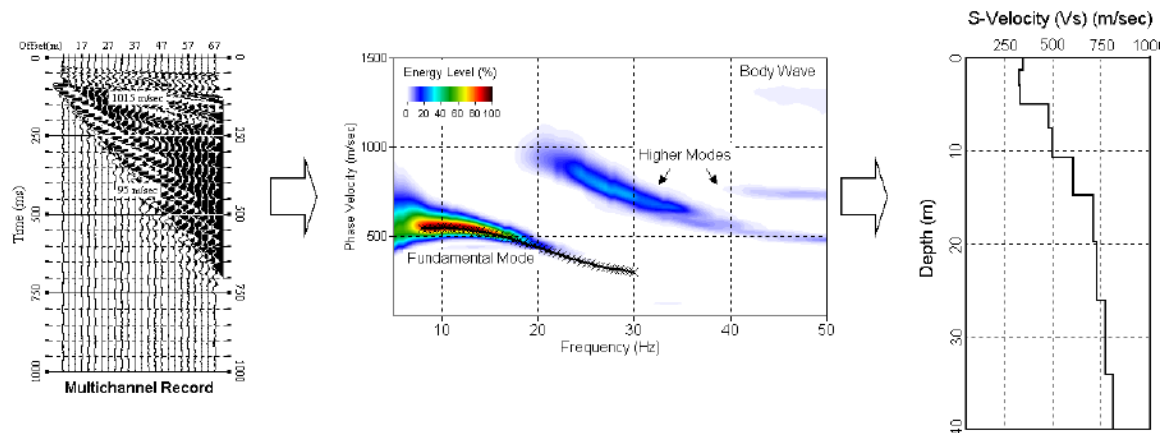


Figure 2.15 Processing Steps to Estimate Shear Wave Velocity (Park et al. 2004)

After field surveying is complete, each collected shot record is processed, highlighting the present surface wave signatures. The raw shot record may contain other wave forms, such as refracted waves, body waves, and sources of cultural noise. However, one of the main advantages of the MASW seismic technique is that the strength of the utilized surface wave is much greater than other wave forms; therefore surface waves are more discernable in the presence of noise. In a record presenting good signal to noise (S/N) ratio, the signal strength of the surface wave should be evident by the linear sloping features of the dispersive wave forms. Surface waves, on an active shot record, are often identified noted by the smooth sloping behavior as the wave travels down the geophone array (Ivanov, Park and Xia 2009). This linear slope represents the phase velocity of the particular surface wave, and can be used to transform the shot record data into a dispersion curve relating phase velocity to wave frequency (Park et al. 2000). Developed analysis software, such as SurfSeis, can process shot records and extract dispersion curves through the initial processing sequences (Ivanov, Park and Xia 2009).

Before the phase velocity and frequency information can be inverted, the fundamental mode of the surface wave must be identified. The dispersion curve is produced by processing the shot record data using specialized algorithms (e.g. frequency-wavenumber spectrum, slowness-frequency transformation, KGS wavefield transformation). The resulting dispersion

curve plot relates phase velocity within the frequency domain. As shown in Figure 2.15, the generated image contains the fundamental mode, as well as artifacts from higher modes and other wave forms. The fundamental mode of the dispersion curve is identified by the strongest energy signature in the dispersion curve. At this time, automated selection of dispersion curves is not available, therefore it is still necessary to manually identify the curvature of the fundamental mode. Higher mode contamination of the shot record can hinder the selection of the fundamental mode, and introduce error into the MASW analysis (Ivanov, Park and Xia 2009).

The inversion process for MASW is similar to the inversion process used for ERT analysis. A forward modeling algorithm is used to generate an earth model with layers of varying shear wave velocity. The generated model is an attempt to match an actual layered earth model, for which the exhibited shear wave condition could exist. A root mean square analysis is used to evaluate the fitting of the derived curve with the actual curve extracted from the field data. Before the iterative process is ended, the derived model must either satisfy the error tolerance or the number of iterations performed must exceed the number of iterations allowed for convergence. The inverted section represents an estimate of shear wave velocity with respect to depth (Ivanov, Park and Xia 2009).

The inverted section represents an averaged condition below the given geophone spread. To assign a spatial coordinate to the reading, it is assumed that the layered earth model is representative of subsurface conditions below the mid span, or mid station location of the geophone array. Downhole measurements have been used to test the validity of the mid station assumption. Results from testing have indicated that the use of MASW, with the mid station assumption, provides a reasonable estimation of profiled shear wave properties when compared against downhole measurements of the same area (Park et al. 2000).

The inversion process for MASW is performed prior to the development of the tomography profile. Since a unique shear wave velocity profile is generated for each shot along the survey line, the individual profiles can be interpolated to create a single two-dimensional image

representing lateral and vertical variations in shear wave velocity. No additional inversion is required. Interpolation can be performed using an equal weighting or variant weighting system (Ivanov, Park and Xia 2009).

## 2.4 Case Histories

ERT and MASW surveying methods are being used by the engineering public to augment various types of geotechnical investigations. The referenced case histories demonstrate how geophysical testing has been successfully used to improve understanding of site conditions and geology, in various applications. Presented studies also demonstrate how practitioners are attempting to directly correlate results of geophysical testing to geotechnical in-situ testing. These examples are provided to demonstrate how geophysical surveys are best used when combined with other geophysical techniques or geotechnical field and laboratory testing programs.

Particular case histories discussed herein may incorporate the use of other geophysical methods; however, for the purposes of this study, components of the study related to the use of electrical and shallow seismic surface wave methods are highlighted.

### 2.4.1 *Examples of Site Characterization and Assessment*

#### 2.4.1.1 Detailed Site Assessment in Anguilla, BWI

In the British West Indies, on the Island of Anguilla, N.S. Nettles & Associates (NSN) was contracted to perform a large scale site evaluation for a proposed resort community. The purpose of the evaluation was to effectively map the geologic conditions of the site, detect anomalous conditions, determine the depth of the underlying limestone stratum, determine the thicknesses of unconsolidated soils and determine potential drilling paths for flushing channels from an inland salt water pond to Rendezvous Bay. In addition to conventional geotechnical drilling and sampling programs, NSN utilized both ERT and MASW testing to focus drilling efforts to areas of interest and concern. ERT was used to image variations in stratigraphy, while MASW was primarily utilized to evaluate material density.

Geophysical field studies consisted of 63 ERT transects and 33 MASW transects, developed from 371 individual MASW readings (as a side note, ERT measurements were collected using the AGI SuperSting Resistivity system and a dipole-dipole array). ERT and MASW profiles were analyzed and compared to make preliminary assessments on subsurface conditions, and make decisions regarding the sampling program in three regions of the site. Observable areas of weakness within the underlying limestone formations and potentially developing or existing karst conditions were of particular interest to the design team. Such areas of interest, as identified by the geophysical testing, were targeted. Overall, 45 SPT borings, 71 CPT soundings, and 60 four-inch rock core borings were performed to observe underlying soil conditions and validate conclusions drawn by the geophysical testing. The final earthen model derived from the combined effort allowed the design team to compile design parameters for the various commercial, residential and infrastructure additions associated with the proposed development.

Electrical resistivity profiling was also used to evaluate the composition of a land-locked saltwater pond located along the western shoreline of Rendezvous Bay. The pond area was studied to determine potential directional drilling paths for flushing channels and to assess whether sufficient volumes of sediment at the pond bottom was available provide the needed fill for the development during construction. ERT profiles were used to direct drilling paths away from unstable subsurface features such as deposits of loose sand and sediment, as well as weak or fractured rock. Electrical resistivity measurements were also used by the project team to discern pockets of sand and gravel within the bed of the pond, for potential use as fill. Initial estimations suggested that approximately 500,000 cubic yards of fill material would be needed to complete the proposed project. Based on ERT imagery and excavation plans generated from the ERT analysis, approximately 450,000 cubic yards of sands and gravels would be readily available excavation, with the remaining 50,000 cubic yards to be acquired by ripping underlying limestone exposed through the removal of sediment overburden (Nettles, Jarrett and Cross 2008).

#### 2.4.1.2 Missouri Department of Transportation Field Test of MASW

Researchers from the University of Missouri-Rolla tested MASW technology against known geological conditions along Interstate 70 near St. Louis, Missouri. The objectives of the study was to determine the reliability of shear wave measurements derived using MASW testing method, and whether the bedrock or “acoustic bedrock” level could be accurately depicted using MASW.

In order to perform the analysis, a seismograph was used to receive trace signals from a series of 12, 4.5 hertz geophones. Surface wave signal were generated using a 20 pound sledgehammer striking a steel plate coupled with the ground surface. The SurfSeis software, developed and produced by the Kansas Geologic Society, was used to process the individual shot records, generate a series of one dimensional profiles and inverts the generated profiles into a tomography image. The test segment of Interstate 70 was approximately 6,400 feet in length, for which three prior geotechnical borings were available. To enhance the study, additional boring data and seismic cone penetration testing (SCPT) was performed along Interstate 70, adjacent to the MASW survey line. A total of 19 borings and 6 SCPT soundings were completed along in conjunction with this study. The additional boring data allowed for more reference points of bedrock depth, while SCPT allowed for of side-by-side comparisons of shear wave velocity readings with depth.

The depth to the bedrock interface was evaluated in two fashions. First, the generated shear wave profile was visually assessed to derive an initial profile of the rock. Based on this image, it appeared that the bedrock elevation varied between 26 feet and 44 feet. This information correlated well with the existing boring data. Further, one dimensional profiles were extracted from the tomography readings, at station numbers which correlated with borings and SCPT soundings. In a comparison between borings, the difference in between top of rock measurements derived from boring data and MASW readings only varied by an average of 0.7 feet. Further, results of SCPT measurements were relatively similar to those deduced from the

MASW testing. Discrepancies between the MASW interpretation, boring data and SCPT soundings can partially be attributed to the fact that borings and SCPT readings were not taken directly atop the respective station location assigned to the MASW survey. Rather readings were offset a nominal distance off of Interstate 70. Therefore, variations in geologic conditions can cause some variations in seismic response.

Overall, researchers felt that the MASW test method accurately and effectively depicted the bedrock profile. Further by comparing the inversion data to SCPT readings, researchers felt comfortable that the MASW measurements were comparable to the other direct means of measuring seismic shear waves (Thitimakorn et al. 2005).

At a later date, the authors conducted additional cross-hole (CH) seismic testing at the Interstate 70 test site, and performed a similar analysis at a test location in Poplar Bluff, Missouri, where CH, SCPT and MASW testing were performed. The purpose of this comparative analysis was to evaluate the effectiveness of SCPT and MASW seismic analyses, when compared against CH testing. Since CH analysis is considered superior to both of the aforementioned methods, the authors used CH readings to provide benchmark readings for comparative purposes. The final conclusions of the comparative analysis were that MASW, although not equivalent to CH data acquisition, was more reliable than SCPT measurements and provided an acceptable degree of accuracy. Further, researchers concluded that the MASW represents a cost effective alternative to CH testing and can be performed in areas for where drilling equipment cannot readily access. Researchers also were pleased that the MASW measurements could effectively map various conditions (e.g. densities, voids) within a given rock formation as SCPT is limited to depth of cone penetration (Thitimakorn et al. 2006).

#### 2.4.1.3 Site Characterization for Retaining Wall near Atlanta, Georgia

In this case, the authors were asked to perform a site assessment for the purposes of designing a mechanically stabilized earth (MSE) wall at the site of an existing landfill. The retaining wall was required by the governing regulatory agency so that the volume of the existing



waste facility could be expanded. In order to successfully design the retaining wall, geologic conditions in the area had to be adequately defined. The engineers were aware that the location of the retaining wall is located in the southern piedmont region of Georgia, which is characterized as having alluvial deposits, saprolites and bedrock in various conditions of weathering. One of the primary objectives of the wall designer was to determine a depth to bedrock across the proposed area.

In order to optimize the drilling program, seismic refraction and MASW techniques were both utilized at the site. Seismic refraction is a conventional technique used to determine bedrock horizons; however, there was thought to be a potential for encountering shallow lenses of rock which might effectively “hide” other important subsurface features. So by combining surface wave and P-wave analysis tools, a more complete analysis of subgrade could be obtained.

Testing was focused along the alignment of the berm for the proposed MSE wall. The berm was approximately 2,700 linear feet in length. Geophysical surveying was concentrated in known areas of shallow rock conditions. Seismic refraction surveys were conducted over 1,140 feet of the alignment and MASW surveying was conducted over approximately 500 feet. Geophysical testing was performed using a 24 channel Geode seismograph, with 14 hertz geophones for the refraction survey and 4.5 hertz geophones for the MASW survey. Source signal was provided by using a 20 pound sledgehammer and steel strike plate. In order to acquire samples of soil and rock and validate geophysical surveying results, 16 soil borings and 9 rock core borings were collected.

For the P-wave analysis, the Geometric software package, SeisImager, was used to determine first wave arrivals and plot respective bedrock horizons. For shear wave analysis, SurfSeis, produced by the Kansas Geologic Society, was utilized for shot analysis and inversion.

After reviewing the P-wave analysis and the boring data, it was concluded that the depth to rock was accurately depicted by the geophysical analysis, which provided validity to refraction readings between boring locations. Likewise, the MASW analysis indicated areas within the

underlying rock formation where zones of weaker material were present. Such conditions were validated through the collection of rock core samples in those isolated areas. The combined geotechnical and geophysical efforts accurately depicted the horizon of bedrock, and various degrees of densities within the underlying rock formation (Tomeh et al. 2006).

#### 2.4.1.4 Time-lapse Analysis of Texas Levee

Researchers from the Kansas Geologic Survey performed various seismic surveys, including MASW, at a common site, to evaluate whether the effects of flood conditions could be discerned with either P-wave and/or S-wave analyses. The test site was located at an existing levee site in South Texas, within the San Juan Quadrangle. Flood conditions were modeled by rapidly filling the reservoir.

The area of interest, a suspected fracture within the levee core, was initially detected through the use of a previous ERT evaluation. To establish a baseline condition, both P- and S-wave analyses were performed across the crest of the levee specific, in the area of the perceived discontinuity. The MASW profile, used to evaluate shear wave properties of the levee, imaged the discontinuity thought to be present in the core material.

Water levels adjacent to the levee were elevated to assess the gradual effects of saturation on the levee. Additional profiles were collected at 12 hour intervals as the water level increased. After assessing the levee for a 36 hour period, both P- and S-wave profiles were analyzed for changes. Results of the P-wave analysis showed little variation in the compression wave velocity, indicating that, in this instance, the sensitive of the P-wave to material saturation was marginal. However, the time lapse analysis of the shear wave profiles showed an increase in stiffness with respect to an increase in saturation. The researchers concluded that the discontinuity observed in the levee core was in fact desiccation of the clay material. As the levee core saturated, it was evident that the core material expanded effectively closing the discontinuity in the core and improving the shear properties of the soil (Ivanov et al. 2005).

## 2.4.2 *Attempts to Correlate Geophysical and Geotechnical Data*

### 2.4.2.1 Analysis from Thermal Power Plant Sites in India

The authors of this study use geotechnical site data collected at the locations of two thermal power plant projects in India to evaluate the potential for correlating penetration test results with findings of ERT geophysical testing. The selected sites are located in Aligarh and Jhansi in Uttar Pradesh, India.

Electrical resistivity measurements were collected using a Syscal Junior multi-electrode system, with 72 electrodes. A Wenner-Schlumberger array was used for data acquisition, and inversion of apparent resistivity measurements was conducted using the RES2DINV software package. The researchers recognize that the inherent non-unique interpretation of data was a potential drawback to the study. To address this, down-hole data was used to set boundary constraints to the interpreted data. During the geotechnical investigations, borings were sampled to a depth of 16 meters, therefore the inverted resistivity models were limited to a depth of 24 meters.

ERT results from both sites were relatively similar. Near surface, unsaturated soils were represented by higher resistivity readings, while underlying saturated soils were represented by lower resistivity measurements. Anomalous near-surface readings were identified at both sites as being localized boulder deposits, some of which were visible from the ground surface.

Geotechnical testing at each site was compiled showing the variation in SPT and DCP readings at similar intervals. Averaging of corrected N-values and DCP readings were used to show general trends in penetration resistance with depth. Boundary conditions and data dispersion were assessed by evaluating data points within one standard deviation of the average value trend line. Laboratory testing to determine grain size was performed to characterize the makeup of soils in the different site profiles. At Aligarh, with the exceptions of two depth intervals where a predominance of fine grained sands were noted, the site was primarily composed of

coarser sand material. However, the Jhansi site was characterized by a predominance of fine grained sands. Gravel contents at both sites were relatively low.

In order to compare the results, researchers attempted to compare the corrected SPT N-values to representative one-dimensional resistivity profiles from each site, as well as transverse resistivity profiles. Transverse resistivity was defined as a summation of the product of respective resistivity measurements and layer thicknesses, as expressed in Equation 2.18.

$$T = \sum \rho_i h_i \quad (2.18)$$

Researchers concluded that there was no direct correlation with resistivity measurements and corrected penetration readings. Authors did correlate a general increase in transverse resistivity with penetration resistivity; however, relations were site-dependent. Variation in relationships was attributed to different geologic environments present at each site (Sudha et al. 2009).

#### 2.4.2.2 Field Testing of Geophysical Techniques in Garchy, France

This study focuses on the author's attempts to correlate findings from conventional geotechnical field and laboratory testing to the results of electrical geophysical techniques at a common site in Garchy, France. The author's premise is that the performance of the conventional geotechnical testing can be time consuming and expensive, and that being able to extract geotechnical information from either vertical soundings or profile data would benefit site investigations.

In order to conduct this investigation, the researchers used both VES and ERT methods of acquiring electrical resistivity measurements, as well as ground penetrating radar (GPR). For geotechnical testing, dynamic cone penetrometer (DCP) and vane shear readings were utilized. The author recognizes that the use of more conventional testing methods, such as cone penetration testing (CPT), would be more beneficial; however, the use of the aforementioned field methods provided an efficient and convenient means of analysis, for the purposes of the study.

Garchy is located in the southeastern sedimentary basin of Paris. This particular area was selected based on the open and uninhibited nature of the site, the absence of foreign (particularly metal) objects, relatively level terrain, low to negligible background noise, and the distinct variations in lithology. Upper portions of the site are believed to be comprised of an alluvial stratum consisting of silty clays and coarse sands, and the lower portions are expected to be comprised of limestone. The groundwater levels are estimated to reside at depths ranging from 5 to 11 meters below grade.

As noted, various VES, ERT and GPR measurements were taking at this site. DCP measurements were taking in common areas along the various transects. Electrical resistivity measurements were taken using a SYSCAL R1+ resistivity meter with both Wenner and Alpha-Wenner arrays. Collected apparent resistivity measurements were inverted using the RES2DINV software package. General findings from the geophysical testing at the site indicated that layering could be divided into three distinct strata. The upper formation was identified as a thickness of alluvial soils. Below this stratum, a more conductive middle layer was thought to be associated with the Bourbonnias clay formation. The third stratum was identified as the underlying weathered limestone. Other geophysical testing performed at the site was complemented of the findings from the resistivity measurements and inversions.

The authors evaluated the results in two fashions: by directly correlating penetration data with ERT measurements and also by making comparisons between extracted one dimensional profiles and penetration resistance. When comparing penetration test result and profile data from ERT, it was visibly possible to discern the transition between strata. However, the data dispersion was too great to make a direct correlation with the information when attempting to numerically correlate penetration resistance with electrical resistivity measurements (Cosenza et al. 2006).

### 2.4.2.3 Analysis of Shear Wave Velocity Penetration Testing

The objective of the author was to derive correlations between field penetration testing methods and corresponding measurements of shear wave velocity. A test site located near Erzincan, Turkey, was used due to the known presence of deep alluvial deposits. To complete the study, SPT, CPT and DCP testing were performed for field penetration data. Shear wave velocity measurements were collected by means of crosshole and downhole analysis. Samples collected from the site were analyzed in the laboratory so that respective material properties were known.

Upon completion, the author was able to correlate shear wave velocity to various forms of penetration testing data. The analysis of data included both linear and non-linear data fittings, in an attempt to optimize the fit of the correlation. Examples of proposed relationships, and respective measure of correlation with data, are provided in Table 2.5 below.

Table 2.5 Derived Correlations between Shear Wave Velocity and Penetration Resistance

Soil Type	$V_s$ Correlation (m/s)	Correlation Coefficient (%)
All Types	$51.5 N^{0.516}$	81
All Types	$61 N^{0.267} \sigma_v^{0.283}$	83
Clay	$43.7 N^{0.324} \sigma_v^{0.270}$	90
Sand	$54 N^{0.332} \sigma_v^{0.221}$	90
Gravel	$205.7 N^{0.074} \sigma_v^{0.177}$	64
Sand	$408 D_{50}^{0.247}$	54
Sand	$116.6 D_{50}^{0.289} \sigma_v^{0.409}$	78
Clay	$55.3 q_c^{0.377}$	80
Sand	$0.7 q_c + 218$	75
All Types	$41 q_c^{0.212} \sigma_v^{0.461}$	70
All Types	$86.4 N_{10}^{0.367}$	71

In the conclusions, the author recognizes that the derived correlations are not a substitute for site specific testing; however can be useful when analyzing the validity field data in the presence of geotechnical testing (lyisan 1996).

## CHAPTER 3

### FIELD DATA COLLECTION

The intent of this study is to evaluate how the performance of geophysical testing enhances the effectiveness of a geotechnical site characterization. In an effort to meet this objective, a single site is needed for both geotechnical and geophysical analysis. With permission from the City of Gladewater, Texas, testing was allowed at the site of the City's earthen dam. Previous geotechnical works have been completed at this location relating to the condition of the dam for water retention purposes. In addition, to past geotechnical studies, the city commissioned an electrical resistivity tomography study to validate and confirm the findings of the previous geotechnical evaluation. In a collaborative effort with the City of Gladewater, Texas, Geometrics, Inc., and Apex Geoscience, Inc., MASW seismic testing was performed at the same location for the purposes of additional study at this site.

The dam at Lake Gladewater was constructed in 1952, damming Glade Creek for the purpose of creating a water reservoir for municipal use. The constructed height of the dam, measured from the toe of the dam to crest, is estimated to be approximately 38 feet. The normal water level of the lake is approximately 301 feet (MSL), and the elevation of the dam crest is approximately 314 feet (MSL), approximately 13 feet above the normal lake level. The length of the dam is approximately 1,100 to 1,200 linear feet. Angle of side slopes is estimated to range from 1 to 1 (horizontal to vertical) to 2 to 1. (Texas Commission of Environmental Quality 2005).

#### 3.1 Site Assessment and Geotechnical Sampling

In 2005, a routine condition assessment, as required by the Texas Commission of Environmental Quality (TCEQ), was performed for Lake Gladewater Dam. Observations made during this inspection included standing water related to seepage at various locations along the



downstream toe of the dam, heavy vegetative growth and localized sloughing or sliding failures along the face of the downstream slope. Recommendations provided in this assessment suggested further monitoring of the downstream seepage condition, and also suggested maintenance and repairs for reconditioning areas near the toe of the dam and along the face of the downstream slope (Texas Commission of Environmental Quality 2005).

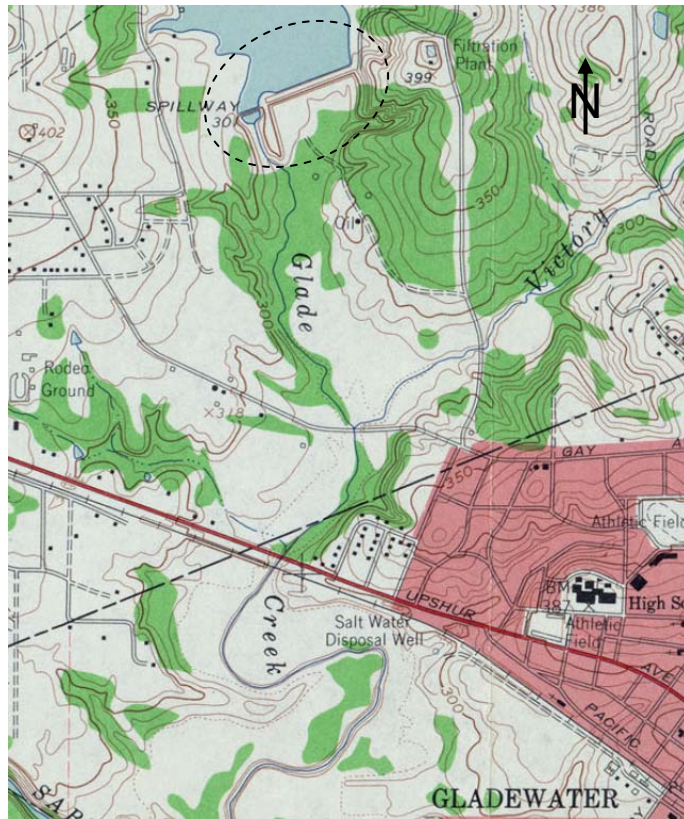


Figure 3.1 Map of Lake Gladewater Dam from Gladewater Quadrangle (United States Geologic Survey 1960)

### 3.1.1 *In-Situ Geotechnical Testing*

In response to the provided visual assessment, a geotechnical site assessment was authorized by the City of Gladewater, Texas. The focus of the geotechnical study was assessing

the seepage and sloughing conditions described in the 2005 TCEQ report, and providing recommendations for maintenance and remedial repairs.

The geotechnical assessment was limited to the central portion of the dam where the most significant observations of seepage and slope degradation were made. Sampling could not be performed at the toe of the dam due to accessibility. Geotechnical sampling was performed for the purpose of identifying the composition of the dam, assessing the condition of subsurface soils, and to observe seepage through the dam structure. Sampling was performed at three locations along the crest of the dam, as presented in Figure 3.2. Borings were spaced approximately 100 to 150 feet apart and each boring was drilled and sampled to an approximate depth of 40 feet. Drilling was completed using a track mounted, CME 45 drilling rig. Borings were advanced using dry auger drilling techniques, and samples were retrieved by means of split spoon and Shelby tube sampling methods. The in-situ testing program included standard penetration testing (SPT) and hand penetrometer testing of acquired Shelby tube samples. Samples were collected in a semi-continuous manner to a depth of 10 feet. Thereafter, samples were collected to at 5 foot intervals until the termination depth was achieved. Standard penetration testing (SPT) and Shelby tube sampling were performed in accordance with ASTM Standards D 1589 and D 1587, respectively.

Groundwater observations were made both during and after the completion of drilling activities. During drilling and sampling activities, a notation was made at the depth for which initial contact was made with groundwater seepage. Upon completion of sampling, borehole excavations were observed to assess changes in groundwater condition over time. Final borehole groundwater readings were taken prior to the abandonment of borehole excavations.

Field testing data and initial material descriptions were transcribed on field logs and returned to the laboratory with the respective samples. Samples and field logs were reviewed and assessed by the supervising engineer, and selected samples were assigned and prepared for laboratory testing. Results of field and laboratory testing were recorded in a final form on

boring logs after a cursory review by the supervising engineer. Boring logs are provided in Appendix B for review.



Figure 3.2 Approximate Boring Locations along Crest of Dam

### 3.1.2 Laboratory Testing

Samples returned from the field were inspected by the supervising engineer to confirm and verify notations made in the field and to determine the appropriate laboratory testing. Initial observations indicated that the composition of the sampled area was either a sandy clay or clayey sand. Samples at the dam's foundation level soils also possessed sandy clay materials with trace amounts of iron ore gravel.

Table 3.1 Summary of Assigned Testing Program

Description of Testing Method	ASTM Designation
Soils Finer than No. 200 Sieve	D 1140
Unconfined Compressive Strength of Cohesive Clay	D 2166
Moisture Content Determination	D 2216
Atterberg Liquid Limit and Plastic Limit Determination	D 4318

Table 3.1 provides a summary of the assigned laboratory testing program. Testing was primarily focused on identifying physical characteristics of the dam and foundation materials. Upon completion of testing and review of results by the supervising engineer, test results were transferred to final log documents, prepared for further evaluation by engineering staff and final reporting. Final boring logs contain results of field and laboratory testing, respective USCS soil classifications, and pertinent field observations including approximate strata breaks and groundwater measurements. Boring logs are provided in the Appendix for further review.

### *3.1.3 Comments*

Results of field and laboratory testing and associated findings were provided to a civil engineering firm consulting with the municipality on future modifications to the dam and hydraulic analysis of the associated water shed.

## 3.2 Electrical Resistivity Survey

In November of 2008, the City of Gladewater authorized the performance of an electrical resistivity tomography analysis along the crest of the Lake Gladewater Dam. The purpose of the tomography study was to confirm observed geotechnical observations, image the structure of dam, and to evaluate the presence of voids or other anomalous conditions within the dam structure (Tayntor and Wright 2008).

### *3.2.1 Survey Preparations*

Since field activities had been conducted at this site previously, it was known that the crest of the dam was relatively flat. The crest could be modeled as a flat and level plane; therefore, no terrain modifications would be necessary during the final analysis. The crest area had recently been cleared of vegetation, so access to the exposed subgrade was readily available. Additional information was needed to ensure that foreign objects or conditions would not introduce noise into the survey. Through a review of dam schematics and previous documentation related to the lake, it was determined that an underground release valve was identified traversing the dam at an unknown depth. Further, metallic railing and grates,

associated with a raw water intake facility located in the lake, would be in close proximity to the crest of the dam during the study. This information was noted for later use during interpretation, as the presence of metallic objects can impact current flow and effectively skew measurements of apparent resistivity (Advanced Geosciences Incorporated 2008).

### 3.2.2 *Equipment*

The SuperSting Resistivity System, produced by Advanced Geosciences, Incorporated, was used to complete the survey. The SuperSting R8 transmitter/receiver is a self regulated eight channel digital volt meter, capable of transferring up to two amps of current to the ground. Without auxiliary switch boxes, the SuperSting R8 is capable of conducting multiple readings using a string of up to 56 electrodes. The equipment was supplied with the SuperSting R8, 4 electrode cables, each cable with 14 electrodes takeouts, and 56 steel stakes. Due to technical difficulties experienced in the field, the electrical resistivity survey was conducted using 28 electrodes as opposed to 56 electrodes. The SuperSting R8 system requires an external 12 volt battery source; however, the performance of the equipment can be optimized by using a pair, 12 volt batteries connected in series (Advanced Geosciences, Incorporated 2006). Deep cycle marine batteries were utilized for this application. The use of dry cell batteries, such as the deep cycle marine batteries is preferred due to the ability to repeatedly drain the battery source and recharge, within minimal impact to the battery core (Advanced Geosciences Incorporated 2008).

The SuperSting R8 requires commands in order to properly trigger electrodes for current induction and measurement of potential difference (Advanced Geosciences Incorporated 2008). AGI Administrator software package, provided with the SuperSting Resistivity System, allows the user to input array parameters to model resulting survey psuedosections. The generated model will give the user an estimate of penetration depth, data point coverage, and an estimation of time required to perform the survey. An example of a generated psuedosection is provided in Figure 3.3. After an array configuration is created, the user can create a unitless command file usable by the SuperSting R8 transmitter/receiver. Another notable feature of the AGI Administrator

software is the ability to reverse the array direction, so that points are collected starting from the end of the electrode string and progresses towards the first electrode in the array. This progression is advantageous during a roll-along survey. The SuperSting R8 stores all measurements of current and potential difference during the course of a survey. Each measurement is coordinated with the address of the four electrodes associated with the respective reading. With the capability of referencing coordinate or nodal locations of past readings, the equipment can conclude a survey once all readings within a new domain are acquired. By not overlapping existing data, the use of a reverse array provides an efficient means of surveying and data storage for roll along applications (Advanced Geosciences Incorporated 2008).

For the purposes, of this survey, a dipole-dipole array was selected due to the need for high lateral resolution and the relatively shallow depth of interest. A depth of 50 feet would resolve the depth evaluated during the original geotechnical assessment. The array was modeled in the in the AGI Administrator program, and then transferred to the SuperSting R8 equipment for surveying purposes. Figure 3.3 shows the completed model of the dipole-dipole array used during the dam survey.

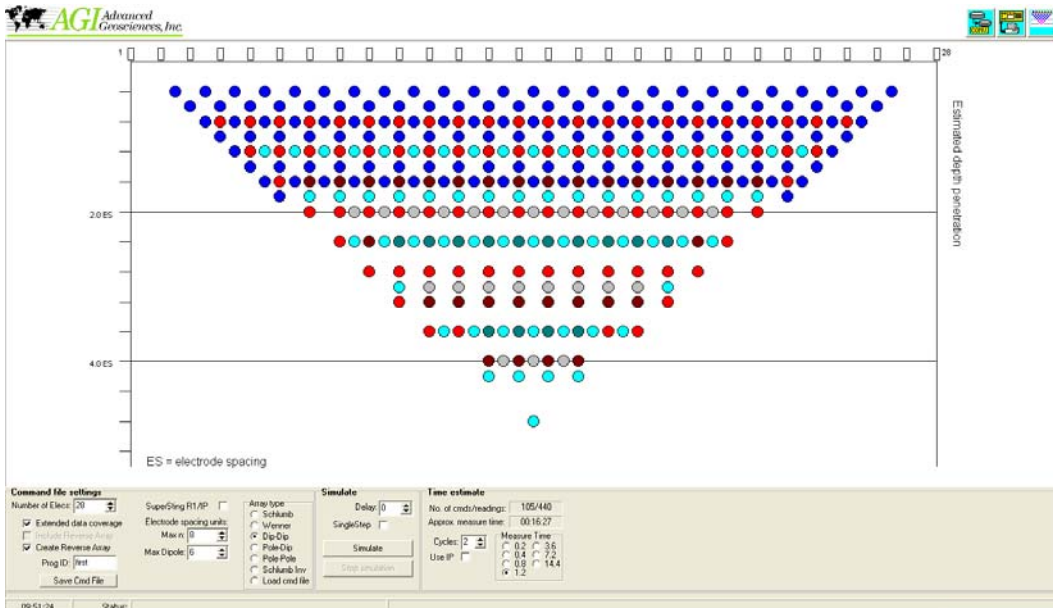


Figure 3.3 Pseudosection Model of Dipole-Dipole Array Used During Data Acquisition

Additional information is provided in Appendix B regarding the development of the survey's data spread, relative to electrode locations along the cable spread.

### 3.2.3 Data Acquisition

Consideration was given to the desired resolution, depth of investigation, and available equipment. For the purposes of this study it was determined that an interval spacing of 10 feet would adequately profile the core material as well as foundation soils. It was estimated that for 28 electrodes, at an interval spacing of 10 feet, the approximate depth of penetration would be approximately 54 feet. This is based on the assumption that the penetration depth is approximately 20 percent of the survey length (Advanced Geosciences Incorporated 2008). Each run would cover 270 linear feet of the dam. The estimated depth of penetration can also be viewed in the model presented in Figure 3.3. It should be noted that the AGI Administrator program generates a generic command file which can be used with any given interval spacing. The y-axis of the display provides a depth range based on electrode spacing, *ES*; therefore a depth of 4.0 *ES* would correspond to a depth of 40 feet, if the electrode spacing was 10 feet.

In order to traverse the length of the dam, a roll-along survey would be necessary. To perform the roll-along with 2 strands of 14 electrodes, the first 14 electrodes would have to be relocated to the end of the survey line, making the same electrodes the last 14 electrodes of the next run. This configuration is considered a half spread roll along. An example of the described roll-along movement can be viewed in Figure 2.5 (a).

The first electrode was located on the northeast end of the dam, with the string extending along the crest towards the spillway on the southwest end of the dam. The location of the first probe was marked with a nail and surveying tape for future referencing. Figure 3.4 shows an approximate location of the initiation point of the survey and direction of the roll-along survey.



Figure 3.4 Origination Point and Direction of Electrical Resistivity Tomography Survey.

From the reference point, a tape measure was used to layout the interval spacing of the electrodes. Steel stakes were used to couple the cable electrodes with the soil. Stakes were driven into the ground using a hammer. Each stake was driven approximately 6 to 10 inches into



the ground so that stakes would couple with the soil. After stakes were placed, the electrode cables were laid out along the survey line and coupled with the stake.

Prior to starting the survey, the survey command file was retrieved and site specific inputs (e.g. interval spacing, units) were manual entered into the SuperSting R8. Contact resistance checks were also performed prior to beginning the survey. Contact resistance checks are performed by measuring the contact resistance present at each electrode location. The resistance check provides two quality controls to the survey by ensuring that that the electrodes are sufficiently coupled with the ground and also to verify that all elements in the system are connected and functioning. The addition of a saline solution improves coupling between the stake and earth, and may be added around stakes before beginning a survey to reduce contact resistances. Reducing contact resistance allows for a more complete transfer of current and clear signal reception, both key elements in reducing the signal to noise ratio of the survey (Advanced Geosciences Incorporated 2008).

Once launched, the acquisition of field measurements was performed by automated processes in the SuperSting Resistivity system. While the survey was being performed, the upcoming roll-along was laid out (i.e. measurement of interval spacing, placement of stakes, and application of saline solution).

The SuperSting R8 unit will shut down after completing the inputted survey routine. During a roll-along, the instrument is informed by the user that the roll-along is or is not complete. If told that the roll-along is not complete, the unit will save survey data and shut down for movement purposes. After relocating the unit and attaching necessary cables, the unit is given the respective configuration of electrodes being used for the next acquisition and the location along the survey line. After performing the contact resistance test, data acquisition is started again. The roll-along process is continued until the survey is complete. After the last run is complete, the SuperSting R8 is informed that the survey is over, and all data associated with the current survey is stored for later use (Advanced Geosciences Incorporated 2008).



Figure 3.5 Performance of Electrical Resistivity Tomography Survey at Lake Gladewater

#### 3.2.4 *Data Processing and Inversion*

The raw data stored in the SuperSting R8 must be extracted and converted into a form suitable for processing. The AGI Administrator software is used to download and convert field data into a form readable for the AGI EarthImager 2D analysis software. In the raw form, measurements of apparent resistivity can be plotted into the respective pseudosection. The EarthImager 2D software uses the measured apparent resistivity pseudosection during the inversion process to recreate an earth model fitting the conductive characteristics of the recorded raw model. The default model used to begin the inversion process is a homogenous half-space with an assigned resistivity equivalent to measured apparent resistivity values, in log form. Other models may be used to begin the inversion by manual selecting available user-defined functions (Advanced Geosciences, Incorporated 2009).

The inversion process is iterative in two ways. First, EarthImager uses an iterative routine to develop a matching earth model, using an error tolerance or maximum number of iterations as criteria for terminating the inversion. Secondly, if the level of error in a given model is beyond acceptable limits (i.e. root mean square or L2 Normalization terms), the raw data can be evaluated to determine whether outlier measurements are causing unwanted error in the inverted model. Disruptive points, or noise, can result from cultural conditions present at the time of the survey, recordings of negative values, or malfunctioning equipment. Corrupting data points can be isolated by using the misfit histogram generated in the EarthImager program, manually eliminating data points in the pseudosection or by suppressing the readings collected from particular electrodes. The iteration process can stop when the user is satisfied that the represented model demonstrates the subsurface condition, within the accepted error tolerances for the survey (Advanced Geosciences Incorporated 2009). Figure 3.6 represents the final inverted section for the resistivity analysis conducted at the Lake Gladewater Dam in 2008.

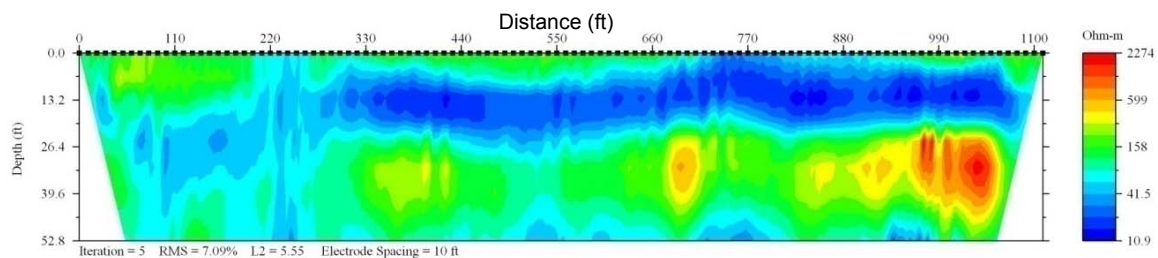


Figure 3.6 Electrical Resistivity Profile of Lake Gladewater Dam (Tayntor and Wright 2008)

### 3.2.5 Comments

The collection of field data and data inversion were performed by John Tayntor, P.E. and Joshua Hubbard, E.I.T. of Apex Geoscience, Incorporated. Field data, for approximately linear 1,100 feet, was acquired in one 10-hour day. An interpretative analysis of the profile was provided to the City of Gladewater in December of 2008.

### 3.3 Multi-Channel Analysis of Surface Wave (MASW) Survey

Since 2008, the City of Gladewater has worked with consulting firms to plan repairs and design modifications to the earthen structure. In April 2009, the City of Gladewater was approached with the opportunity to perform additional field testing at the site of the Lake Gladewater Dam, for research purposes associated with this study. As presented, the MASW analysis would provide the city with information estimating stiffness characteristics of the dam and subsurface soils, which could be correlated with previous geotechnical and geophysical data. Permission to conduct the study and access to the site were granted by the municipality. Field testing commenced in May 2009. Equipment and support staff for the study was provided through charitable contributions by Geometrics, Incorporated and Apex Geoscience, Incorporated.

#### 3.3.1 *Survey Preparations*

As noted, the terrain at the site was relatively flat, and little to no change in surface conditions were noted between the times of the two geophysical surveys. The research site provided a relatively quiet atmosphere for seismic data acquisition, as ambient and cultural noise was limited. The dam location was positioned away from city streets and a significant distance from a nearby public park. Weather conditions were mild on the day of the survey, presenting only slight wind conditions and minimal surface impact from lake waves. Potential cultural noise, from operating transfer pumps, was noted to the south of the dam. However, it was later determined that the pump equipment was too far away for vibrations to be picked up by the survey equipment. Conditions were identified and noted for later use during data interpretation.

#### 3.3.2 *Survey Setup*

Soundings for the MASW survey were recorded using a PC laptop, one 24 channel Geode Seismograph and 4.5 Hz geophones. The Geode seismograph is used to receive and digitize received analog electrical impulses generated by each geophone in the linear array. Digital signals are then transmitted to the laptop and interpreted by the Geometric Siesmodule

Controller software. No shot records are saved in the Geode instrument. The Seismodule Controller software is used to setup each shot record, view acquired seismic data, convert received digital signals into a SEG-2 format, and monitor survey location and progress (Geometrics Incorporated 2003). Figure 3.8 provides a screenshot of the Seismodule Controller, as being used during the MASW survey.

The interval spacing of the geophones was set at 4 feet, which was also the maximum distance provided between connecting leads on the geophone cable. Using this spacing, the spread length of the geophone array was approximately 92 feet. The maximum 4 foot interval spacing was used to maximize the length of the geophone array which is noted to improve modal separation (Park 2005).

One geophone was connected to each of the 24 available leads. The natural frequency of the geophones was 4.5 Hz, making the receivers optimal for recording lower frequency signals. Steel spikes were not used to couple geophones with the ground, due to past observations of cemented soils and gravels present at the ground surface. Steel spikes were replaced with plates in order to circumvent poor coupling at the surface. The use of steel plates also provided an efficient means of moving survey equipment from location to location. Geophones were positioned in a linear array, and in line with the seismic source.

A 16 pound sledge hammer and aluminum strike plate was used as the seismic source for the survey. The strike plate, needed to be flush with the ground surface so a complete transfer of energy was transmitted. The trigger was taped to the handle of the sledge hammer and connected to the Geode seismograph. During use, the trigger was positioned away from the hammer strike. The seismic source was positioned 12 feet from the first receiver.



(a)



(b)

Figure 3.7 Instrumentation and Setup for MASW Field Testing.

### 3.3.3 *Data Acquisition*

Prior to beginning the survey, parameters related to the geometry of the field survey and data acquisition were provided to the Seismodule Controller program. With the exception of the source offset distance, the selection of field parameters was based on documented guidance provided by the Kansas Geologic Survey (Ivanov, Park and Xia 2009). For data acquisition, the recording time and sampling intervals were set at 1 second and 0.5 milliseconds, respectively. Parameters recommended by Geometrics, Inc. were used to coordinate the triggering system with the Geode seismograph.

After the initial setup of Seismodule Controller, the system was ready for the first shot record. As a check, the receiver signal window of the Seismodule Controller was monitored while one team member walked by the geophone array. The induced vibrations from the footsteps returned a small, but visible, signal to the receiver indicating proper oscillation of the geophone core.

Recording sequence is started by initializing the recording software and arming the trigger system. When ready, the party responsible for swinging the hammer is signaled, and the hammer blow initiates the survey. The response from the triggering system notifies the seismograph that the survey has begun. Signals recorded through the designated recording time and at the designated time interval. Figure 3.8 shows an example of the visual output provided by the processing software after completing one shot.

After acceptance of the sounding, either the setup can be moved for the next reading or additional readings can be collected in the same locations for the purpose of staking records. Staking records is used to improve the definition of the record, and generally used in noisy environments. Staking was not thought to be needed due to the low noise levels present at the research site.

To prepare for the next shot record, the geophone spread was translated 12 feet down the survey line, representing a shift equivalent to three geophone interval spacing. After

equipment was moved, systems checked, and recording system initialized, another shot was recorded. For this survey, 72 soundings were recorded over a length of 852 feet.

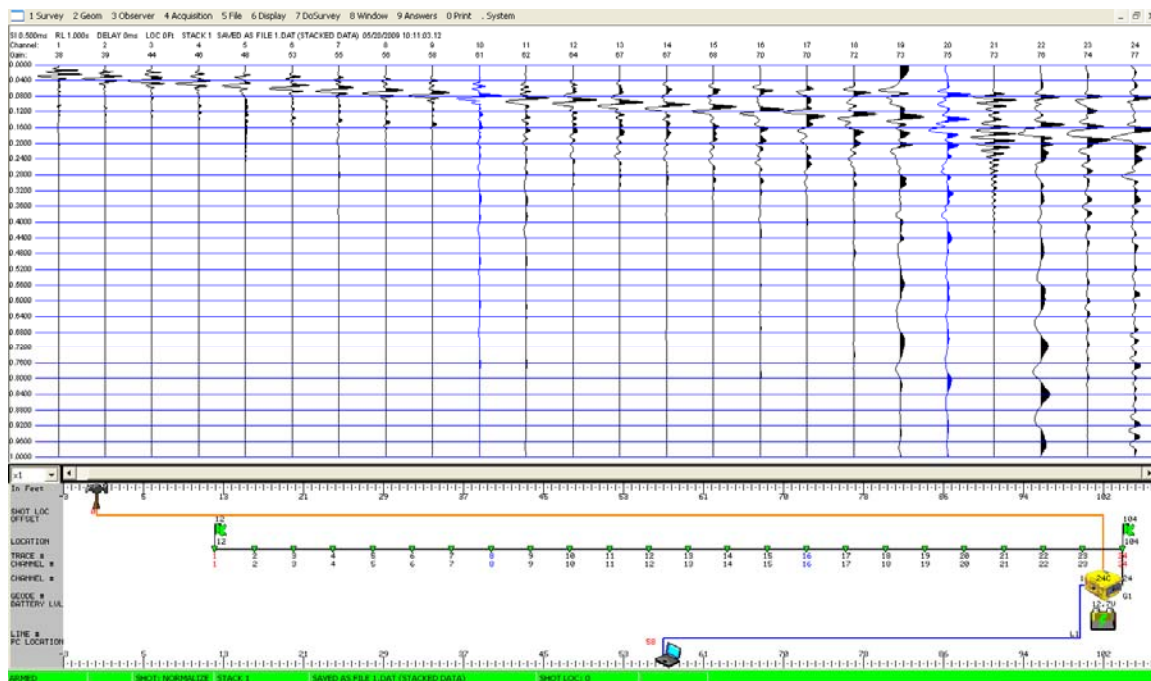


Figure 3.8 Example of Acquired Shot Record during Lake Gladewater MASW Survey

### 3.3.4 Data Processing and Inversion

Processing of shot records was performed using the SurfSeis software package, developed by the Kansas Geologic Survey. The purpose of the software is to process and analyze shot records for Rayleigh wave dispersion characteristics, develop representative dispersion curves, allow manual isolation and extraction of fundamental modes, invert extracted curvatures into one-dimensional shear wave sounds, and interpolate series of one-dimensional models into a single two dimensional tomography image (Ivanov, Park and Xia 2009). Appendix A provides a flowchart detailing the processing steps used for analyzing MASW profiles.

Processing begins by up loading SEG-2 field records into SurfSeis. Records are processed and converted into KGS format, which is recognizable by the program. After the



conversion into KGS format, the program will collect information pertain to the nature of the survey (i.e. active or passive method of data acquisition), the setup of the survey, and how the survey was advanced. Data files are processed a second time scanning for signatures of surface waves within the record (Ivanov, Park and Xia 2009)

Algorithms in the SurfSeis routine are used to analyze each KGS file and determine surface wave phase velocity and frequency properties, and used to plot representative dispersion curves. Due to the energy of surface waves, related measurements of amplitude can be used to highlight the energy of the fundamental mode (Ivanov, Park and Xia 2009). Figure 3.9 is an example of a generated dispersion curve, and markings indicating the selected curvature of the fundamental mode. Each shot record has a unique dispersion curve, and each curve must be analyzed manually, by the processor, to identify and select best fit for the fundamental mode (Ivanov, Park and Xia 2009).

The dispersion curve can also be used to evaluate the depths of analysis. As seen in Figure 3.9, the fundamental mode is identified by the marked curvature in the bottom left of the exhibit. The node on the far left of the curvature corresponds with a frequency of approximately 7 Hz and a phase velocity of 1,000 feet per second. Referencing (2.13, the wavelength is equivalent to the phase velocity divided by the frequency. In this example, the corresponding wave length would be approximately 143 feet. Assuming that the maximum depth of penetration is approximately half of the maximum recorded wavelength (Ivanov, Park and Xia 2009), the depth of penetration would be approximately 71 feet. The minimum depth of resolution can be determined in a similar fashion, by using the nodal point to the far right of the extracted curve. For the given example, the shallowest observable depth is approximately 8 to 10 feet below the surface.

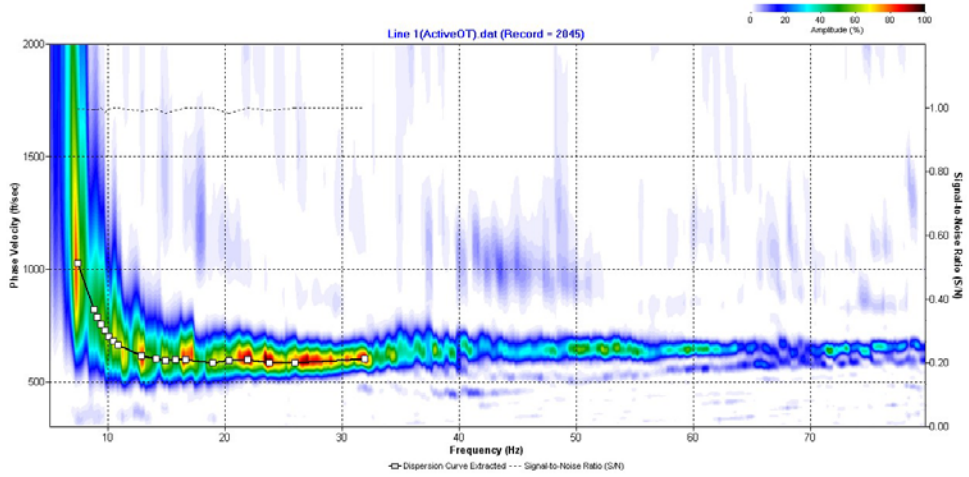


Figure 3.9 Dispersion Curve from Sounding No. 45 of Lake Gladewater Dam

After all records have been evaluated and the fundamental modes are selected, curves are then used as comparative tools during the inversion process. SurfSeis attempts to generate a layered earth, shear wave model that would produce a similar fundamental mode curvature as that extracted from field testing. The iterative process continues until the predetermined error tolerance is achieved or the maximum number of iterations is performed.



Figure 3.10 Inversion of Sounding No. 45 from Lake Gladewater Dam

The multiple layered earth models are compiled to form a single tomography profile. The tomography image is an interpolative representation of the multiple one-dimensional shear wave profiles. An inversion algorithm is not required to generate the tomography image (Ivanov, Park and Xia 2009). The tomography image presented in Figure 3.11 represents the shear wave analysis performed at the Lake Gladewater Dam in 2009 using MASW survey techniques.

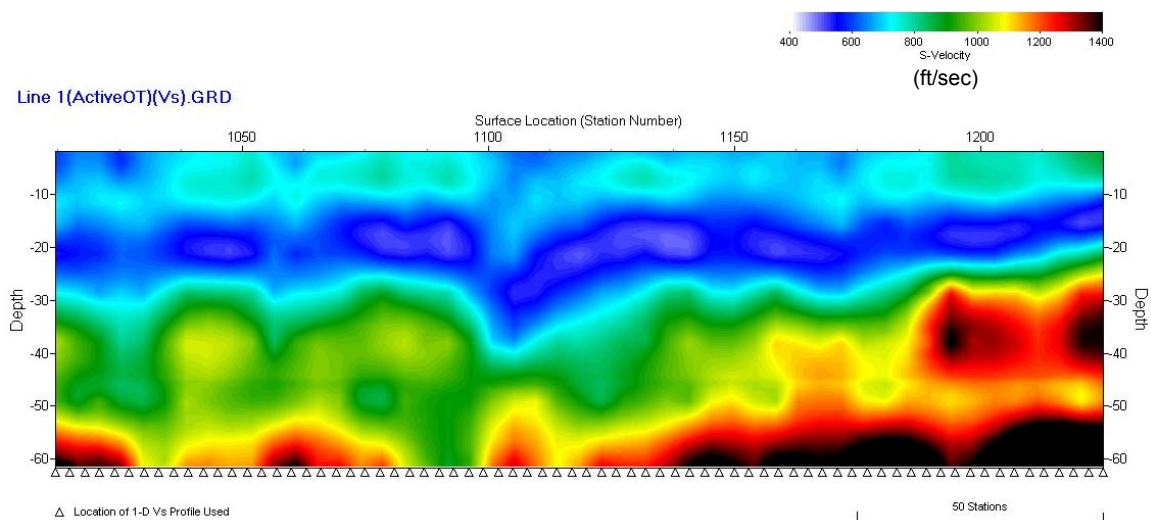


Figure 3.11 Shear Wave Profile using MASW Seismic Tomography.

### 3.3.5 Comments

The collection of field data and data inversion were performed by John Tayntor, P.E. and Joshua Hubbard, E.I.T. of Apex Geoscience, Incorporated. Field data, for approximately linear 852 feet, was acquired in one 10-hour day. The MASW profile was provided to the City of Gladewater in July of 2009.

## CHAPTER 4

### FINDINGS AND OBSERVATIONS

Testing at the site of the Lake Gladewater Dam was performed over a period of three years, and findings at each phase of the evaluation were determined based on the availability of data, to date. In keeping with this fact, findings are presented based on the information available at the conclusion of each assessment. This is done to demonstrate progressively improving knowledge of site conditions with the addition of each test.

#### 4.1 Geotechnical Site Assessment

##### 4.1.1 *Findings*

As part of the original geotechnical site assessment, three borings were drilled and sampled near the mid span of the dam. The mid span of the dam, based in a visual assessment of downstream slope and toe conditions, was thought to be the primary area of interest for the study. Soils acquired from the three test sites are relatively consistent in nature. Performed laboratory testing indicates that soil classifications include clayey sand, sandy lean clay, and lean clay with sand. Appendix A can be referenced for boring logs and detailed soil profile information. Encountered soils are consistent with those of the Queen City Sand formation. United States Geologic Survey (USGS) characterizes the Queen City Sand formation as containing a mixed deposit of sands and clays, with concentrations of iron ore, sandstone and lignitic material. Clays are described as being silty in nature (United States Geologic Survey 2009).

Table 4.1 Percent Fine Content and Plasticity Index Test Summary

Material Description	Value Ranges of Laboratory Testing	
	Percent Passing No. 200 Sieve (%)	Plasticity Indices
Clayey Sand (SC)	41 – 44	9 – 15
Sandy Lean Clay (CL)	51 – 68	13 – 21
Lean Clay with Sand (CL)	71 – 76	24 – 28

Table 4.1 demonstrates how physical characteristics and material composition were similar among the sampled soils. Moisture content profiles are also relatively consistent at each location. An increased moisture condition in each boring strongly corresponds with the lake level approximately 13 feet below the top of the crest.

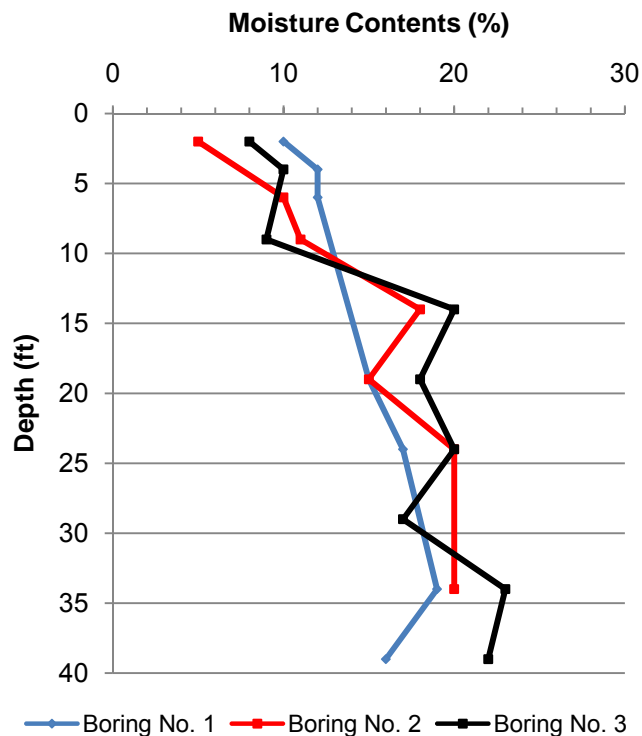


Figure 4.1 Boring Moisture Content Profiles

Comparing the three locations, the moisture content levels were marginally higher at the location of Boring No. 3. Final subsurface water levels observations were noted approximately 27 to 34 feet below crest level.

In-situ testing included SPT and hand penetrometer measurements of collected Shelby tube samples. Field measurements indicate that the majority of the observed soils possessed either a loose to medium dense relative density, or a medium stiff to stiff consistency, based on correlations with SPT N-values and hand penetrometer values. This generalization holds true except for the following notable exceptions:

- At the location of Boring No.1, soft to medium stiff conditions, inconsistent with other borings, were noted from approximately 13 feet to 35 feet; and
- At the location of Boring No. 3, stiffer clay conditions were noted from a depth of 13 feet to 25 feet.

Unconfined compressive strength tests, performed as part of the laboratory testing program, provide reasonable agreement between measured compressive strength and field hand penetrometer values.

#### *4.1.2 Observations*

Materials sampled are consistent with the local geologic formation. It is plausible that the majority of fill material used to construct the dam was from an onsite or nearby source. Without direct testing, it can be inferred that the permeability of compacted clayey sand and sandy lean clay materials is generally on the order of  $1 \times 10^{-5}$  to  $1 \times 10^{-6}$  centimeters per second (cm/s), which is the lower limits for materials used in impervious applications. Moderately plastic and highly plastic clays, more ideal for impervious applications have permeability of  $1 \times 10^{-7}$  cm/s or greater (Day 2006).

The mid span of the dam was isolated prior to field activities due to observations of heavy vegetative growth and shallow sloughing slope failures on the face of the downstream slope. Further, softened soil conditions and standing water were found near the downstream toe. All three described conditions are believed to be related to developed seepage and elevated moisture condition within the earthen structure. Data from field and laboratory observations validate the previous assumptions. Specific examples of correlating field data and observations include (see Figure 4.3 for additional information on field observations and boring locations relative to locations on the dam):

- Heavy vegetation exists near the location of Boring No. 3. Boring No. 3 was noted to have elevated moisture contents below the lake mud line, more so than the other two boring locations. Elevated moisture levels are believed to be the source for moisture for vegetative growth.
- Mid slope failures were noted to correspond with Boring Nos. 1 and 2. Subsurface groundwater levels were measured at 27 feet below crest elevation at both boring locations. Previous reports indicated that the gradient of the existing downstream slope was estimated at 2 to 1 (horizontal to vertical), and as steep as 1 to 1 along certain areas of the dam. Given the geometry and composition of the slope, it is believed that the destabilization of surface soils is due to the flow path of the developed steady-state seepage condition and the occurrence of natural erosion over the face of the downstream slope.
- Standing water and softened soils conditions were noted at different locations near the toe of the dam. The most prominent areas were correlated to location of Boring Nos. 1 and 2. During field testing, low density material was encountered within Boring No. 1 at depths ranging from approximately 25 feet to 35 feet. It is possible that the low density material observed is providing a seepage path to the identified softened and saturated areas.

The geotechnical assessment included the following components: review of documents, visual observations of the site, in-situ testing, soil sampling, and laboratory testing. With the geotechnical data available general inferences were made regarding the composition of the structure and the general behavior of the structure. Soil composition and conditions are known at three locations at the mid span of the dam.

## 4.2 Electrical Resistivity Survey

### 4.2.1 *Findings*

The inverted profile was initially analyzed to detect potential deficiencies or weaknesses in the model. The first identifiable area is located on the eastern portion of the dam, in the vicinity of the known raw water intake and low flow outlet embedded within the dam. The exact effect of the metallic objects on the survey results is unknown; therefore, it was prudent to neglect this area during any further analysis. The second area selected was based on engineering judgment. The inverted profile is a model representing a true earth condition for which the measured apparent resistivity could exist. By virtue of the model assumptions of the inversion software, the extents of the generated profile could be used without modification. However, boring data was only available to a depth of 40 feet, and only within a selected portion of the dam. No additional drilling was to be performed at this time. In addition, as observed in the final survey pseudosection, the density of data points decreases with depth. As an engineering judgment, it was decided that the interpretation would not include data presented at a depth of 40 feet and below, as these areas could not be confirmed with boring data and represented a higher degree of inference. Areas neglected during the interpretation of the electrical resistivity analysis are represented in Figure 4.2.

The accepted quality of the final resistivity profile was thought to be representative of the observed and known conditions. The root mean square error analysis (calculated at 7.09%) was below the maximum allowable value of 10%. L2 Normalization ranging from 3% to 5% suggests a good data fit, with an improving fit as the L2 Normalization approaches 1% (Advanced



Geosciences Incorporated 2009). For the performed survey, the L2 Normalization of 5.55 was accepted given the known presence of the metallic objects on the east side of the dam. As a secondary quality check, visual comparison between the measured and modeled apparent resistivity pseudosections provided strong correlation with each other.

After the initial analysis, the profile was correlated with existing boring data and field observations. Borings positions were estimated based on drilling log information from the original project. Estimated boring locations may be viewed on Figure 4.3.

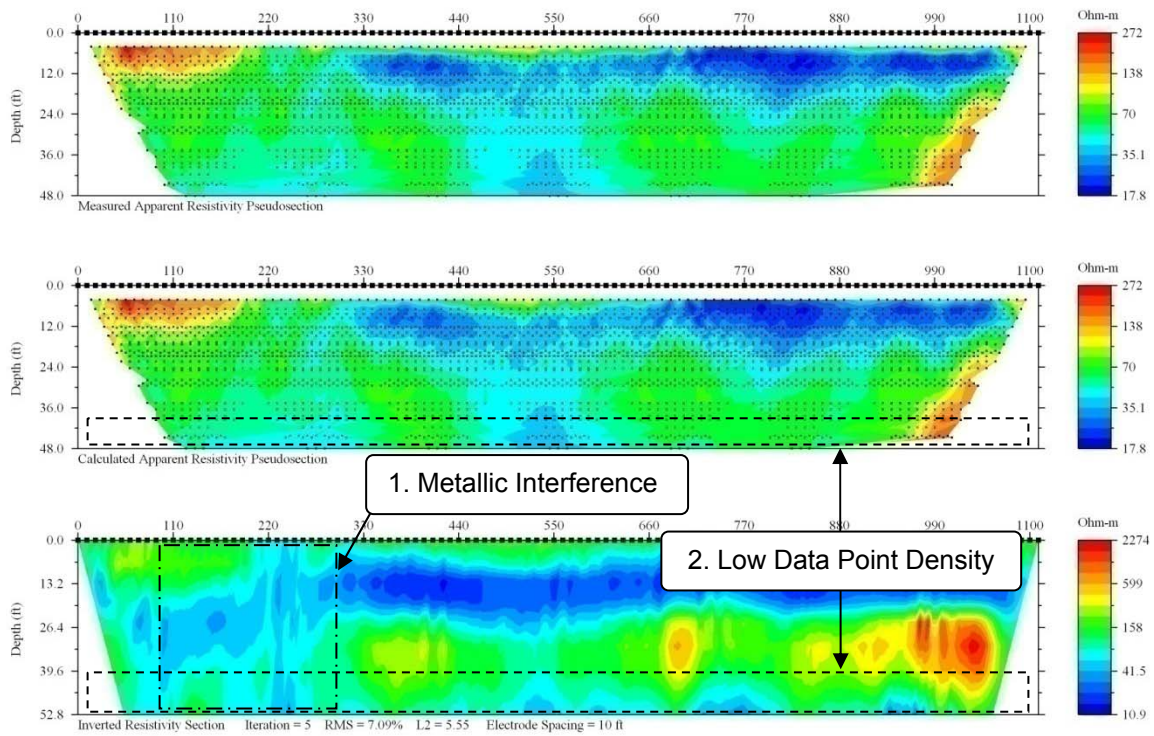
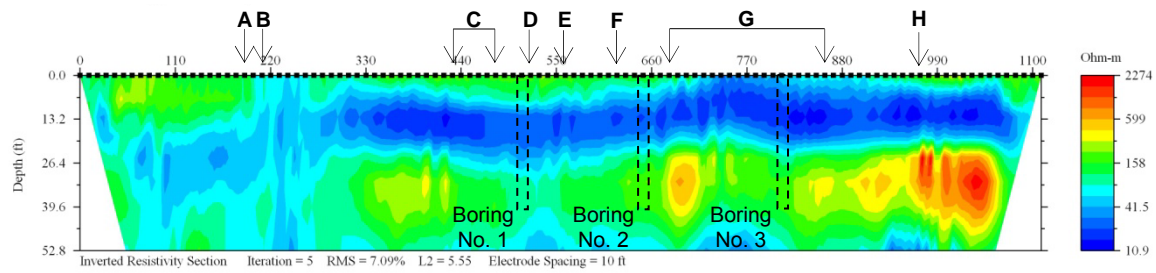


Figure 4.2 Neglected Areas of Electrical Resistivity Profile



- |                                     |                                    |
|-------------------------------------|------------------------------------|
| A. Existing drainage outlet at toe  | E. Standing water at toe           |
| B. Raw water intake structure       | F. Mid slope failure               |
| C. Mid slope failure/seepage at toe | G. Heavy vegetation/seepage at toe |
| D. Soft soils at toe                | H. Seepage at toe                  |

Figure 4.3 Location of Borings and Downstream Slope Observations

The range of resistivity values, for the survey, fluctuated from approximately 11 to 2,300 ohm-meters. Based on documented ranges of material resistivity (refer to Table 2.4), the range of measurements for the survey correspond well with deposits of clay, sands, and gravels. Correlations with the logs suggest that the lower resistivity values (10.9 to 100 ohm-meters) are complimentary of clayey sand and sandy clay fill material, generally with a higher saturation level. Mid range values, between 100 and 400 ohm-meters, are representative of the clayey sands and stiffer clay materials. Resistivity measurements above 400 ohm-meters are believed to be higher concentrations of sand and gravel.

#### 4.2.2 Observations

Since soils identified on the boring log were only marginally varied in composition, the primary correlation between the boring data and the electrical resistivity measurements would be between the soil moisture content and the measured electrical resistivity. As can be seen in Figure 4.4, generally, a decrease in soil resistivity can be noted as the soil moisture content increases. Some deviations from this trend are observable; however, this can be attributed to the heterogeneity of the soil profile. At this time, a direct correlation between soil moisture content and electrical resistivity cannot be made.

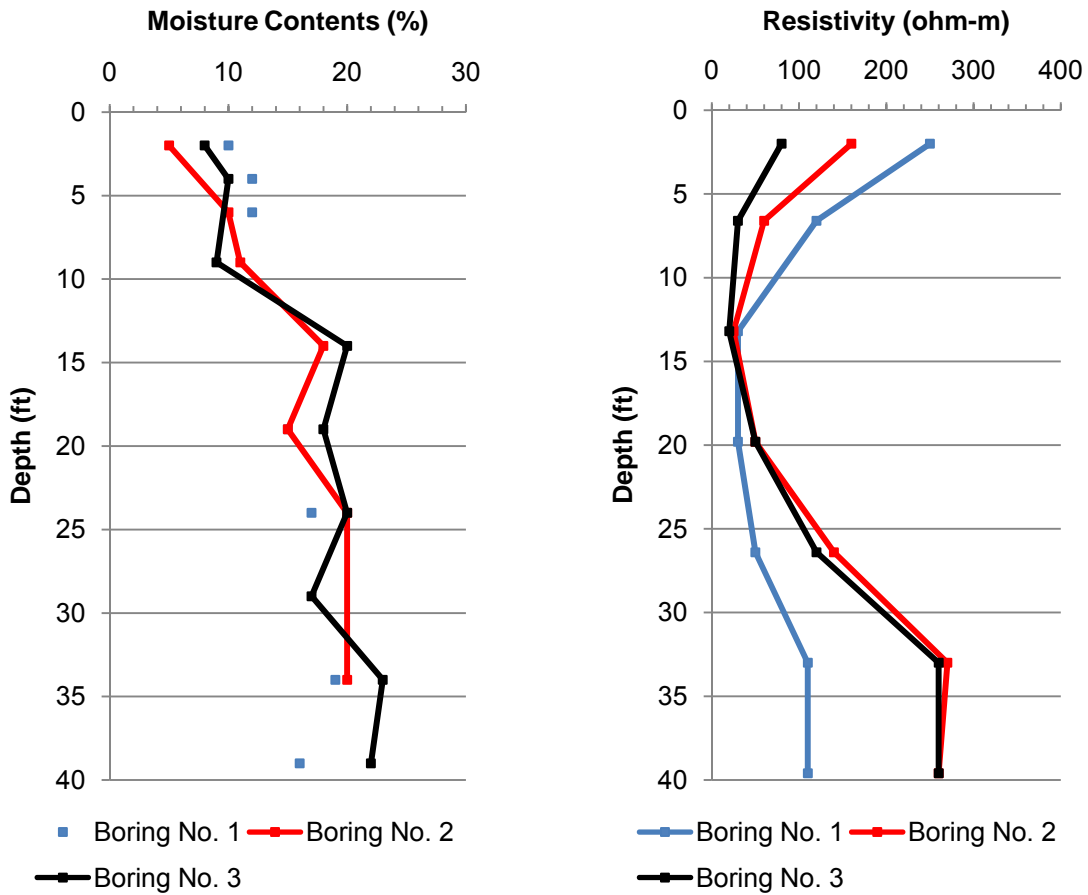


Figure 4.4 Variations in Moisture Content and Resistivity with Depth

Based on previous observations from the site and the findings of the electrical resistivity survey, the following observations are made:

- Observations of soil softening and seepage at the mid span of the dam and mid slope failures correlate with the trough of lower resistivity observations between 440 and 600 feet. Resistivity profile data reinforces the assumptions made during the geotechnical assessment. A deeper fill area may be present, allowing for a seepage path at this location.

- In the vicinity of Boring No. 3, between 660 feet and 880 feet, low resistivity measurements are representative of the elevated moisture conditions corresponding to the vegetative growth on the downstream slope.
- Locations of mid slope failures and standing water at the toe correlate strongly with the lowest resistivity measurements present on the survey, suggesting areas of higher saturation and potential seepage.
- The relatively consistent low resistivity signature (measurements less than 50 ohm-meters) spanning from approximately 300 feet to 1,080 feet, suggests continuity of the core material. Anomalous conditions were not observed from the surface to a depth of approximately 25 feet.

Historical topographic data was unavailable at the time of the original geotechnical assessment and the resistivity survey. However, based on the boring data collected and the resistivity profile, an inference can be made about the varying depth to native soils. As mentioned, the Queen City Sands formation does possess local deposits of sand and gravel. If presumed that the boundary between the native subgrade and the dam fill exists at the abrupt resistivity increase (ranging in depth from 25 to 30 feet), then geologic and resistivity data would suggest that areas presenting higher resistivity would represent natural deposits of coarse sand or gravel material. The permeable nature of sand and gravel deposits may present another seepage path residing below the constructed dam. As seen by the positioning of the borings, these conditions were not identified during the geotechnical survey. Had borings been positioned in a different location, such conditions may have been encountered.

Upon completion of the resistivity survey and with the geotechnical data available, previous inferences regarding the composition of the dam structure and the general behaviors within the structure have been validated. Soil composition and conditions of the three boring locations could be effectively extrapolated across the discernable portions of the dam structure.

Generalizations could be made regarding native soil conditions, which were unevaluated prior to this survey. However, it is noted that although the soil conditions observed during the geotechnical assessment corresponded with the electrical resistivity profile, other conditions were present within the dam which were not identified during geotechnical sampling. Therefore, it is reasonable to assume that the performance of the electrical resistivity profile improved the knowledge base for the site assessment.

#### 4.3 Multichannel Analysis of Surface Waves (MASW) Survey

The MASW shear wave profile presented in Figure 3.11 is scaled according to station numbers used by the SurfSeis program during processing. For observation purposes, Figure 4.5 provided below, represents the shear wave profile scaled in linear feet. It should be noted that the survey line begins at 161 feet, with respect to the origination point of the electrical resistivity survey. This starting point represents the mid station location of the first shot record. The origination points for the two surveys did not coincide due to logistics associated with the MASW field setup. However the area of interest was effectively mapped using the seismic technique.

##### 4.3.1 *Findings*

As with the resistivity survey, the interpolated shear wave profile was initially analyzed to detect potential deficiencies or weaknesses in the model. The final shear wave profile presents findings from the ground surface to a depth of 60 feet. The SurfSeis program can determine the maximum observable depth, based on the results of the dispersion curve analysis. The minimum depth of resolution must be determined manually by evaluating dispersion curves on an individual basis, as discussed previously in Section 3.3.4. Looking at the dispersion curve analysis, it appears that the minimum depth of resolution is between 5 to 10 feet. For this evaluation the upper 7 feet of the profile was neglected.

As previously mentioned, the presence of the raw water intake piping and low flow valve was believed to interfere with the results of the electrical resistivity analysis. Since seismic analysis is not sensitive to the presence of metallic objects, as is the electrical resistivity methods,

these objects could be resolved during the MASW analysis. Looking at the east side of the dam (between the 161 and 317 feet designations), a square notched area between the depths of 30 and 45 feet is believed to outline the excavation for the installed lines.

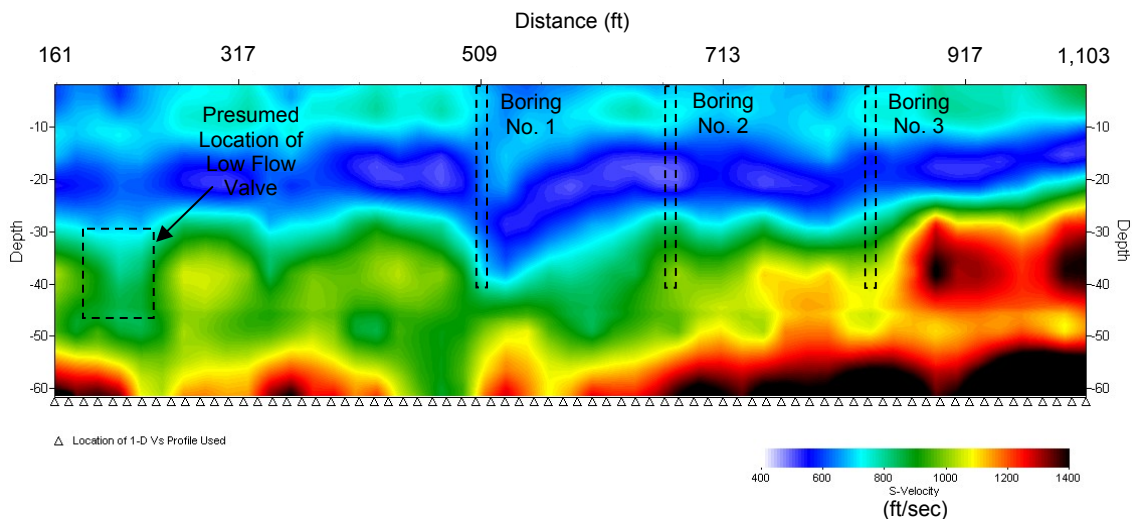


Figure 4.5 MASW Shear Wave Profile of Lake Gladewater Dam, Scaled in Linear Feet

No root mean square error analysis was performed during the formation of the shear wave profile; however, a minimum root mean square tolerance of 10% was used during the inversion of the one-dimensional shear wave profiles. The tomography image was generated by equally weighting each of the profiles and interpolating between each.

Shear wave velocities ranged from approximately 400 feet per second to 1,400 feet per second. Referencing Figure 2.14, the represented range of shear wave velocities is consistent with a material stiffness ranging from soft to hard (conversion between units of velocity is provided in Table 4.2).

Table 4.2 Correlations between material stiffness and shear wave velocity

Material Stiffness	Shear Wave Velocity Range	
	(meters per second)	(feet per second)
Very Soft	Less than 100	Less than 300
Soft	100 – 300	300 – 1,000
Hard	200 – 500	600 – 1,700
Very Hard	500 or greater	1,700

4.3.2 Observations

To compare the mapped shear wave velocity with boring data, field penetration testing was used as measure of material density. Figure 4.6 presents the relationships between SPT N-values with depth, and shear wave velocity with depth, at each of the respective boring locations.

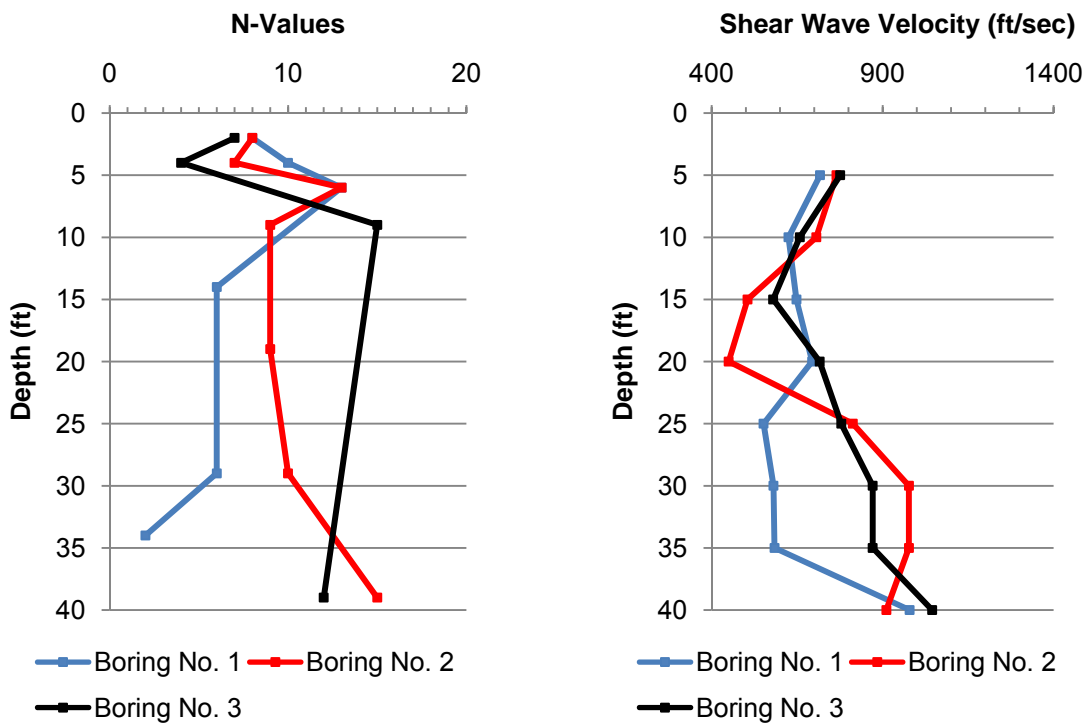


Figure 4.6 Variation in SPT N-Values and Shear Wave Velocity with Depth

Due to the limited number of N-Value measurements, a direct correlation cannot be made between the SPT N-values and the shear wave velocities.

Although increasing N-values generally indicate an increase in relative density in cohesionless soils and stiffness in cohesive soils, in a mixed soil profile the N-values should be viewed in conjunction with associated soil types as N-value measurements do not correlate between cohesionless and cohesive soils without some discontinuity. This can be seen in the general SPT correlations provided in Table 2.1 and Table 2.2. As an example, in Figure 4.7, trends can be observed in the general soil descriptions and the shear wave velocity profile (shear wave velocity ranges are from Table 4.2).

Depth	Soil Condition/ Shear Wave Range
5 – 15 ft	Medium Dense Sand/Medium Stiff Clay (300 – 1,000 ft/sec)
15 – 20 ft	Very Stiff Clay (600 – 1,700 ft/sec)
20 – 35 ft	Medium Stiff Clay (300 – 1,000 ft/sec)
35 – 40 ft	Very Stiff Clay (600 – 1,700 ft/sec)

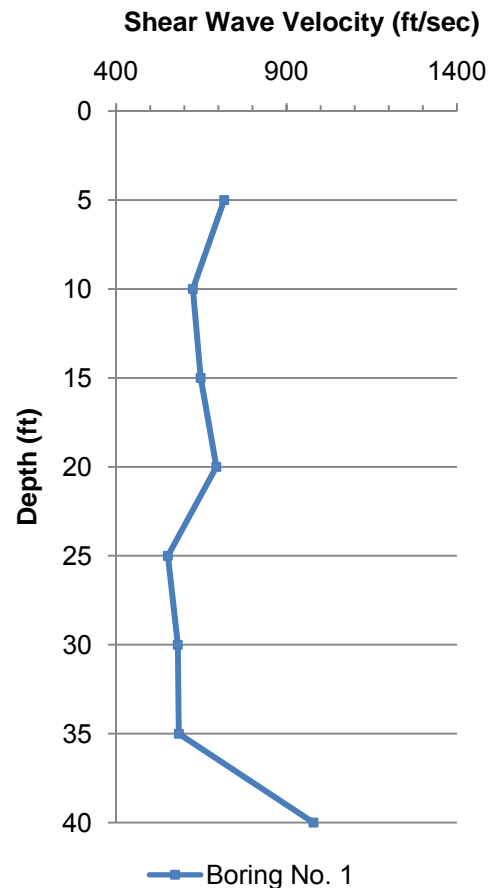


Figure 4.7 Comparison of General Soil Conditions and Shear Wave Velocity with Depth at Boring No. 1



Common soil conditions present as relatively linear patterns. Such conditions can be seen at depths of 5 to 15 feet and from 25 to 35 feet. Abrupt increases in stiffness were noted at depths of 20 feet and 40 feet. Such increases are consistent with the increased hand penetrometer values at both the 20 and 40 foot depth. Further, at all depths, the shear wave velocity measurements are within the ranges of associated with material descriptions corresponding to the field penetration testing.

Strong correlations can be observed when comparing the general trends and curvatures of the MASW and electrical resistivity profiles. The previously identified trough of low resistivity present at the mid span of the dam also appears on the MASW survey as a region of low density material, in a similar location.

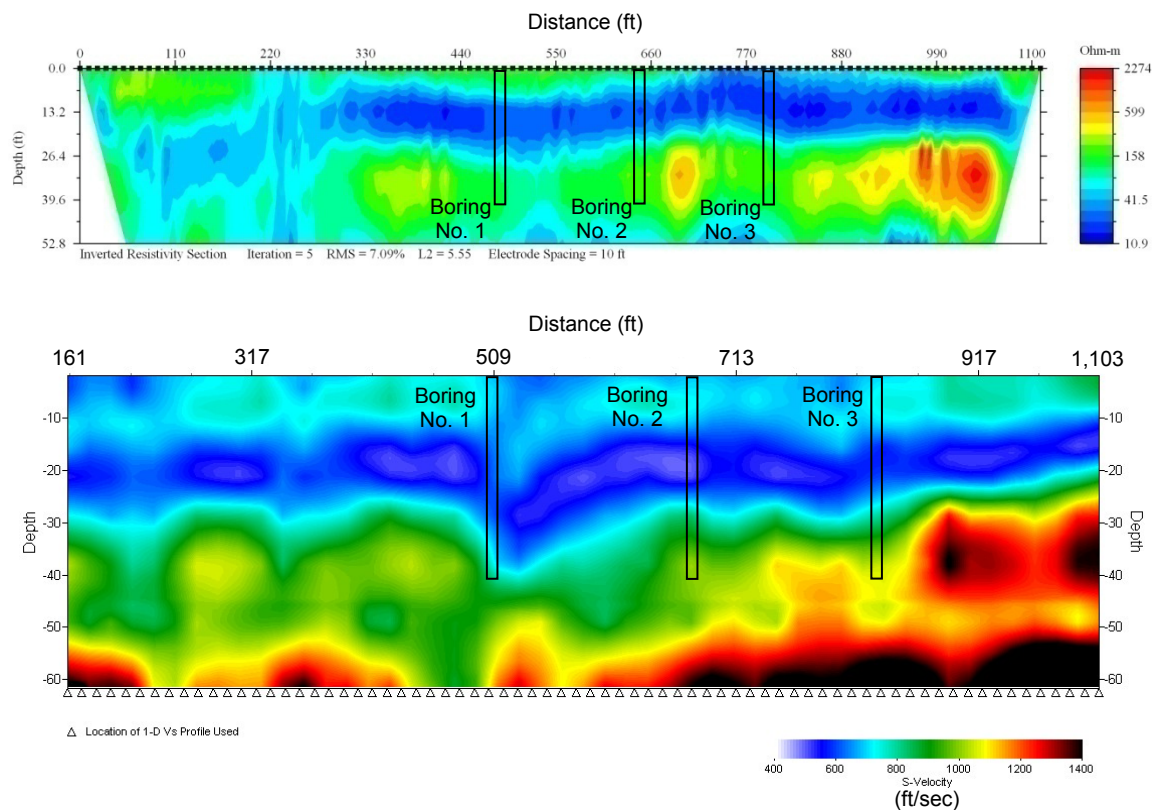


Figure 4.8 Electrical Resistivity and MASW Tomography with Boring Overlay

The trough condition observed in both surveys may represent the basin of the original Glade Creek. Another notable feature is the common regions of high resistivity and high shear wave velocity measurements. These common areas further suggest that concentrations of sands and gravels are present within the dam profile. Further, the previous assumption regarding the horizon of the natural subgrade is strengthened the distinct variation in shear wave properties between 25 and 35 feet. In addition, the lowest presented shear wave readings correspond well with the observations of seepage, mid slope failure and vegetative growth.

The findings from the MASW profile, when combined with the findings and observations of the original geotechnical observations and electrical resistivity survey, provide a comprehensive assessment of the dam site. Analysis and mapping of material density strengthens the correlations previously seen in the electrical resistivity survey and geotechnical observations.

## CHAPTER 5

### CONCLUSIONS

#### 5.1 Findings and Conclusions

The primary objective of this study was to establish that geotechnical site assessments are enhanced through the implementation of applicable geophysical testing methods. Three methods of analysis were used during the study of the dam structure; geotechnical sampling and in situ testing, electrical resistivity tomography, and multichannel analysis of surface waves (MASW) seismic tomography. After comparing the different forms of data, the following inferences can be made regarding the progression of testing.

- Profile data from electrical resistivity and MASW analyses was comparable with data collected during the original geotechnical analysis.
- Dissimilarities between profiles and boring log data can exist due to the heterogeneity of the earthen structure, as well as the resolution capabilities and data smoothing associated with each method.
- Areas of low resistivity and low density corresponded with areas of observed seepage, slope failures, and vegetative growth, possibly indicating seepage paths through the dam structure.
- By comparing electrical resistivity and MASW profiles, stronger inferences can be made about the composition of the earthen structure (e.g. depth to original native subgrade, existence of sand and gravel deposits).
- The use of two different classes of geophysical methods (i.e. electrical and seismic methods) allowed for different features in the dam structure to be resolved (e.g. near

surface features seen in the electrical resistivity profile, raw water intake and low flow valve piping in MASW profile).

- The use of geophysical profiling resolved features within the dam structure not observed during the initial geotechnical assessment (i.e. concentrations of sands and gravels present between Boring Nos. 2 and 3 and west of Boring No. 3).

A definitive conclusion cannot be drawn based on the performance of this study alone. However, findings from this study do support the objective. From this study, the following conclusions can be made regarding the progression of testing.

- Correlating geotechnical boring data with tomography imaging allows for improved interpolation of between geotechnical data sets, subsequently reducing risk in the overall analysis.
- The incorporation of geophysical testing into a geotechnical site assessment can be done with marginal impact to performance schedules due to the speed of data acquisition and processing, as each analysis was performed during a single 10 hour work day.
- When compared with results of the original geotechnical assessment (i.e. boring data, site observations), the correlation of multiple geophysical methods improve overall understanding and resolution of the earthen structure.

## 5.2 Recommendations for Future Work

The performance of similar analyses is needed in order to validate the primary objective of this study. It is believed that future studies would benefit by utilizing and/or incorporating the following measures in the methodology:

- Perform all testing and data acquisition during the same analysis period to limit any potential variations in site conditions.

- Use a common field penetration technique (e.g. SPT analysis, Cone Penetration analysis) to monitor in-situ conditions, to provide a stronger data set for correlating geophysical data with in situ material density.
- Evaluate the affects of variable equipment selection and setup, selection of array type, and performance of site-based calibrations on survey performance.
- Look at the effectiveness of other geophysical methods in common applications (e.g. comparison with seismic and resistivity downhole testing).
- Incorporate GPS and/or GIS information into data acquisition and presentation of findings to enhance the location of survey features and testing results.

## APPENDIX A

### PROCEDURE FOR DEVELOPMENT OF TWO DIMENSIONAL MASW PROFILE

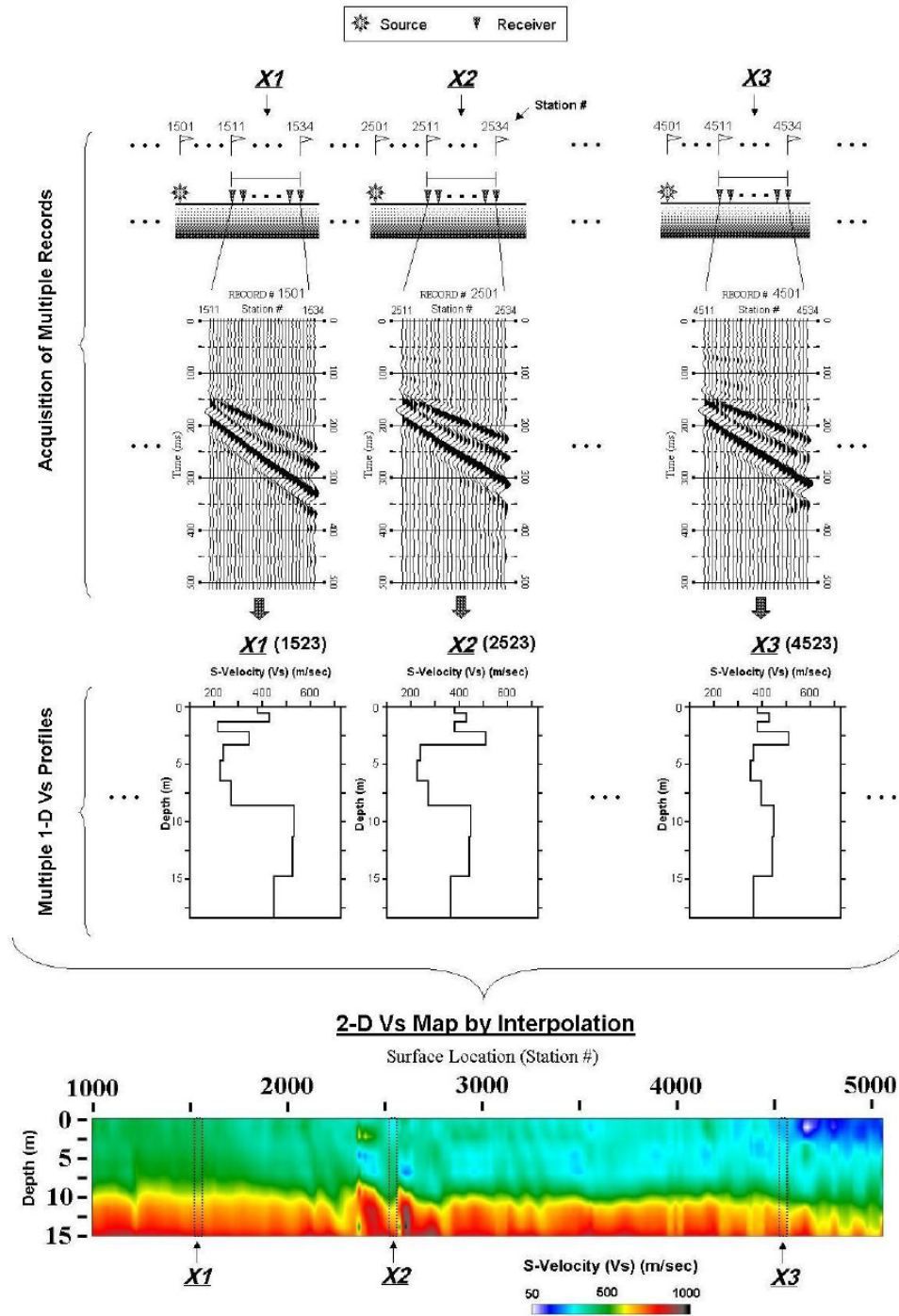


Figure A.1 Procedure for development of 2-D MASW Profile (C. B. Park 2005)

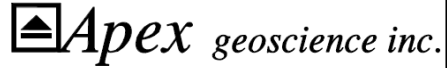
APPENDIX B

BORING LOGS FROM LAKE GLADEWATER DAM



**LOG OF BORING NO. 1**

Project Description: **Lake Gladewater Dam  
Gladewater, Texas**



Depth, feet	Samples	Graphic Log	MATERIAL DESCRIPTION	Penetration Blows / Foot	Pocket Penetrometer, TSF	Unconfined Compression, TSF	% Passing No. 200 Sieve	Unit Dry Weight, lb/cu ft.	Water Content, %	Liquid Limit	Plastic Limit	Plasticity Index	Other
0			Loose, light tan, with red, CLAYEY SAND (SC), mottled	8			44		10	29	15	14	
5			-medium dense	10									
5.0			Medium dense, light tan and light red, CLAYEY SAND (SC)	13					12				
8.0			Very dense, red and tan, CLAYEY SAND (SC), mottled	2.5			44		12	25	16	9	
10			Medium stiff, light tan, brownish tan, SANDY LEAN CLAY (CL), mottled	6									
13.0			Very stiff, dark tan with red, SANDY LEAN CLAY (CL), mottled	3.5			51		15	29	16	13	
18.0			Medium stiff, tan and red, SANDY LEAN CLAY (CL), mottled	0.5					17				
23.0			Medium stiff, gray, tan and red, SANDY LEAN CLAY (CL), mottled	6									
28.0			Soft, dark tan and light red, SANDY LEAN CLAY (CL), mottled	2			59		19	35	18	17	
33.0			Very stiff, dark tan and red, SANDY LEAN CLAY (CL), mottled	2.5					16				
38.0			Boring terminated at 40'										
40.0													
45													

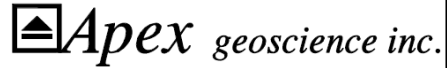
Completion Depth: **40.0**  
 Date Boring Started: **6/13/06**  
 Date Boring Completed: **6/13/06**  
 Logger: **E. Wilson**  
 Project No.: **106-157**

Remarks: **Seepage noted at 34' during drilling. Water level at 27'3" at final check.**

Figure B.1 Lake Gladewater Dam Boring No. 1

**LOG OF BORING NO. 2**

Project Description: **Lake Gladewater Dam  
Gladewater, Texas**

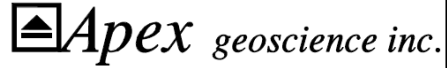


Depth, feet	Samples	Graphic Log	MATERIAL DESCRIPTION	Penetration Blows / Foot	Pocket Penetrometer, TSF	Unconfined Compression, TSF	% Passing No. 200 Sieve	Unit Dry Weight, lb/cu ft.	Water Content, %	Liquid Limit	Plastic Limit	Plasticity Index	Other
0			Loose, tan, CLAYEY SAND (SC), with organics	8			41		5	27	15	12	
3.0													
5			Loose, tan and red, CLAYEY SAND (SC), mottled	7									
5.0													
8.0			Medium dense, light tan and red, CLAYEY SAND (SC)	13			45		10	29	14	15	
10													
13.0			Loose, light tan and tan, CLAYEY SAND (SC)	9			45		11	25	14	11	
15													
18.0			Very dense, gray and red, CLAYEY SAND (SC), mottled	2.0					18				
20													
23.0			Loose, light tan and gray, CLAYEY SAND (SC), mottled	9					15				
25													
28.0			Very stiff, gray, tan, and red, SANDY LEAN CLAY (CL), mottled	2.0		68		18	42	19	23		
30													
33.0			Stiff, red and gray, SANDY LEAN CLAY (CL)	10									
35													
38.0			Very stiff, light red and tan, with gray, LEAN CLAY WITH SAND (CL), mottled	2.5		71		20	45	17	28		
40.0			Very stiff, gray, red, and tan, SANDY LEAN CLAY (CL)	15				20					
40			<b>Boring terminated at 40'</b>										
45													
Completion Depth: <b>40.0</b> Date Boring Started: <b>6/13/06</b> Date Boring Completed: <b>6/13/06</b> Logger: <b>E. Wilson</b> Project No.: <b>106-157</b>				Remarks: <b>Seepage noted at 39' during drilling. Water level at 27'6" at final check.</b>									

Figure B.2 Lake Gladewater Dam Boring No. 2

**LOG OF BORING NO. 3**

Project Description: **Lake Gladewater Dam  
Gladewater, Texas**

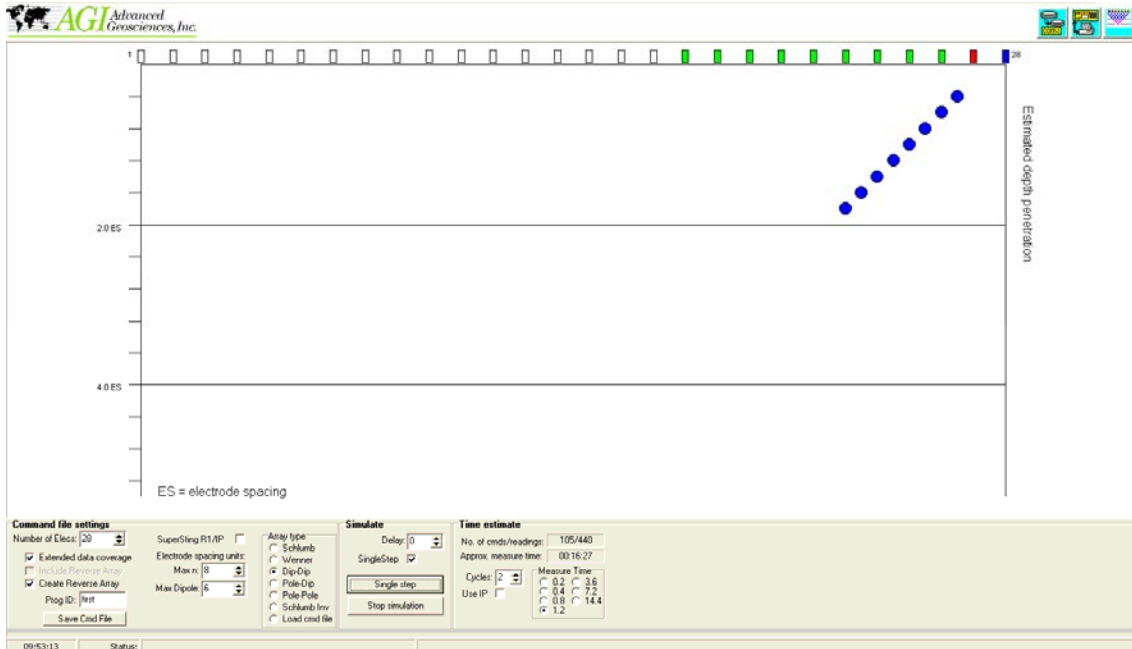


Depth, feet	Samples	Graphic Log	MATERIAL DESCRIPTION	Penetration Blows / Foot	Pocket Penetrometer, TSF	Unconfined Compression, TSF	% Passing No. 200 Sieve	Unit Dry Weight, lb/cu ft.	Water Content, %	Liquid Limit	Plastic Limit	Plasticity Index	Other
0			Loose, light tan and red, CLAYEY SAND (SC)	7					8				
3.0			Loose, tan and red, CLAYEY SAND (SC)	4			43		10	26	14	12	
5.0			Very dense, light tan, red, with gray, CLAYEY SAND (SC), mottled		2.5								
8.0			Medium dense, brown, CLAYEY SAND (SC)	15					9				
13.0			Stiff, light brown, red, and tan, SANDY LEAN CLAY (CL), mottled		1.5	2.5		123	20				
18.0			Very stiff, light tan, red with tan, SANDY LEAN CLAY (CL), mottled		3.5		55		18	39	18	21	
23.0			Stiff, red and tan with gray, SANDY LEAN CLAY (CL), mottled		1.5				20				
28.0			Dense, red, light tan, and gray, CLAYEY SAND (SC), mottled		1.0		43		17	27	14	13	
33.0			Very dense, gray and red with tan, CLAYEY SAND (SC), mottled		2.0	1.9		100	23				
38.0			Medium stiff, red, gray, tan, LEAN CLAY WITH SAND (CL), mottled	12			76		22	41	17	24	
40.0			<b>Boring terminated at 40'</b>										
45			Completion Depth: <b>40.0</b> Date Boring Started: <b>6/13/06</b> Date Boring Completed: <b>6/13/06</b> Logger: <b>E. Wilson</b> Project No.: <b>106-157</b>										
				Remarks: <b>Seepage noted at 24' during drilling. Water level at 34'9" at final check.</b>									

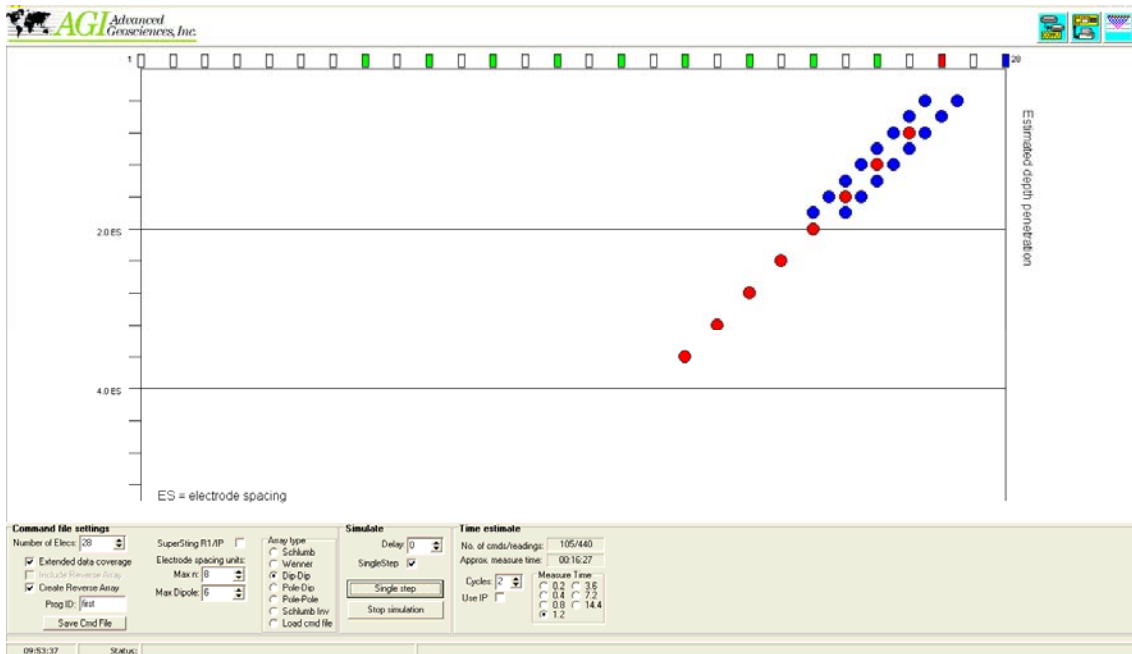
Figure B.3 Lake Gladewater Dam Boring No. 3

APPENDIX C

DEVELOPMENT OF SUBSURFACE MAPPING SCHEME FROM DIPOLE-DIPOLE ARRAY  
USING AGI ADMINISTRATOR PROGRAM

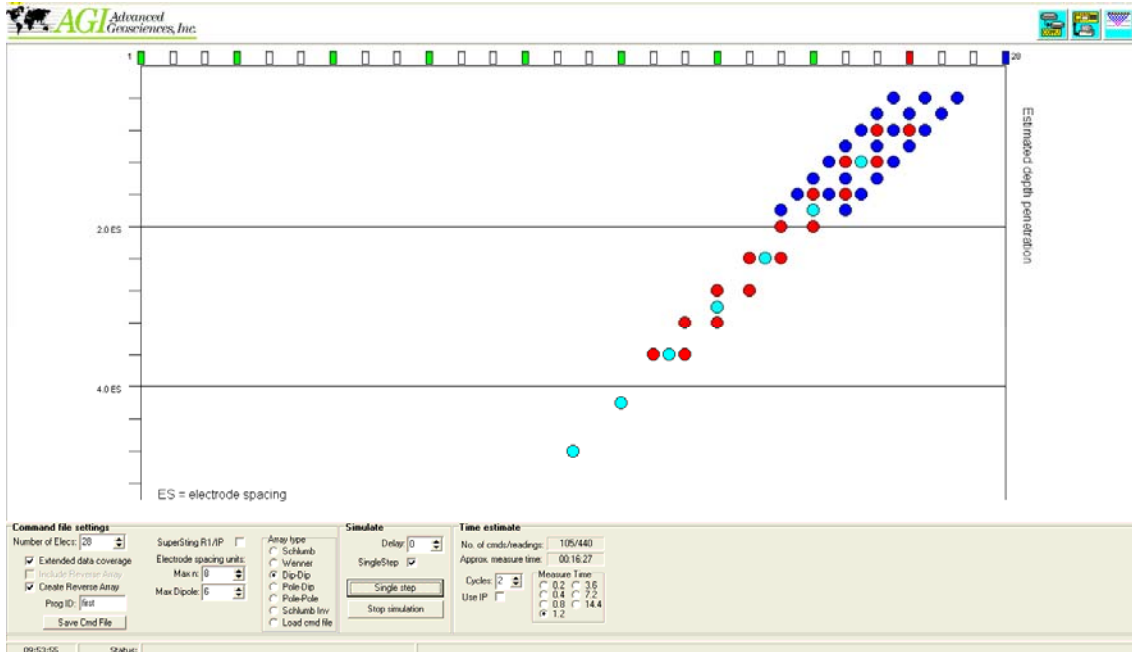


(a)

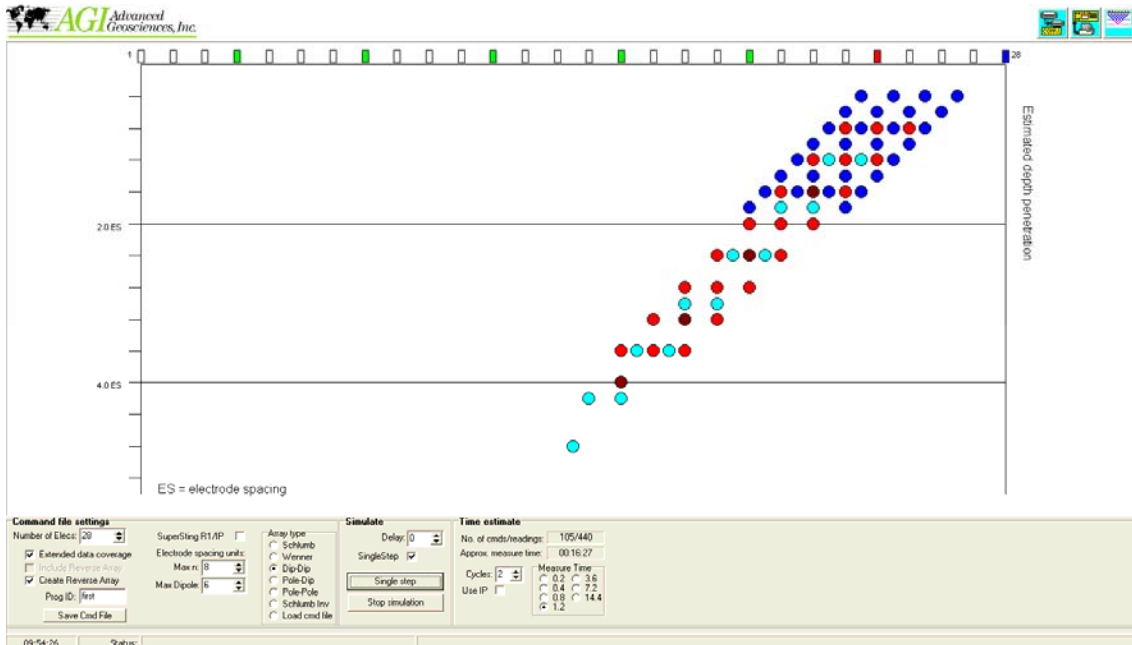


(b)

Figure C.1 Construction of Dipole-Dipole Survey Array

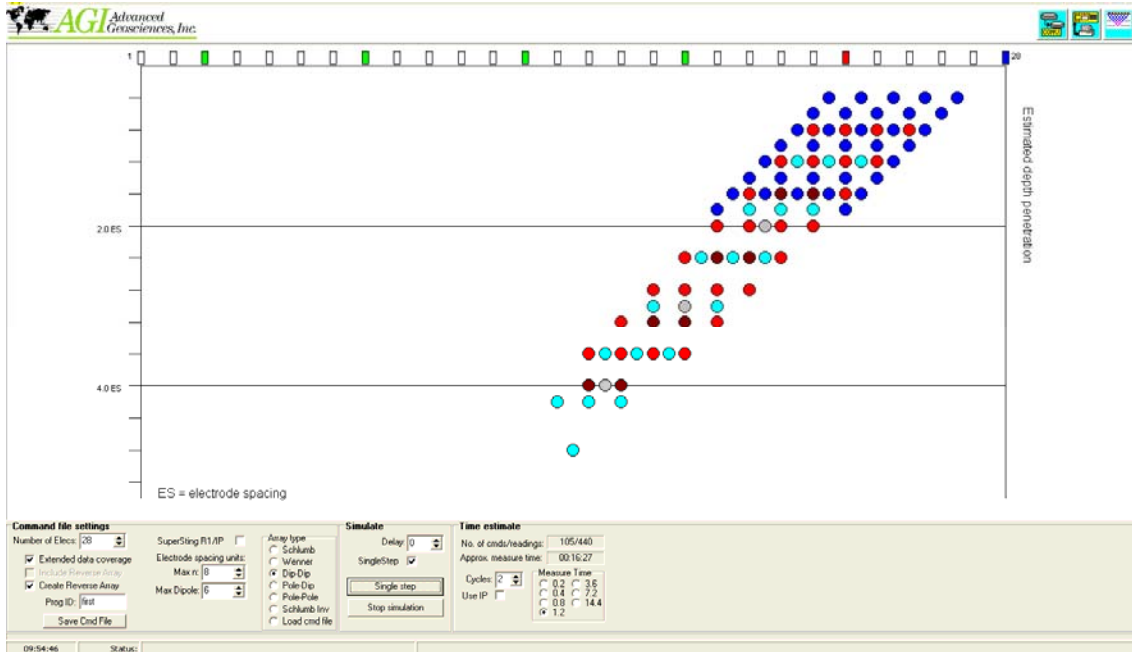


(a)

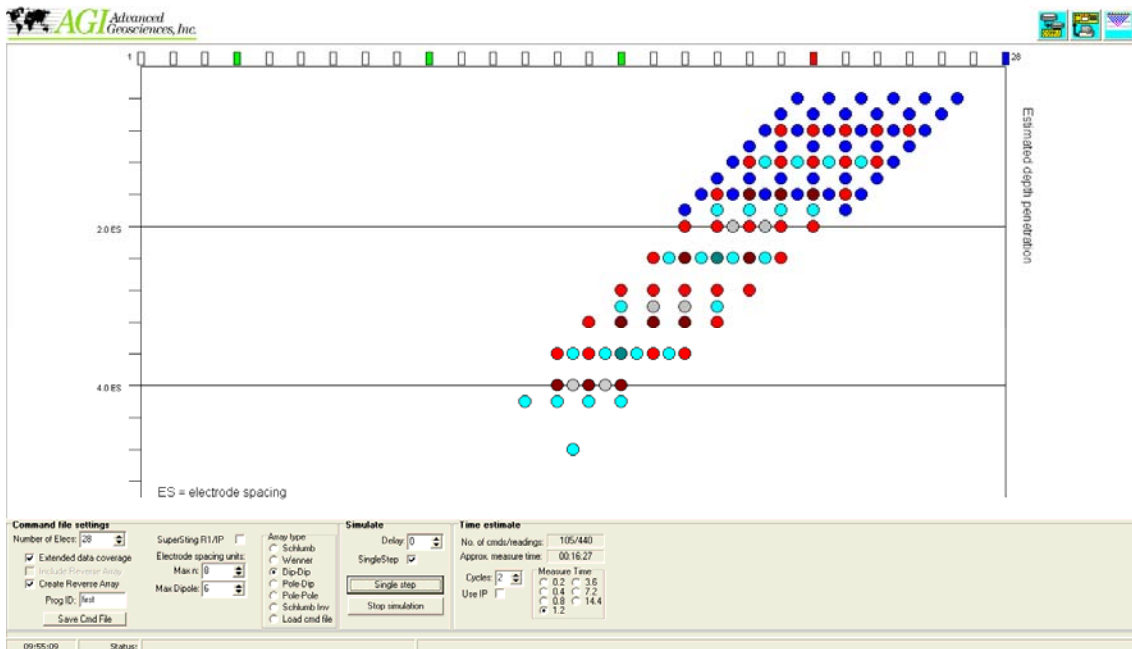


(b)

Figure C.2 Construction of Dipole-Dipole Survey Array



(a)



(b)

Figure C.3 Construction of Dipole-Dipole Survey Array

APPENDIX D

ENLARGED ERT AND MASW TOMOGRAPHY IMAGERY



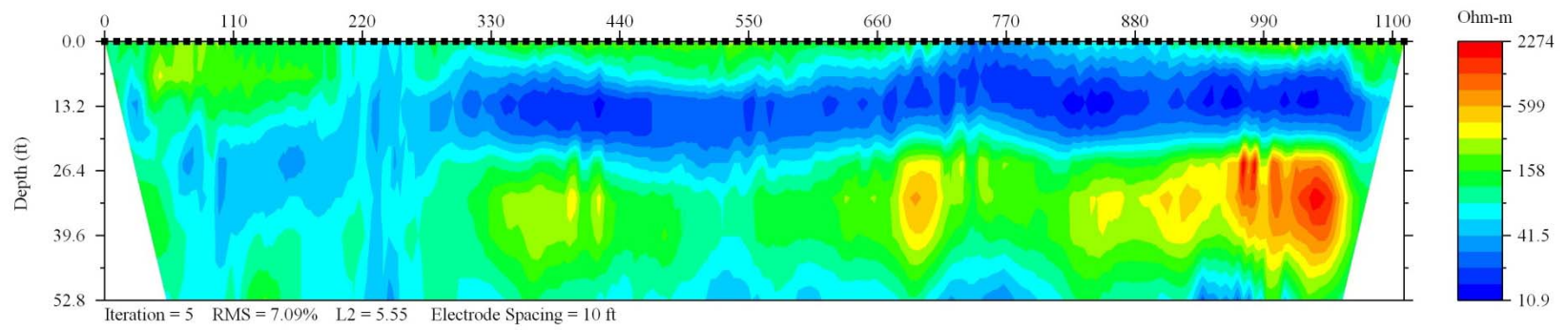


Figure D.1 Lake Gladewater Dam Electrical Resistivity Profile

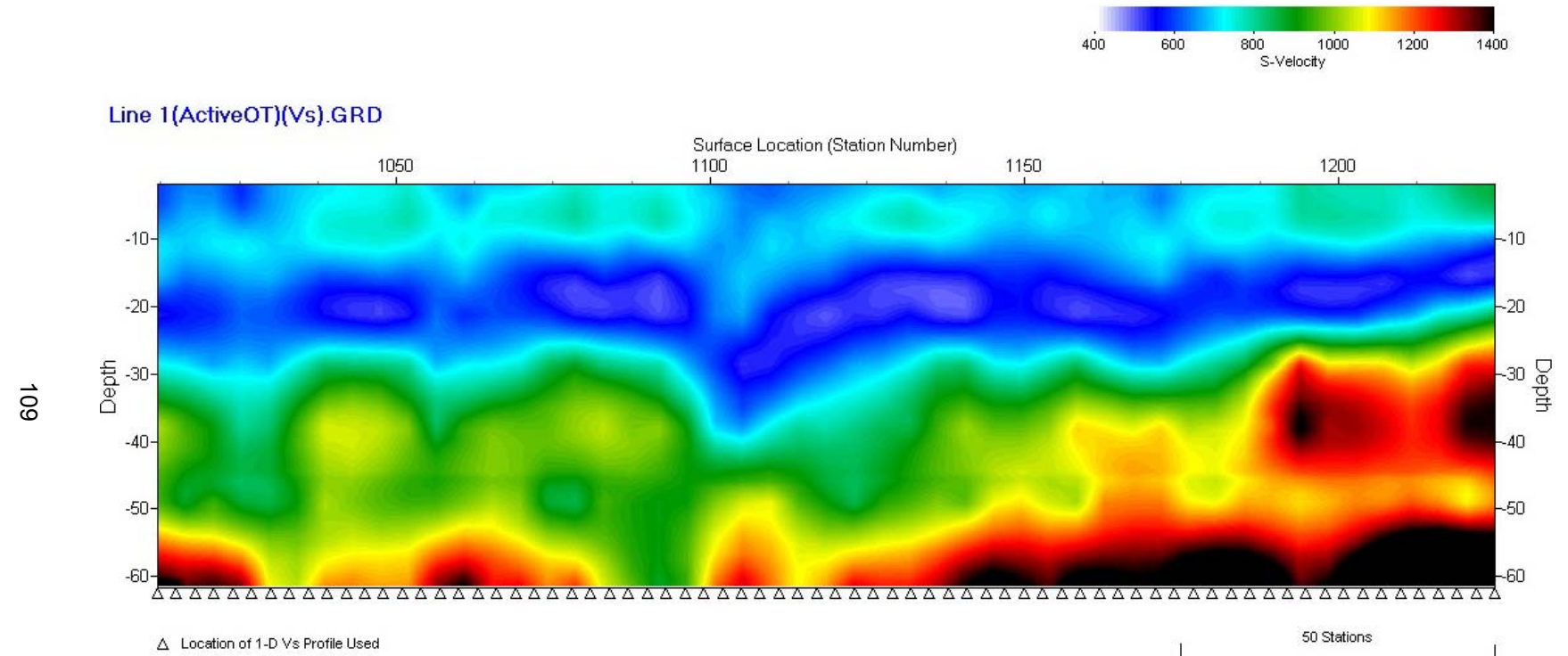
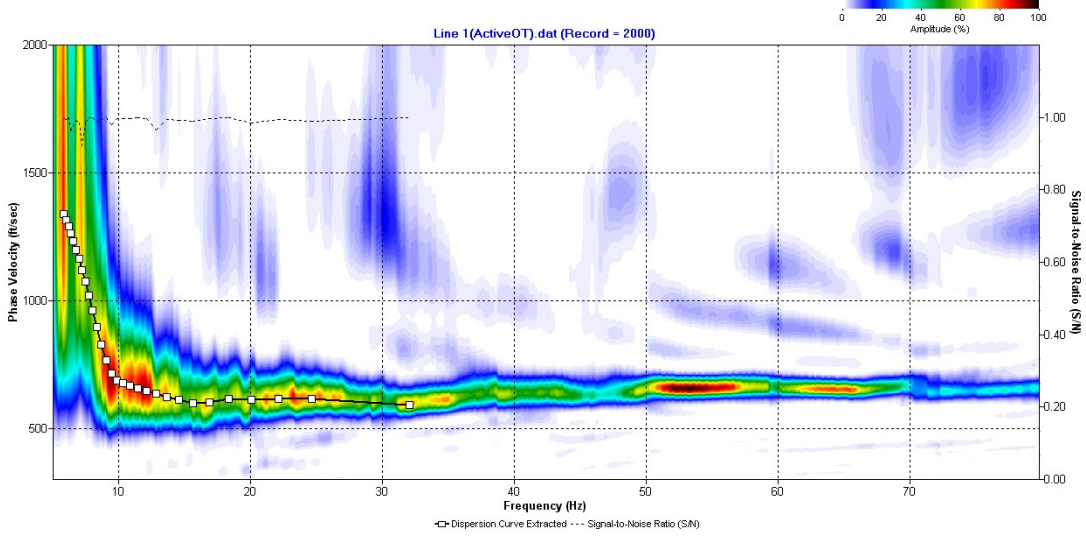


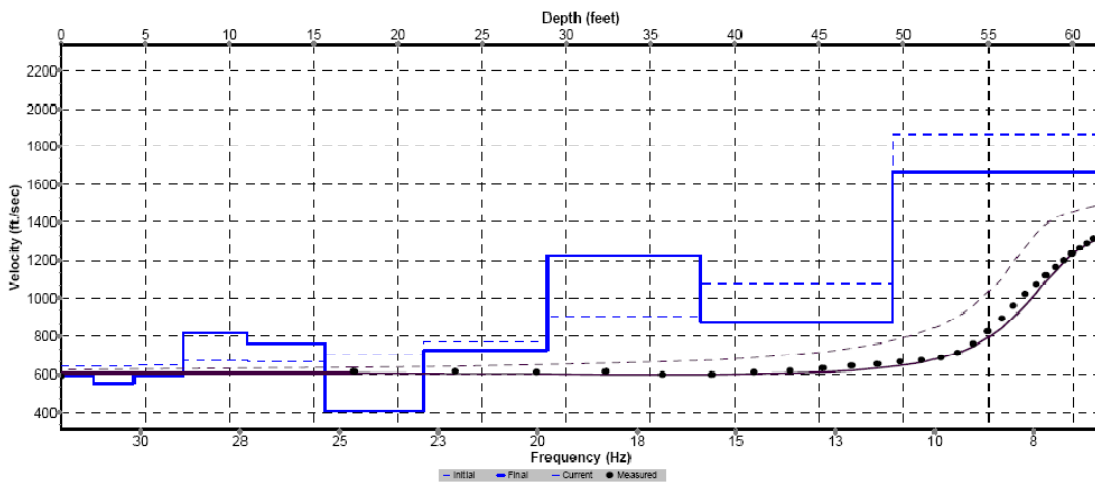
Figure D.2 Lake Gladewater Dam Electrical Resistivity Profile

## APPENDIX E

### MASW DISPERSION CURVE AND SHEAR WAVE PROFILE EXAMPLES

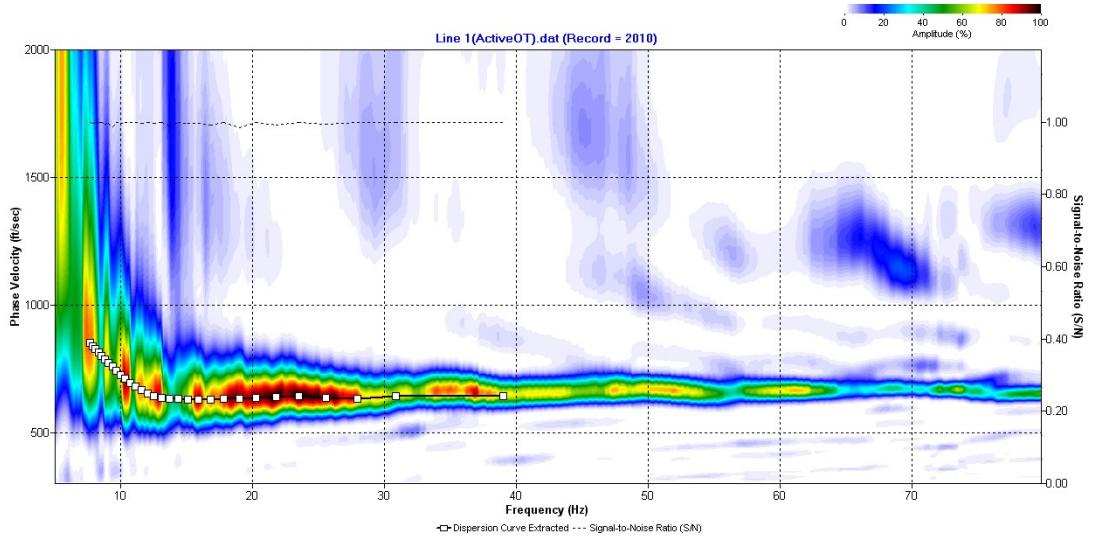


(a)

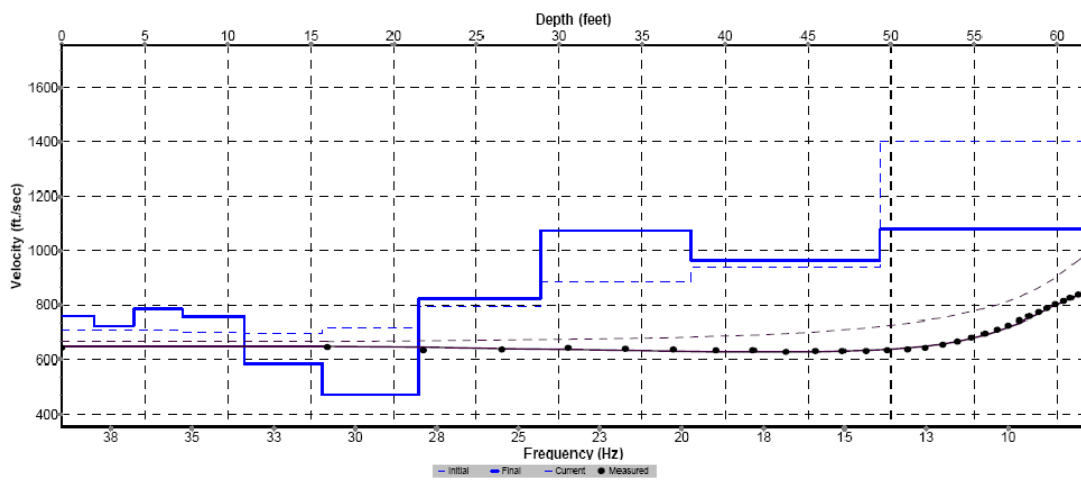


(b)

Figure E.1 (a) Dispersion Curve and (b) 1-D Shear Wave Velocity Profile for Record No. 2000

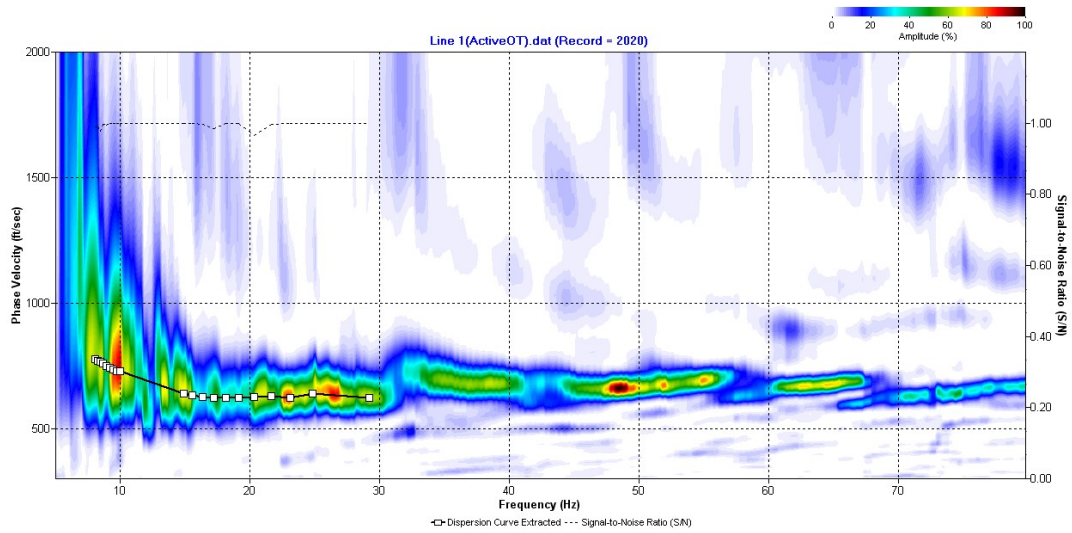


(a)

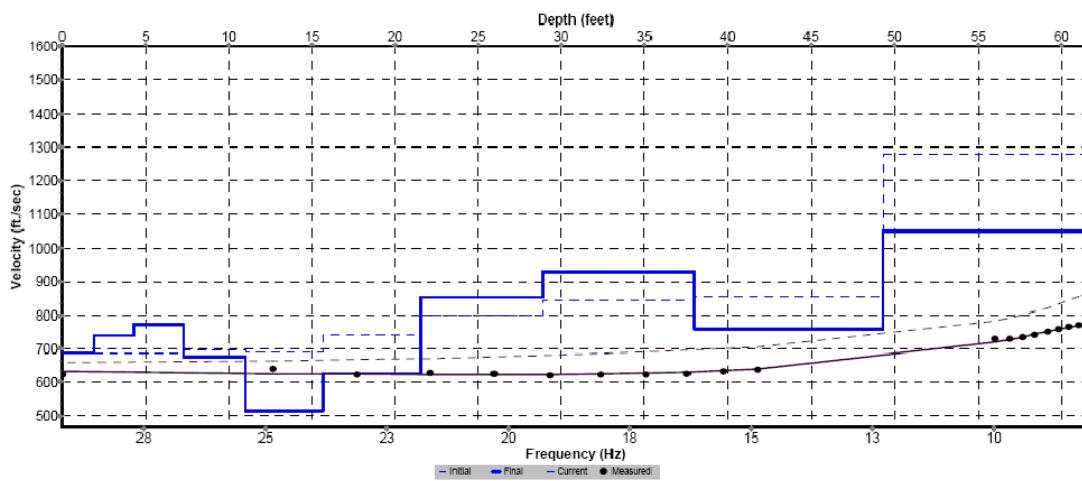


(b)

Figure E.2 (a) Dispersion Curve and (b) 1-D Shear Wave Velocity Profile for Record No. 2010

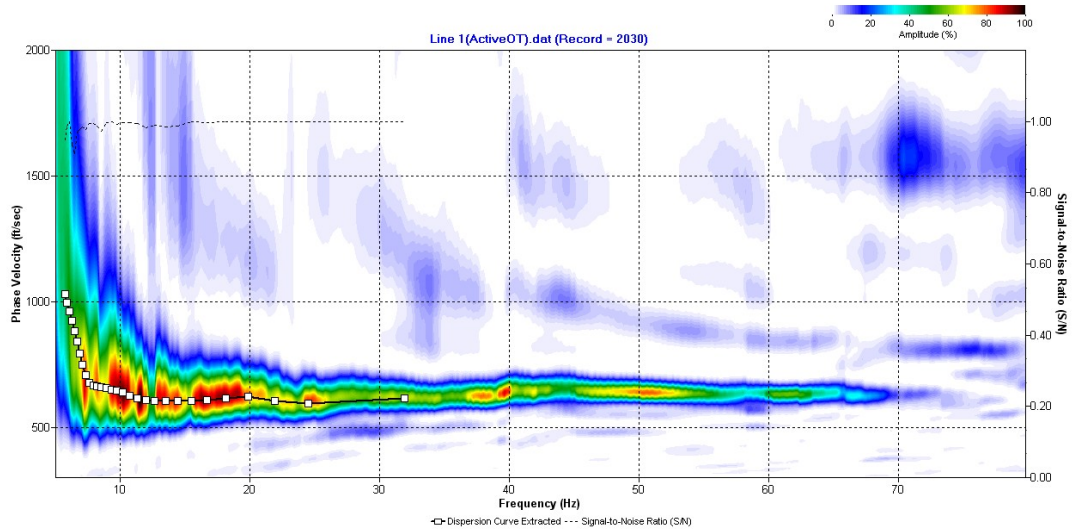


(a)

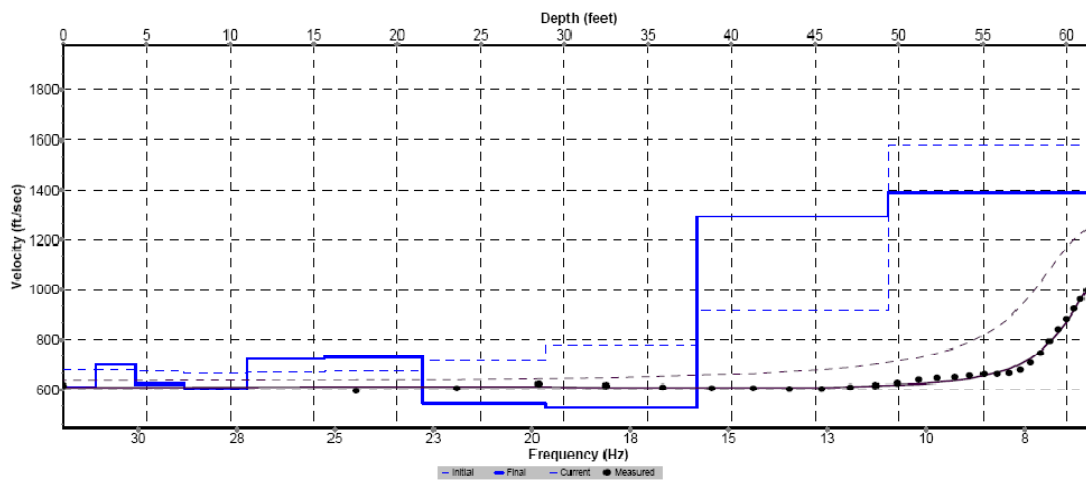


(b)

Figure E.3 (a) Dispersion Curve and (b) 1-D Shear Wave Velocity Profile for Record No. 2020

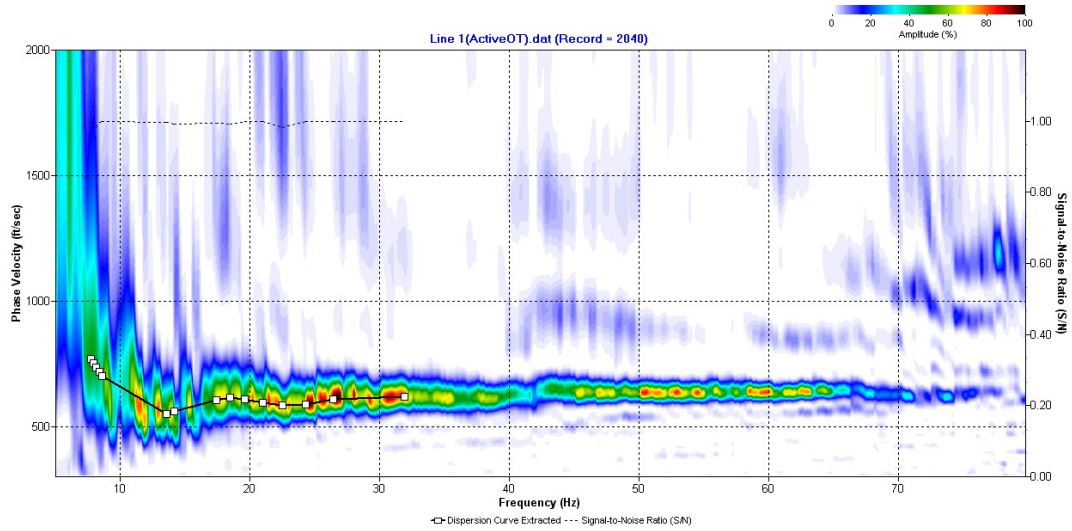


(a)

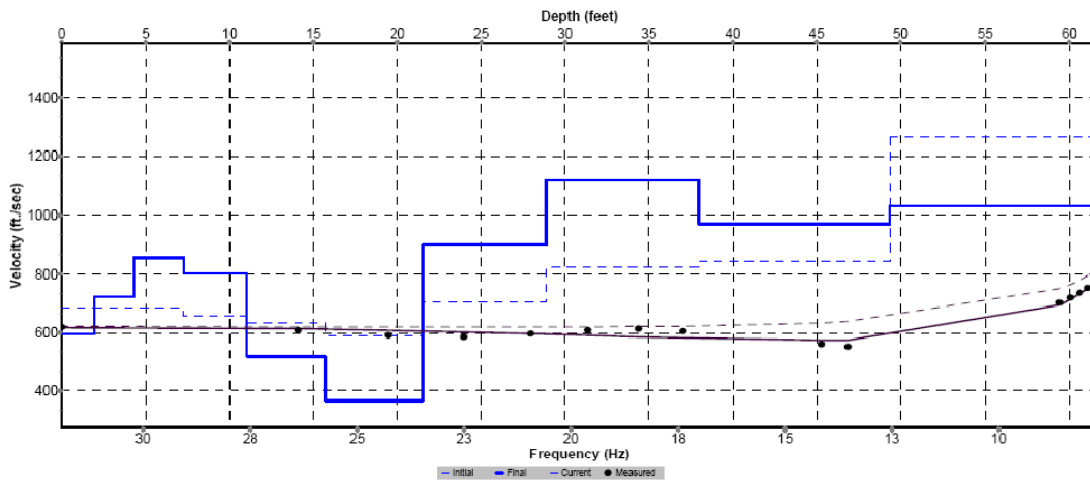


(b)

Figure E.4 (a) Dispersion Curve and (b) 1-D Shear Wave Velocity Profile for Record No. 2030



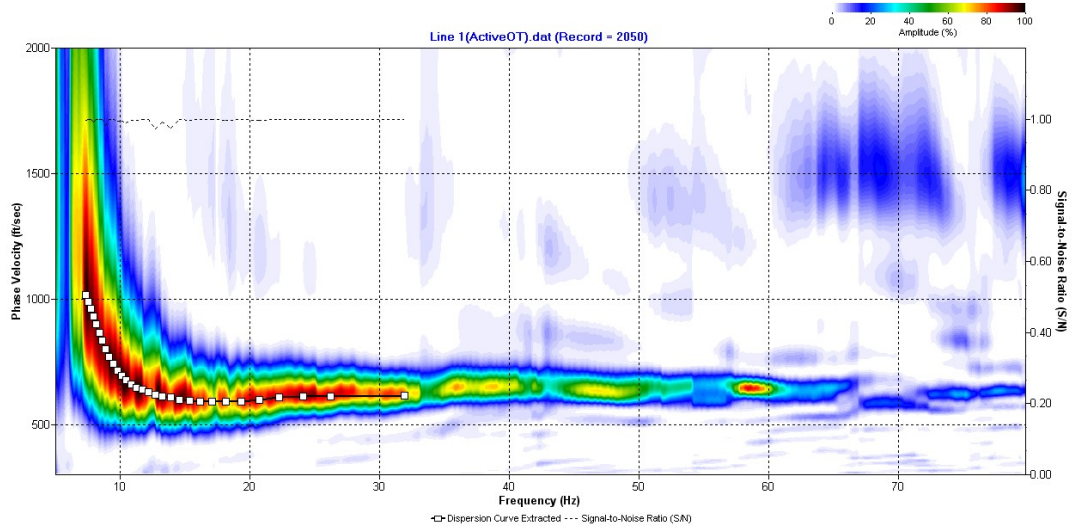
(a)



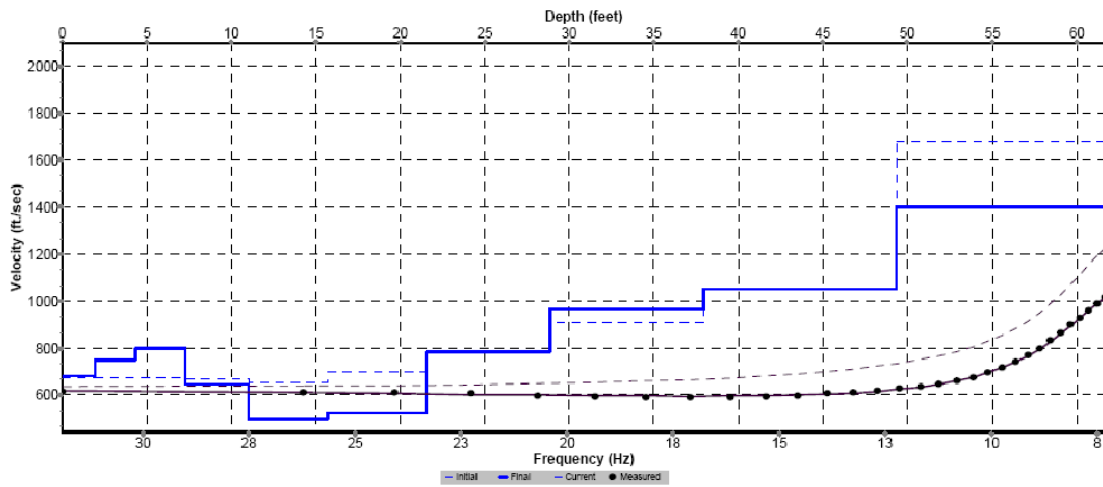
(b)

Figure E.5 (a) Dispersion Curve and (b) 1-D Shear Wave Velocity Profile for Record No. 2040



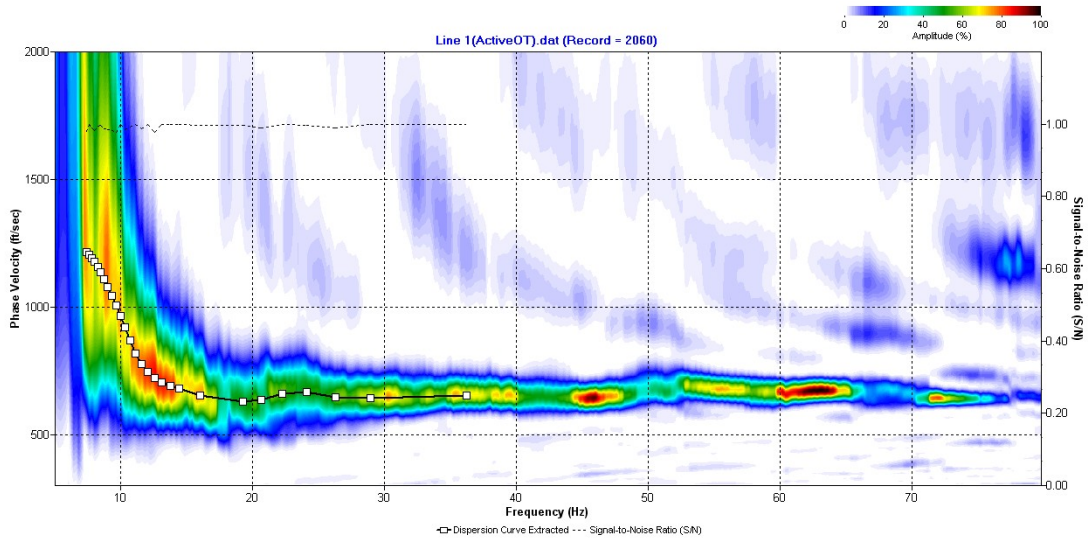


(a)

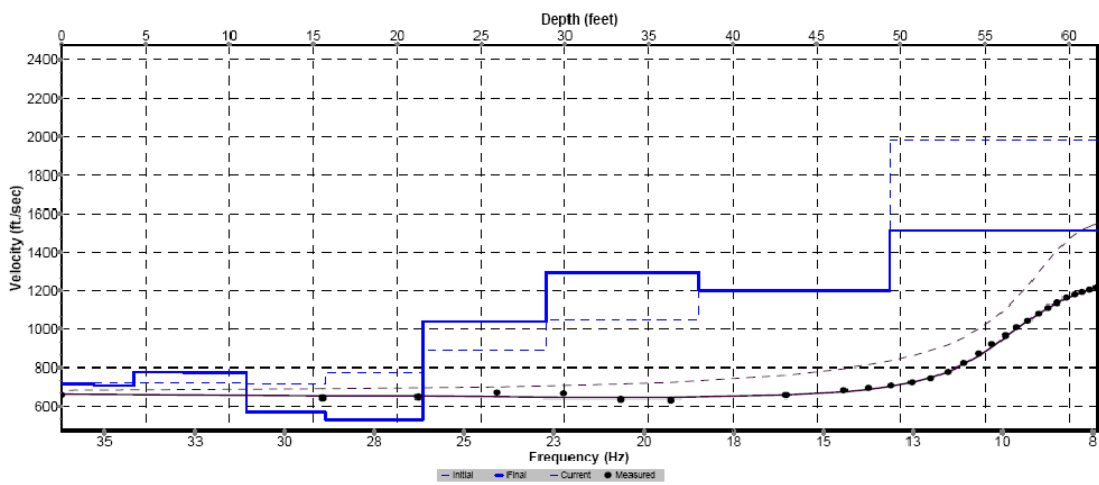


(b)

Figure E.6 (a) Dispersion Curve and (b) 1-D Shear Wave Velocity Profile for Record No. 2050

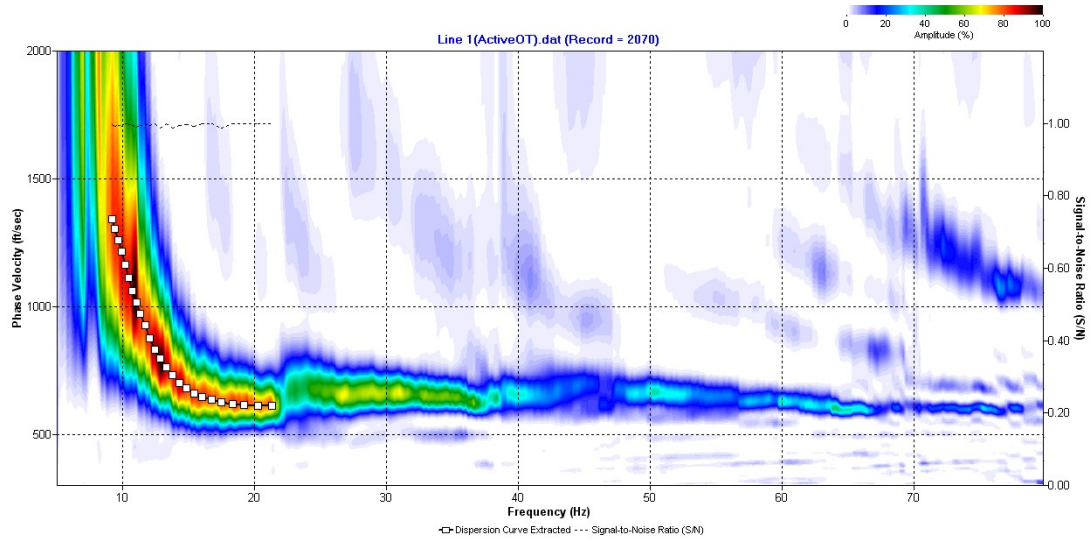


(a)

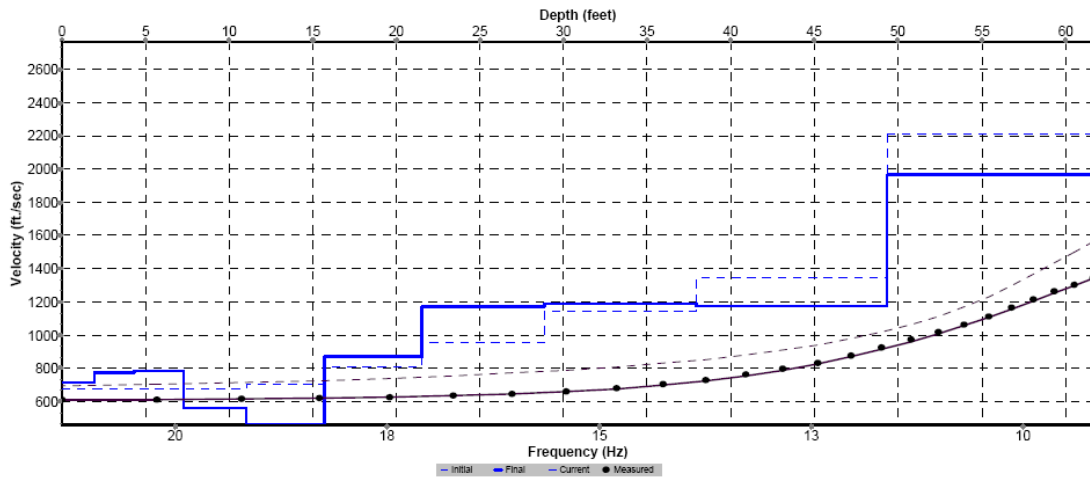


(b)

Figure E.7 (a) Dispersion Curve and (b) 1-D Shear Wave Velocity Profile for Record No. 2060



(a)



(b)

Figure E.1 (a) Dispersion Curve and (b) 1-D Shear Wave Velocity Profile for Record No. 2070

## REFERENCES

- Advanced Geosciences Incorporated. "Workshop/Seminar on Resistivity Imaging." Austin, April 29, 2008.
- Advanced Geosciences, Incorporated. Advanced Geosciences, Inc. January 23, 2009. <http://www.agiusa.com> (accessed April 16, 2009).
- Advanced Geosciences, Incorporated. "Advanced Resistivity Imaging Seminar." Austin, April 16, 2009.
- Advanced Geosciences, Incorporated. "Instruction Manual for The Super Sting with Swift Automatic Resistivity and IP System." Austin, January 2006.
- American Society of Testing and Materials. "ASTM D 1589-99: Standard Test Method for Penetration and Split Barrel Sampling of Soils." 1999.
- American Society of Testing and Materials. "ASTM D 5778-07: Standard Test Method for Electronic Friction Cone and Piezocone Penetration Testing of Soils." 2007.
- Benson, Richard C., and Lynn Yuhr. "An Introduction to Geophysical Techniques and Their Applications for Engineers and Project Managers." SAGEEP. Keystone: Environmental and Engineering Geophysical Society, 1996. 62-87.
- Bowles, Joseph E. Physical and Geotechnical Properties of Soils, 2nd Edition. New York: McGraw-Hill, Inc., 1984.
- Bryson, Sebastian L. "Evaluation of Geotechnical Parameters using Electrical Resistivity Measurements." American Society of Civil Engineers Proceeding No. 158. American Society of Civil Engineers, 2005.
- Butler, Dwain K. "What Is Near-Surface Geophysics." In Near-Surface Geophysics, by Dwain K. Butler, 1-6. Tulsa: Society of Exploration Geophysicist, 2005.

- Callister Jr, William D. Fundamentals of Material Science and Engineering. New York: John Wiley and Sons, Inc., 2001.
- Coduto, Donald P. Foundation Design: Principles and Practices. Englewood Cliffs: Prentice-Hall, Inc., 1994.
- Coduto, Donald P. Geotechnical Engineering: Principles and Practices. Upper Saddle River: Prentice-Hall, Inc., 1999.
- Cosenza, Philippe, Eric Marmet, Faycal Rejiba, Yu Jun Cui, Alain Tabbagh, and Yvelle Charley. "Correlation Between Geotechnical and Electrical Data: A Case Study at Garchy in France." Journal of Applied Geophysics, 2006: 165-178.
- Day, Robert W. Foundation Engineering Handbook: Design and Construction with the 2006 International Building Code. New York: McGraw-Hill, Inc., 2006.
- Gardner, Terry, and David Wright. "Lake Gladewater Dam-Embankment Remediation." Geotechnical Evaluation, Tyler, 2006.
- Geometrics Incorporated. "ES-3000, Geode, and StrataVisor NZ/NZC Operator's Manual, P/N 28519-01 Rev K." San Jose, June 2003.
- Gibson, Paul J, and Dorothy M George. Environmental Applications of Geophysical Surveying Techniques. Hauppauge: Nova Science Publishers, 2003.
- Greenhouse, John, Paul Gudjurgis, and David Slaine. "Introduction to Environmental and Engineering Geophysics." SAGEEP 98. Chicago, 1998.
- Ivanov, Julian, Choon Park, and Jianghai Xia. "MASW/SurfSeis 2 Workshop." Fort Worth: Kansas Geologic Survey, March 28, 2009.
- Ivanov, Julian, Richard D Miller, Jr., Robert F Ballard, Joseph B Dunbar, and Steve Smullen. "Time-lapse Seismic Study of Levees in Southern Texas." Society of Exploration Geophysicist, 2005: 1121-1124.
- Iyisan, Recep. "Correlation Between Shear Wave Velocity and In-Situ Penetration Test Results." Teknik Dergi, 1996: 1187-1199.

- Kearey, Philip, Micheal Brooks, and Ian Hill. An Introduction to Geophysical Exploration. Williston: Blackwell Publishing, 2002.
- Loke, M.H. "Electrical Imaging Survey for Environmental and Engineering Studies." 2000.
- Look, Burt G. Handbook of Geotechnical Investigation and Design Tables. London: Taylor and Francis/Balkema, 2007.
- Milson, John. Field Geophysics. New York: John Wiley & Sons, 1996.
- National Cooperative Highway Research Program. NCHRP Synthesis 368: Cone Penetration Testing. Washington D.C.: Transportation Research Board, 2007.
- Nettles, Sandy, Brett Jarrett, and Eric C. Cross. "Application of Surface Geophysics for Providing a Detailed Geotechnical Assesment of a Large Resort Development Site in Anguilla, BWI." American Society of Civil Engineers Conference Proceedings No. 327. American Society of Civil Engineers, 2008. 110-119.
- Parasnis, D.S. Principles of Applied Geophysics. New York: Chapman & Hall, 1997.
- Park, Choon B, Richard D Miller, Jianghai Xia, and Julian Ivanov. "MASW - An easy seismic Method to map shear-wave velocity of the ground." Chun Cheon: Korean Society of Engineering Geology, 2004.
- Park, Choon B, Richard D Miller, Jianghi Xia, and Julian Ivanov. "Multichannel Seismic Surface-Wave Methods for Geotechnical Applications." First International Conference on the Application of Geophysical Methodologies to Transportation Facilities and Infrastructure. St. Louis, 2000.
- Park, Choon B, Richard Miller, Jianghai Xia, Nils Ryden, and Peter Ulriksen. "The MASW Method - What and Where it is." EAGE 65th Conference and Exhibition. Stavanger, 2003.
- Park, Choon B. MASW - Horizontal Resolution in 2D Shear-Velocity ( $V_s$ ) Mapping. Open-File Report, Lawrence: Kansas Geologic Survey, 2005.
- Pelton, John R. "Near-Surface Seismology: Wave Propagation." In Near-Surface Geophysics, by Dwain K. Butler, 177-218. Tulsa: Society of Exploration Geophysicist, 2005.

Society of Exploration Geophysicist of Japan. Application of Geophysical Methods to Engineering and Environmental Problems. Tokyo: Society of Exploration Geophysicist of Japan, 2004.

Steeple, Don. "Engineering and Environmental Geophysics at the Millenium." Geophysics, 2001: 31-35.

Steeple, Don. "Near-Surface Seismology: A Short Course." Lawrence: Society of Exploration Geophysicist, 1998.

Sudha, Kumari, M Israil, S Mittal, and J. Rai. "Soil Characterization Using Electrical Resistivity Tomography and Geotechnical Investigations." Journal of Applied Geophysics, 2009: 74-79.

Tayntor, John J, and David A. Wright. "Electrical Resistivity Analysis at Lake Gladewater Dam." Geotechnical Evaluation, Tyler, 2008.

Texas Commission of Environmental Quality. "Lake Gladewater Dam Inspection Report." Inspection Report, Austin, 2005.

Thitimakorn, Thanop, Neil Anderson, David Hoffman, and Ahmed Ismail. "A Comparative Analysis of 2-D MASW Shear Wave Velocity Profiling Techniques." Electronic Journal of Geotechnical Engineering, 2006.

Thitimakorn, Thanop, Neil Anderson, R. Stephenson, and Wanxing Liu. "2-D Shear Wave Velocity Profile Along Test Segment of Interstate 70, St. Louis, Missouri." American Society of Civil Engineers Conference Proceedings No. 164. American Society of Civil Engineers, 2005.

Tomeh, Amin A, Sam Alyateem, Hameed Malik, and Billy Malone. "Geophysical Surveying and Data Simulation Application to Geotechnical Investigations: A Cost Effective Approach for Developing Economical Foundation Design Criteria." GeoCongress 2006: Geotechnical Engineering in the Information Technology Age. American Society of Civil Engineers, 2006.

United States Corps of Engineers. "EM 1110-1-1802: Geophysical Exploration for Engineering and Environmental Investigations." Engineering Manual, Washington D.C., 1995.

- United States Corps of Engineers. "Geotechnical Investigations." Engineering Manual No. 1110-1-1804, Washington D.C., 2001.
- United States Geologic Survey. "Gladewater Quadrangle, Texas, 7.5 Minute Series." Denver, 1960.
- United States Geologic Survey. Texas Geologic Map Data: Queen City Sands. October 30, 2009. <http://tin.er.usgs.gov/geology/state/sgmc-unit.php?unit=TXEQqc;0> (accessed October 30, 2009).
- Van Der Hilst, Robert. "Chapter 4: Seismology." MIT Open Course Ware. 2004. <http://ocw.mit.edu/NR/rdonlyres/Earth--Atmospheric--and-Planetary-Sciences/12-201Fall-2004/4813C5AE-9A5F-4440-8A49-39559A713D67/0/ch4.pdf> (accessed October 25, 2009).
- Zonge, Ken, Jeff Wynn, and Scott Urquatt. "Resistivity, Induced Polarization, and Complex Resistivity." In Near-Surface Geophysics, by Dwain K. Butler, 265-300. Tulsa: Society of Engineering Geophysicist, 2005.



## BIOGRAPHICAL INFORMATION

Joshua Hubbard graduated from Texas A&M University in the fall of 2004, receiving a Bachelor of Science Degree in Civil Engineering. Since that time, he has worked as a staff engineer for Apex Geoscience, Incorporated in both the Tyler and Dallas/Fort Worth areas. His works in the geotechnical and construction fields have included a variety of projects, primarily in Texas, Oklahoma, New Mexico, Arkansas and Louisiana. Joshua currently plans to continue practicing in the Dallas/Fort Worth area, and pursue his professional license in 2010.